REMARKS

Status of the Claims

Claims 15-43 are currently pending. Claims 1-14 have been canceled without prejudice or disclaimer of the subject matter claimed therein. Claims 26-38 are withdrawn from examination as being directed to a separate invention. New claims 39-43 have been added. New claims 39-43 are dependent from claim 15, 16, 22, 24, or 25, and are directed to the same invention as claims 15-25. Thus, new claims 39-43 should be examined with claims 15-25.

Support for New Claim

Claims 15, 21, 22, and 26-35 have been amended. These claims have been amended to delete the word "receptor" after "KDR/Flk-1", since "KDR/Flk-1" is the name of the receptor.

New claims 39-43 have been added. Support for these new claims can be found throughout the specification. Representative support is summarized in the table below.

Claims	Representative Support
39	Page 3, line 13
40	Page 8, line 21
41	Page 9, lines 25 and 26
42	Claim 24
43	Claim 25

New claims 39-43 do not introduce prohibited new matter.

Takahashi *et al.* and Lack of Unity Requirement

The Office Action alleges that the invention of Group II (now claims 15-25) was found to have no special technical feature that defined a contribution over the prior art of Takahashi *et al.* (Takahashi).

Applicants respectfully point out that Takahashi teaches that Y1175, but not Y1214, plays a crucial role in the transduction of signals to the MAP kinase pathway and DNA synthesis of endothelial cells (page 2769, left column, first paragraph). Thus, Takahashi teaches away from obtaining a probe that binds the Y1214 site on KDR/Flk-1 for detecting activation of

KDR/Flk-1. Accordingly, claims 15-43 define a contribution over the prior art of Takahashi, and claims 15-43 relate to a single inventive concept under PCT Rule 13.1 and should be examined together.

Rejection Under 35 U.S.C. § 112, First Paragraph

A. Claims 15-25 are rejected under 35 U.S.C. § 112, first paragraph, because the specification allegedly does not provide reasonable enablement for the scope of the claims.

The claims as they stand require that the probe detects activation of KDR/Flk-1 and binds tyrosine residue Y1214 of KDR/Flk-1. Thus, the claims are not directed to any probe. The specification discloses that binding proteins and binding partners are known in the art to bind tyrosine residues on tyrosine kinase receptors and capable of detecting activation of tyrosine kinase receptors. Moreover, the specification discloses antibodies as an example of a binding protein. The specification provides methods for generating antibodies and assays for testing antibodies to determine whether they bind the tyrosine residue of Y1214 of KDR/Flk-1.

The Office Action alleges that the specification does not enable the scope of the claims because the specification only discloses monoclonal and polyclonal antibodies that detect activation of KDR/Flk-1. Applicants respectfully point out that antibodies are an example of a probe that can detect activation of KDR/Flk-1 and binds tyrosine residue Y1214 of KDR/Flk-1. Other examples of probes that bind phosphorylation sites of a tyrosine kinase receptor and detect the activation of the receptor are well known in the art. They include binding proteins or binding partners that interact with tyrosine residues.

The Office Action also alleges that there is no *in vivo* working example for a pharmaceutical composition comprising a probe effective for treating any and all diseases. However, MPEP 2164.02 states that compliance with the enablement requirement does not turn on whether an example is disclosed. MPEP 2164.02 also states that Applicants need not describe all actual embodiments, since only an enabling disclosure is required. Further, the specification need not contain an example if the invention is otherwise disclosed in such manner that one skilled in the art will be able to practice it without undue experimentation. *In re Borkowski,* 422 F.2d 904, 908, 164 USPQ 642, 645 (CCPA 1970).

Moreover, antibodies that act as inhibitors of tyrosine kinase receptors activity are well known and some even have been approved by the FDA for treating cancer. For example, Erbitux

is a monoclonal antibody that targets epidermal growth factor receptors (see attached Baselga, Eur. J. Cancer, 37:S16, 2001), and Erbitux has been approved by the FDA for treating colon cancer (see attached UAB Media Relations). Erbitux binds the epidermal growth factor receptors and blocks ligand-induced EGFR phosphorylation. Avastin is another example of a monoclonal antibody that has been approved by the FDA for the treatment of cancer. Avastin has been approved for the treatment of colorectal cancer (see attached FDA News).

Also, Ycom1D3, a monoclonal antibody against human VEGFR II, has been shown to be efficient in neutralizing VEGF-induced mitogenesis of human endothelial cells (see attached Li *et al.*, Acta Pharmacol Sin. 25(10):1292, 2004). IMC-1C11, an anti-KDR antibody, has been reported to block VEGFR-KDR interaction and inhibit VEGFR-induced endothelial cell proliferation and to be safe and well tolerated by patients with liver metastases from colorectal carcinoma in a phase I study (see attached Posey *et al.*, Clinical Cancer Research, 9:1323, 2003). Additionally, DC101, an anti-VEGFR-II antibody, has been reported to suppress contact hypersensitivity (see attached Watanabe *et al.*, Experimental Dermatology 13:671, 2004). Thus, antibodies have been shown to be effective as pharmaceutical agents for *in vivo* use and for the treatment of diseases.

The Office Action alleges that the specification does not teach the chemical structure of any probe and does not provide assays that are useful for obtaining such a probe. Additionally, the Office Action alleges that the claims do not teach all peptides "comprising" Y1214 of the KDR/Flk-1 for generating the claimed probes. As discussed above, the specification provides antibody as an example of the claimed invention. The specification provides methods for generating antibodies that bind tyrosine residue Y1214 of KDR/Flk-1 and detect activation of KDR/Flk-1 and assays for detecting whether the antibodies bind KDR/Flk-1 and whether the antibodies inhibit KDR/Flk-1 activity. These methods and assays are also well-known to a person of ordinary skill in the art. Moreover, as discussed on page 5, lines 18- 31, assays that are useful for detecting or measuring a change in the activation state of KDR/Flk-1 include fluorimetric assays, chromogenic assays, radiolabelling assays, and chemiluminescence assays which are routinely used by a person of ordinary skill in the art. Takahashi also discloses assays for detecting activation of KDR/Flk-1.

Further, the claims require that the probes not only bind tyrosine residue Y1214 of KDR/Flk-1 but also detect activation of KDR/Flk-1. Thus, the claims are not directed to any

probe but only those that bind tyrosine residue Y1214 of KDR/Flk-1 and detect activation of KDR/Flk-1. Given that assays for determining whether a probe binds the Y1214 of KDR/Flk-1 and whether a probe can detect the activation of KDR/Flk-1 are well known and described by the specification, one would be able to obtain the probes encompassed by the claims and the peptides comprising SEQ ID NO: 1 or 2 useful for generating antibodies encompassed by the claims. Thus, the specification enables one of ordinary skill in the art to obtain such probe without undue experimentation.

Additionally, anti-phosphotyrosine antibodies are known in the art. Some representative examples of such antibodies include 4G10 (see page fig. 2 of Ganju *et al.*, J. of Virology, 72(7):6131, 1998), 5E2 (see fig. 2 of Redemann *et al.*, Mol. and Cell. Biology, 12(2):491, 1992), and PY20 (see fig. 2 of Prochazka *et al.* Biology of Reproduction, 68:797, 2003).

Given that there is guidance in the prior art and in the specification for obtaining anti-phosphotyrosine antibodies, it would not require undue experimentation to obtain peptides comprising SEQ ID NO: 1 or 2 for generating antibodies that bind the Y1214 residue of KDR/Flk-1. It is within the skill of the artisan to obtain peptides comprising SEQ ID NO: 1 or 2 useful for generating an antibody that binds the Y1214 residue of KDR/Flk-1 and to determine whether an antibody generated by such peptide can bind the Y1214 residue of KDR/Flk-1 and detect the activation of KDR/Flk-1, given the assays provided by the specification. Moreover, given the guidance provided by the specification and the prior art, it is within the skill of the artisan to obtain antibodies generated from peptides comprising SEQ ID NO: 1 or 2. Also, it would not require undue experimentation to determine whether antibodies generated from peptides comprising SEQ ID NO: 1 or 2 are able to bind the Y1214 residue on KDR/Flk-1 because it would be routine to test for the binding of such antibodies to the Y1214 residue on KDR/Flk-1 given the assays provided in the specification.

Furthermore, Applicants respectfully assert that given the guidance provided by the specification and what is known in the prior art, it would only require routine experimentation to obtain the probes or the peptides for generating antibodies encompassed by the claims. It is well settled that routine experimentation should not be considered as undue in an enablement assessment. As stated in *Ex parte Jackson* and confirmed in *Ex parte Forman*, the court held:

> The test is not merely quantitative, since a considerable amount of experimentation is permissible, if it is merely routine, or in the

> specification in question provides a reasonable amount of guidance with respect to the direction in which experimentation should proceed to enable the determination of how to practice a desired embodiment of the invention. Because the present specification provides ample guidance and the experimentation is routine, the claims are in compliance with the section 112 first paragraph requirement.

Ex parte Jackson 217 USPQ 804 (Bd. Pat. App. 1982).

Applicants respectfully point out that since it is routine to test whether antibodies generated using peptides comprising SEQ ID NO: 1 or 2 bind the Y1214 residue on KDR/FLk-1, given the assays provided by the specification, the specification enables the scope of the claims and Applicants should not be limited to antibodies generated by peptides consisting of SEQ ID NO: 1 or 2. Given that an infringer could design around the claimed invention by generating an antibody from a peptide by adding one amino acid to SEQ ID NO: 1 or SEQ ID NO: 2, claims directed to antibodies generated by peptides consisting of SEQ ID NO: 1 or 2 would not provide adequate protection to Applicants. The court in *In re Goffe* explained that the claims must provide adequate protection to inventors:

> For all practical purposes, the board would limit appellant to claims involving the specific materials disclosed in the examples, so that a competitor seeking to avoid infringing the claims would merely have to follow the disclosure in the subsequently-issued patent to find a substitute. However, to provide effective incentives, claims must adequately protect inventors. To demand that the first to disclose shall limit his claims to what he has found will work or to materials which meet the guidelines specified for "preferred" materials in a process such as the one herein involved would not serve the constitutional purpose of promoting progress in the useful arts.

In re Goffe 542 F.2d 564, 191 USPQ 429, 431 (CCPA 1976). Accordingly, the specification enables the claimed invention.

B. Claims 15-25 are rejected under 35 U.S.C. § 112, first paragraph, as failing to comply with written description requirement.

Applicants respectfully point out that claims 15-25 as they stand are directed to an isolated probe that detects activation of KDR/Flk-1 and binds tyrosine residue Y1214 of the KDR/Flk-1. The claims recite both structural and functional features to describe the claimed probe.

The Office Action alleges that "a probe without a nucleotide sequence or chemical structure has no structure much less function." Applicants respectfully point out that the claims by requiring the probe to bind tyrosine residue Y1214 of KDR/Flk-1 and to detect activation of KDR/Flk-1 provide a structure and function for the probe. The probe must have a certain structure to bind tyrosine residue Y1214 of KDR/Flk-1. The function of the probe is to detect activation of KDR/Flk-1.

The Office Action also alleges that the term "peptide comprising" is "open-ended" encompassing various peptides and that the specification fails to provide a representative number of species of "probe." The Office Action cites *University of California v. Eli Lilly* and *University of Rochester v. G.D. Searle*. However, in contrast to the claims in the cited cases, the claims of the present application require that the probe bind tyrosine residue Y1214 of KDR/Flk-1 and detect activation of KDR/Flk-1. Thus, the claims are not directed to a broad genus of probes.

Moreover, the MPEP 2163 states that disclosure of any combination of identifying characteristics that distinguish the claimed invention from other materials would lead one of skill in the art to the conclusion that the applicant was in possession of the claimed species is sufficient and that an inventor is not required to describe every detail of his invention because an applicant's disclosure obligation varies according to the art to which the invention pertains. In the present case, the claims recite identifying characteristics such as binding to Y1214 of KDR/Flk-1 and detect activation of KDR/Flk-1. The inventors discovered that Y1124 plays a role in signal transduction from KDR/Flk-1 to the MAP kinase pathway and in the DNA synthesis in endothelial cells.

Further, the claims are not directed to peptides comprising Y1214 of KDR/Flk-1. These peptides are used to generate antibodies that bind Y1214 of KDR/Flk-1 and detect activation of KDR/FLK-1. The claims are directed antibodies that bind Y1214 of KDR/Flk-1 and detect activation of KDR/Flk-1, to methods of generating such antibodies, and to methods of using such antibodies. KDR/Flk-1 is a known tyrosine kinase receptor. The nucleic acid encoding KDR/Flk-1 has been isolated and its amino acid sequence has been determined. Although prior to the present discovery it was not known which tyrosine residue on KDR/Flk-1 is involved in the activation of the receptor, the structure and function of KDR/Flk-1 was known. Accordingly, the specification provides adequate description of the claimed invention.

Rejection Under 35 U.S.C. § 112, Second Paragraph

Claims 15-25 are rejected under 35 U.S.C. § 112, second paragraph as being indefinite for failing to particularly point out and distinctly claim the subject matter which applicant regards as the invention.

Applicants respectfully point out that as explained on page 9, lines 25-30 of the specification, the Terman *et al.* reference discloses that the tyrosine residue at position 1215 instead of 1214 because the sequence begins with an initiator methionine. It is clear that the tyrosine residue is at position 1214 when the initiator methionine is not present, as evidenced by Takahashi (Embo Journal, 2001, 20(11):2768). A quick internet search on Google also indicates that tyrosine at position 1214 on KDR/Flk-1 is well known (see attached search results from Google). Thus, claims 15-25 are not indefinite.

Rejections Under 35 U.S.C. § 103(a)

A. Claims 15-20 and 22-25 are rejected under 35 U.S.C. § 103(a) as being unpatentable over Takahashi *et al.* (Takashi) in view of Harlow *et al.* (Harlow).

The claims as they stand are directed to an isolated probe that detects activation of KDR/Flk-1 and binds tyrosine residue Y1214 of KDR/Flk-1. The present invention is based in part on the discovery by the inventors that tyrosine at position 1214 of KDR/Flk-1 plays an important role in the transduction of signals from the receptor to the MAP kinase pathway and in DNA synthesis in endothelial cells.

In contrast to the present invention, Takahashi teaches that Y1175, but not Y1214, plays a crucial role in the transduction of signals to the MAP kinase pathway and DNA synthesis of endothelial cells (page 2769, left column, first paragraph). Thus, Applicants respectfully point out that Takahashi teaches away from obtaining a probe that binds the Y1214 site on KDR/Flk-1 for detecting activation of KDR/Flk-1.

The Office Action alleges that tyrosine phosphorylation of Y1214 may be important for other signaling pathways of VEGF-1 in endothelial cells such as the stimulation of chemotaxis, cell survival, or the regulation of gene expression. However, Applicants respectfully point out that Takahashi specifically states on page 2775, "whether tyrosine phosphorylation of Y1214 is important for other signal pathways of VEGF-1 in endothelial cells, such as the stimulation of

chemotaxis, cell survival, or the regulation of gene expression remains to be elucidated." Thus, Takahashi does not teach or suggest that tyrosine phosphorylation of Y1214 is important for other signal pathways. Rather, the experimental results of Takahashi indicate that Y1214 on KDR/Flk-1 is not involved in the transduction of signals to the MAP kinase pathway and in DNA synthesis in endothelial cells.

The Office Action also alleges that given the teachings of Takahashi, one would have the motivation to make the claimed probe. Applicants point out that the claims as they stand are directed to a probe that not only binds tyrosine residue Y1214 of KDR/Flk-1, but also detects activation of KDR/Flk-1. Moreover, prior to Takahashi's work, it was known that KDR/Flk-1 utilizes the MAP kinase pathway as the major signaling pathway and that tyrosine residues on KDR/Flk-1 are autophosphorylated in response to VEGF-A. Thus, Takahashi performed experiments to better understand the signal transduction mechanism of KDR/Flk-1 and discovered that Y1214 of KDR/Flk-1 was not involved in the transduction of signals to the MAP kinase pathway. Accordingly, given the results obtained by Takahashi, one would not have been motivated to obtain a probe that that binds tyrosine residue Y1214 for detecting activation of KDR/Flk-1, since activation of KDR/Flk-1 does not involve the phosphorylation of tyrosine residue Y1214.

Harlow discloses methods of producing antibodies to any antigen of interest. However, Harlow does not cure the deficiencies of Takashi. Harlow neither teaches a probe that binds the tyrosine residue Y1214 of KDR/Flk-1 and detects activation of KDR/Flk-1 nor provides the motivation for obtaining such a probe.

Accordingly, neither the combination of the cited references nor each of the references individually renders the claimed invention obvious.

B. Claim 21 is rejected under 35 U.S.C. § 103(a) as being unpatentable over Takahashi *et al.* (Takahashi) in view of Harlow *et al.* (Harlow) as applied to claims 15-20 and 22-25 and further in view of U.S. Patent 6,204,011 ('011).

Claim 21 is directed to a kit for detecting the activation of KDR/Flk-1.

The deficiencies of Takahashi and Harlow are discussed above. U.S. Patent '011 does not cure the deficiencies of Takahashi and Harlow. U.S. Patent '011 is relied upon for teaching a kit comprising a human KDR protein. However, U.S. Patent '011 neither teaches a probe that

binds tyrosine residue Y1214 of KDR/Flk-1 and detects activation of KDR/Flk-1 nor provides the motivation for obtaining such a probe.

Accordingly, the cited references do not render the claimed invention obvious.

Conclusion

The foregoing amendments and remarks are being made to place the application in condition for allowance. Applicants respectfully request entry of the amendments, reconsideration, and the timely allowance of the pending claims. A favorable action is awaited. Should an interview be helpful to further prosecution of this application, the Examiner is invited to telephone the undersigned.

If there are any additional fees due in connection with the filing of this response, please charge the fees to our Deposit Account No. 50-0310. If a fee is required for an extension of time under 37 C.F.R. §1.136 not accounted for above, such an extension is requested and the fee should also be charged to our Deposit Account.

Respectfully submitted,
Morgan, Lewis & Bockius LLP

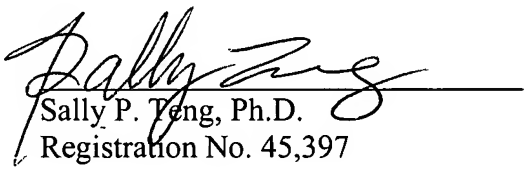

Sally P. Teng, Ph.D.
Registration No. 45,397

Date: April 4, 2007
Morgan, Lewis & Bockius LLP
Customer No. **09629**
1111 Pennsylvania Avenue, N.W.
Washington, D.C. 20004
Tel: 202-739-3000
Fax: 202-739-3001

PERGAMON

European Journal of Cancer 37 (2001) S16–S22

European Journal of Cancer

www.ejconline.com

The EGFR as a target for anticancer therapy—focus on cetuximab

J. Baselga*

Medical Oncology Service, Hospital General Universitari Vall d'Hevron, Paseo Vall d'Hebron 119-129, 08035, Barcelona, Spain

Received 7 March 2001; accepted 25 June 2001

Abstract

The anti-epidermal-growth-factor-receptor (EGFR) monoclonal antibody cetuximab specifically binds to the EGFR with high affinity, blocking growth-factor binding, receptor activation and subsequent signal-transduction events leading to cell proliferation. Preclinical studies, both *in vitro* and *in vivo*, have shown that cetuximab enhances the antitumour effects of chemotherapy as well as radiotherapy by inhibiting cell proliferation, angiogenesis and metastasis and by promoting apoptosis. As of June 2000, 526 patients with advanced solid tumours were treated with cetuximab in phase I/II clinical trials. Analysis of the results of three phase I trials showed that cetuximab has non-linear pharmacokinetics, with saturation of drug-elimination pathways occurring at doses between 200 and 400 mg/m^2. Adverse-event data for 239 patients across most of the completed or ongoing phase I–III trials indicated that the antibody was generally well tolerated. Cetuximab has been evaluated both alone and in combination with radiotherapy and various cytotoxic chemotherapeutic agents in a series of phase I/II studies that primarily treated patients with either head and neck or colorectal cancer. Although not a primary objective of these studies, clinical responses to cetuximab were observed in many patients who had previously failed chemotherapy and/or radiotherapy or were otherwise unlikely to achieve a therapeutic outcome. Based on these promising results, additional phase II and phase III trials are currently underway in head and neck and colorectal cancer.

Keywords: Antibodies; Monoclonal; Antineoplastic agents; Chimeric proteins; Cisplatin; Colorectal neoplasms; Drug; head and neck neoplasms; Receptor, Epidermal growth factor

1. Introduction

Decades of research investigating the molecular basis of cancer have produced a new generation of promising therapies designed to target specific molecular processes that promote tumour growth and survival. One of the first important milestones in the development of these novel antitumour agents was the concept of therapy based on inhibiting activation of the epidermal growth factor receptor (EGFR). The EGFR is a transmembrane receptor tyrosine kinase stimulated by growth factors, such as transforming growth factor (TGF)-α or EGF, that bind to the extracellular domain of the receptor (reviewed in Ref. [1]; Fig. 1a). Ligand binding induces receptors to dimerise and activates the intracellular kinase domain present on each receptor, resulting in phosphorylation of tyrosine residues on each member of the receptor pair. Signalling complexes then form in the cytoplasm and activate gene transcription, which in turn induces responses such as cell proliferation. Ultimately, receptor–ligand complexes are internalised and the signal is terminated.

The concept of the EGFR as a therapeutic target developed from several key observations made both at the laboratory bench and in the clinic. First, preclinical studies showed that EGFR activation promotes multiple tumorigenic processes, stimulating proliferation, angiogenesis and metastasis as well as protecting cells from apoptosis (reviewed in Ref. [2]). In addition, Sato and colleagues [3] found that monoclonal antibodies (MAbs) directed against the EGFR inhibited EGF-induced cell proliferation. Finally, clinical evaluations showed that many different types of solid tumours exhibit elevated levels of EGFR and/or its ligands, both of which are often associated with aggressive disease and poor patient outlook [4].

This has led to the development of a number of anti-EGFR strategies that target different components of the EGFR signalling network or cells that express EGFRs.

* Tel.: +34-93-274-6077; fax: +34-93-274-6059.
E-mail address: baselga@hg.vhebron.es (J. Baselga).

0959-8049/01/S - see front matter
PII: S0959-8049(01)00233-7

For example, tyrosine-kinase inhibitors block signal transduction by inhibiting the intrinsic kinase activity of the EGFR, while ligand–toxin conjugates activate EGFRs and then, when the ligand and its toxic cargo are internalised, kill EGFR-expressing cells. Antisense approaches are also being developed to inhibit the synthesis of growth factors or their receptors. This review focuses on one of these therapeutic strategies—using anti-EGFR MAbs to block EGFR function.

2. Cetuximab—a chimeric anti-EGFR MAb

Cetuximab (also known as C225) is a chimeric MAb that specifically binds to the EGFR with high affinity, preventing the ligand from interacting with the receptor (Fig. 1b). It has a higher affinity for the EGFR than either TGF-α or EGF and effectively blocks ligand-induced EGFR phosphorylation [5]. Preclinical studies have shown that cetuximab also inhibits growth-factor-induced activation of the downstream mitogen-activated protein kinase (MAPK). There is a strong correlation between cetuximab concentrations sufficient to block MAPK activation and those that inhibit cell proliferation [6], raising the possibility that MAPK phosphorylation may serve as a useful pharmacodynamic marker in clinical studies.

In addition to preventing ligand from binding to the receptor, there is also evidence suggesting that cetuximab promotes receptor internalisation [7]. This may reduce the number of receptors available to interact with ligand on the cell surface. Recent studies with trastuzumab (Herceptin®, Roche), an antibody specific for the related HER2 receptor, have shown that trastuzumab stimulates both the internalisation and degradation of HER2 receptors [8]. It is possible that cetuximab has similar effects on the metabolism of EGFRs.

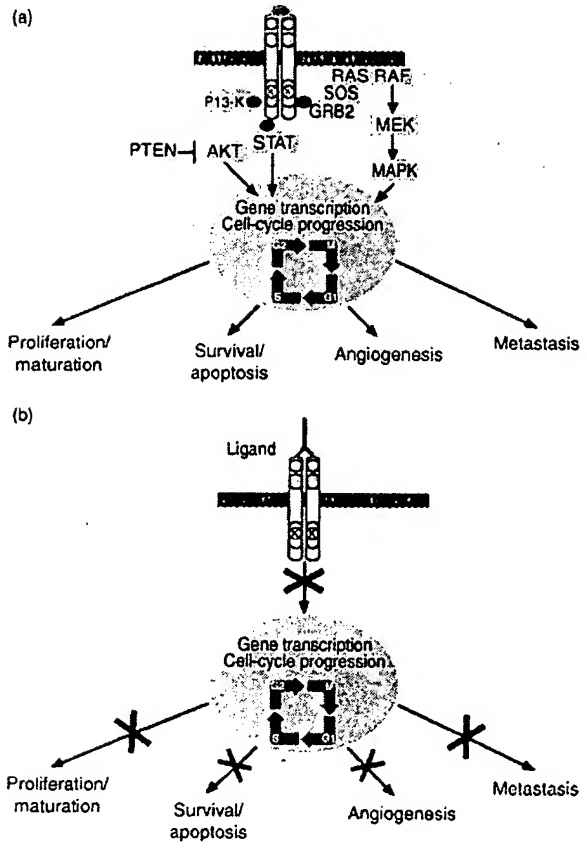

Fig. 1. Epidermal growth factor receptor (EGFR) signal transduction and cetuximab. (a) EGFR signal transduction is initiated when growth factor induces receptor dimerisation and phosphorylation. A transient signalling pathway composed of effector and adapter proteins forms in the cytoplasm and activates gene transcription. The EGFR signalling network then stimulates multiple cellular responses including proliferation, survival, angiogenesis and metastasis. MAPK, mitogen-activated protein kinase; PI3K, phosphatidyl inisitol-3-phosphate kinase. (b) The chimeric anti-EGFR monoclonal antibodies, cetuximab, binds to the EGFR with high affinity, blocking growth factors from both accessing the receptor and stimulating EGFR signal transduction pathways.

3. Cetuximab—mechanism of action

3.1. Cell-cycle progression

The antitumour activity of cetuximab has been attributed to several distinct mechanisms. Both cetuximab and M225, its murine progenitor, inhibit cell-cycle progression in many cell lines, causing cells to arrest in the G1 gap phase that occurs prior to DNA synthesis. An elegant series of experiments has shown that anti-EGFR antibody treatment causes an increase in the expression of the cell-cycle inhibitor $p27^{kip1}$ [9–11]. This in turn results in an increase in the formation of inhibitory $p27^{kip1}$–Cdk2 complexes which prevent cells from exiting the G1 phase of the cell cycle [9,10]. Similar antiproliferative effects have been observed *in vivo*, as cetuximab treatment led to an increase in $p27^{kip1}$ levels and a reduction in proliferating cell nuclear antigen (PCNA) expression in human tumour xenografts in nude mice [12].

3.2. Angiogenesis and metastasis

There is a growing body of data characterising cetuximab's anti-angiogenic properties, which were first reported by Petit and colleagues [13]. This group found that established A431 tumour xenografts treated with cetuximab displayed a significant decrease in the production of angiogenic factors, and these data have since been confirmed with additional tumour cell lines [14,15]. For example, in cultured transitional bladder carcinoma cells, cetuximab inhibited EGF-induced secretion of angiogenic factors in a dose-dependent manner. More pronounced effects were observed in the absence of

EGF stimulation in human tumour xenografts. In this study, the expression of vascular endothelial growth factor (VEGF), basic fibroblast growth factor (bFGF) and interleukin (IL)-8 was correlated with microvessel density, and cetuximab therapy was associated with a decrease in angiogenic factors as well as a decrease in the number of microvessels [14]. There is also evidence indicating that cetuximab therapy inhibits tumour-cell invasion and metastasis. For example, Perrotte and colleagues [14] found that cetuximab therapy significantly inhibited lung metastasis in mice with established human tumour xenografts. While all of the control animals had lymph-node metastases and 40% had lung metastases, none of the cetuximab-treated animals had either type of metastasis. Cetuximab and similar antibodies directed against the external region of the EGFR have also been shown to inhibit the expression and activity of several matrix metalloproteinases (MMPs) that play a key role in tumour-cell adhesion, including the gelatinase MMP-9. Several studies have correlated this antibody-mediated decrease in MMP production with both a significant reduction in *in-vitro* tumour-cell invasion and the inhibition of tumour growth and metastasis in nude mice [16–18]. These inhibitory effects on the invasion, metastasis and angiogenesis of cancer cells may explain why cetuximab treatment is often more effective *in vivo* than *in vitro*.

3.3. Apoptosis

Cetuximab has also been shown to influence apoptosis. Cell survival is dependent, in part, upon the ratio of Bax, which promotes apoptosis, and Bcl-2, which protects cells from apoptosis [19]. Several reports have shown that treatment with cetuximab or similar anti-EGFR antibodies may alter the balance of Bax and Bcl-2 expression. In DiFi human colon carcinoma cells which express high levels of EGFR, cetuximab treatment induced programmed cell death [20]. In these cells, anti-EGFR antibodies caused an increase in the expression of Bax [21] and activated multiple apoptotic caspases [22]. Similarly, in a squamous-cell carcinoma (SCC) cell line, cetuximab treatment led to elevated Bax and decreased Bcl-2 expression and a corresponding increase in the frequency of apoptotic cells [11]. In addition, when cetuximab was applied to breast adenocarcinoma cells, an increase in the inactive phosphorylated form of Bcl-2 was observed [23]. Nevertheless, cetuximab treatment alone was not sufficient to induce cells to undergo programmed cell death and generally had cytostatic effects on cell growth in most of the tumour cell lines that have been studied to date [12]. In combination with several chemotherapeutic agents, however, cetuximab has been shown to increase the incidence of human tumour-cell apoptosis both *in vitro* and *in vivo* in a number of model systems [15,23–26]. It is not yet entirely clear whether the combination of radiotherapy and cetuximab similarly promote programmed cell death *in vivo*.

3.4. Enhancement of the antitumour effects of chemotherapy and radiotherapy

In addition to influencing cellular growth and survival, a number of preclinical studies have shown that cetuximab also potentiates the antitumour effects of chemotherapeutic agents. The synergistic effects of anti-EGFR antibody and chemotherapy (CTX) were first reported by Aboud-Pirak and colleagues [27]. In this study, the combination of anti-EGFR antibody plus cisplatin produced significantly greater growth inhibition of KB oral epidermoid carcinoma-cell xenografts in mice than either treatment alone. Subsequent studies have shown a similar enhancement of antitumour effects in a variety of cancer types. For example, one investigation [28] showed that the maximum tolerated dose of doxorubicin did not inhibit the growth of well-established A431-cell xenografts and that M225 treatment alone only partially reduced tumour growth. In contrast, combined treatment with doxorubicin and M225 produced a marked inhibition of growth, and tumours were eradicated in 40% of the animals [28]. Even more dramatic effects were reported by Fan and colleagues [29] who showed that the combination of M225 and cisplatin completely eradicated well-established A431 cell xenografts in 85% of animals. Furthermore, mice with regressed tumours remained tumour-free for over 6 months, indicating that the therapeutic benefits persisted long after cessation of treatment. In addition to cisplatin and doxorubicin, cetuximab has also been shown to enhance the anti-tumour activity of gemcitabine [15], docetaxel [23,30], paclitaxel [26] and topotecan [25]. Striking synergistic anti-tumour effects on human epidermoid cancer-cell xenografts have also been observed when cetuximab treatment is combined with radiotherapy (RTX; Fig. 2) [31,32].

4. Clinical studies

The efficacy of cetuximab in preclinical tumour models has led to the initiation of many clinical trials. As of June 2000, 526 patients with various tumour types had participated in clinical studies with cetuximab (Table 1). Early phase I dose-ranging trials demonstrated that cetuximab displays non-linear, dose-dependent pharmocokinetics that are not altered by the co-administration of cisplatin. Saturation of drug-elimination pathways occurred at doses between 200 and 400 mg/m^2, and the current recommended dose level is an initial loading dose of 400mg/m^2 followed by weekly maintenance infusions of 200 mg/m^2 [33].

Table 1
Summary of clinical experience with cetuximab

Clinical studies	Completed or ongoing studies[a]	Cancer	Patients treated[a]
Phase I/II, dose-ranging	8	Breast EGFR$^+$-tumours Lung Prostate SCCHN	132
Phase II/III	7	CRC Pancreatic Renal-cell SCCHN	394
Total	15		526

CRC, colorectal cancer; SCCHN, squamous-cell carcinoma of the head and neck; EGFR$^-$, epidermal growth factor receptor positive.
[a] As of June 2000.

4.1. Safety and tolerability

In general, cetuximab appears to be well tolerated, both alone and in combination with CTX or RTX. As of June 2000, safety data were available for 189 patients treated with cetuximab, and drug-related adverse events (AEs) were usually mild to moderate. Grades 1–4 AEs were experienced by 62% of patients, with grades 3–4 AEs reported by 12% of patients. The most common AEs were asthenia (18%), fever (16%), nausea (16%) and acne (15%). Allergic reactions (4% grades 3–4) and acne-like rash (11% grades 3–4) were the most clinically relevant AEs reported. Allergic reactions occurred only during the first infusion. Patients with allergic reactions responded to standard treatments, and subsequent recurrences were controlled with prophylactic antihistamine therapy and increased infusion time. Acne-like rash is now considered to be an expected event, thought to be due to the presence of EGFRs in the epidermis. The rash is not dose-limiting and resolves fully upon cessation of treatment [34].

As cetuximab is a chimeric MAb, it has the potential to stimulate the production of human antichimeric antibodies (HACAs) which may interfere with therapy. However, HACAs were detected in only 3% (4/120) of patients, with neutralising antibodies present in 3 cases.

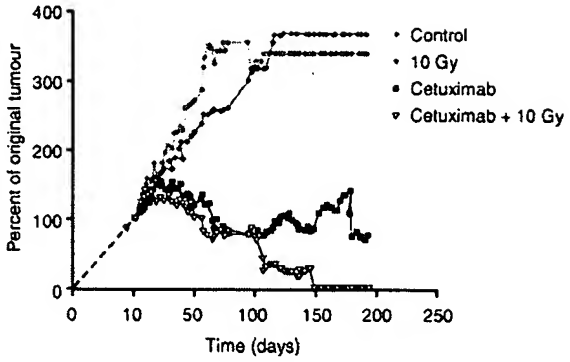

Fig. 2. Synergistic effects of anti-epidermal growth factor receptor (EGFR) antibodies plus radiation on A431 tumour xenografts. Human squamous carcinoma A431 cells were implanted subcutaneously in nude mice. Thirteen days later groups of 8–18 mice received either 10 Gy of ^{60}Co irradiation alone (◆), 10 Gy followed 4 h later by intraperitoneal injections of cetuximab (1 mg) with additional injections administered twice weekly for 4 weeks (▼), cetuximab injections only (■) or no treatment (●). Tumour surface area at each time point is shown as the median for each treatment group. Combination therapy with cetuximab and radiation was associated with a significant increase in the rate of tumour regression. Reproduced with permission from *Cancer Biother Radiopharm* [31].

Patients with detectable HACAs did not experience allergic or anaphylactic reactions, and HACA responses had no clinically limiting effect following weekly infusion of cetuximab [35].

4.2. Cetuximab combined with CTX—evidence of efficacy

More than 100 patients with squamous-cell carcinoma of the head and neck (SCCHN), colorectal cancer (CRC), non-small cell lung cancer (NSCLC) and androgen-independent prostate cancer have received cetuximab in combination with CTX in early phase I and II studies, and in many cases clinical responses have been observed in heavily pretreated patients (Table 2). For example, in a phase I study with advanced SCCHN patients, 67% (6/9) experienced clinical responses to cetuximab combined with cisplatin [36]. Although response to therapy was not a primary objective of this study, this evidence of efficacy—particularly in 3 patients who were previously treated with cisplatin—

Table 2
Response to cetuximab plus CTX

Study phase	Indication	Treatment	Response rates	Reference
Phase I	Advanced SCCHN and NSCLC	Cetuximab + cisplatin	58% (11/19) SD	Baselga and colleagues [33]
Phase I	Advanced SCCHN	Cetuximab + cisplatin	67% (6/9) PR + CR	Mendelsohn and colleagues [36]
Phase I/II	Androgen-independent prostate cancer	Cetuximab + doxorubicin	5% (1/19) SD; 5% (1/19) PR	Slovin and colleagues [38]
Phase II	Refractory SCCHN and CRC	Cetuximab + CTX	22% (14/63) PR + CR	Rubin and colleagues [37]; ImClone Systems Inc. data on file

CRC, colorectal cancer; CR, complete response; CTX, chemotherapy; NSCLC, non-small cell lung cancer; PR, partial response; SD, stable disease; SCCHN, squamous-cell carcinoma of the head and neck.

was promising and led to the initiation of several additional studies. Early phase II studies combining cetuximab with CTX have also yielded positive preliminary results. As of October 2000, 63 patients with SCCHN or CRC who had previously failed surgery, RTX and/or CTX received cetuximab plus either cisplatin or CPT-11. Of the patients with cisplatin-unresponsive SCCHN, 26% (6/23) experienced clinical responses (Fig. 3), and 20% (8/40) of patients with CPT-11-refractory CRC experienced partial or complete responses ([37]; ImClone Systems Inc., data on file). In total, 14 patients experienced clinical responses to cetuximab and a chemotherapeutic compound to which they had previously been resistant.

4.3. Cetuximab and RTX—evidence of efficacy

Promising results have also been obtained from clinical trials with cetuximab and RTX in SCCHN. In a recent phase I study, patients with advanced unresectable disease were treated with either conventional or hyperfractionated radiation combined with weekly doses of cetuximab (100–400 mg/m^2 loading dose and 100–250 mg/m^2 maintenance dose). Although all of the 15 evaluable patients had EGFR$^+$ tumours, which are associated with poor prognosis in SCCHN [39], complete responses were experienced by 87% (13/15) of patients, and the remaining patients (2/15) experienced partial responses [40].

Although caution should be used in drawing conclusions based on retrospective analysis, in the absence of data from comparative phase III studies it is useful to evaluate the response to cetuximab therapy with the data that is currently available. The results of the cetuximab and RTX study described above [40] compare favourably with those of previous trials that treated SCCHN patients with conventional or hyperfractionated RTX alone (Fig. 4a) [41–43]. Of the studies shown in Fig. 4(a), the patients participating in the cetuximab trial had the poorest prognosis, as all of the patients had unresectable disease and the majority (80%) of patients had oropharyngeal carcinomas [40]. The study reported by Zakotnik and colleagues [42] contained the most similar patient population in terms of size and the incidence of oropharyngeal carcinoma and unresectable disease. However, only 31% (10/32) of the patients treated with RTX alone achieved complete responses. In contrast, 87% (13/15) of the patients who received cetuximab plus RTX experienced complete responses, suggesting that cetuximab may enhance the efficacy of RTX. When other response parameters, such as 2-year disease-free survival rates were examined, the combination of cetuximab and RTX also compared well with historical controls (Fig. 4b).

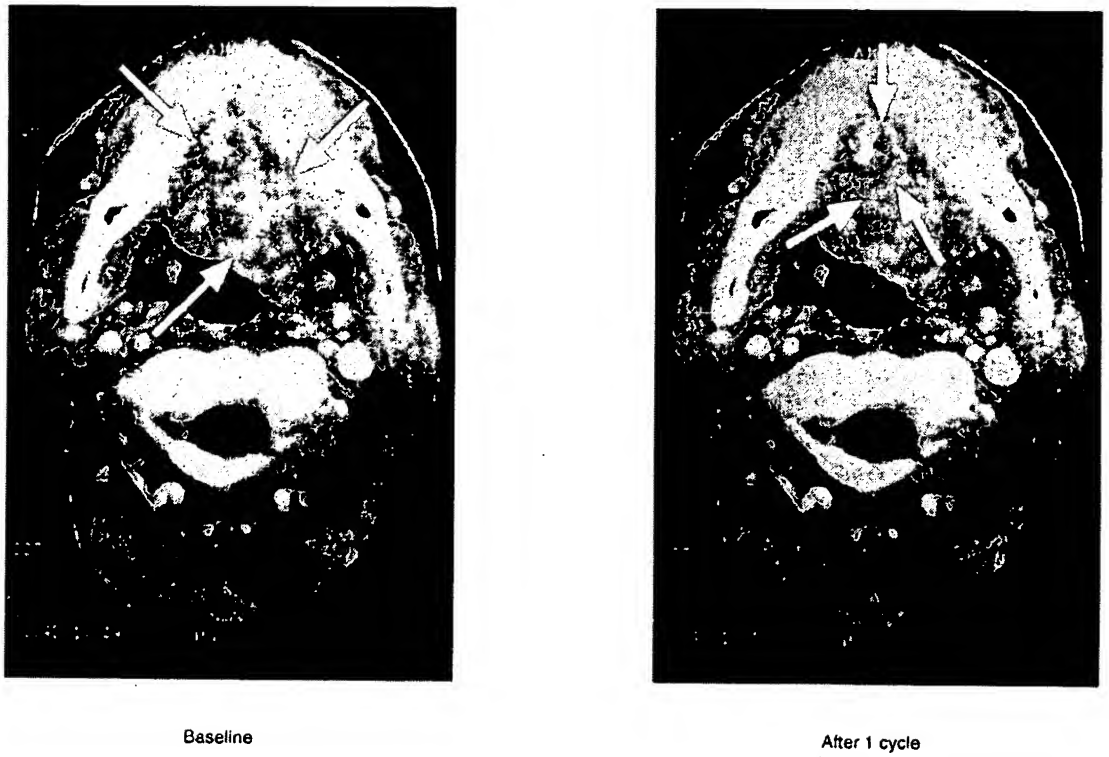

Fig. 3. Response to cetuximab plus cisplatin in squamous cell carcinoma of the head and neck (SCCHN). This patient with recurrent SCCHN had previously received surgery, radiotherapy (RTX), cisplatin, 5-fluorouracil (5-FU) and paclitaxel. After one 7-week cycle of cetuximab (400 mg/m^2 loading dose followed by weekly 250 mg/m^2 maintenance doses) plus cisplatin (100 mg/m^2 every 3 weeks), the patient experienced a partial response. Reproduced with kind permission from J. Mendesohn.

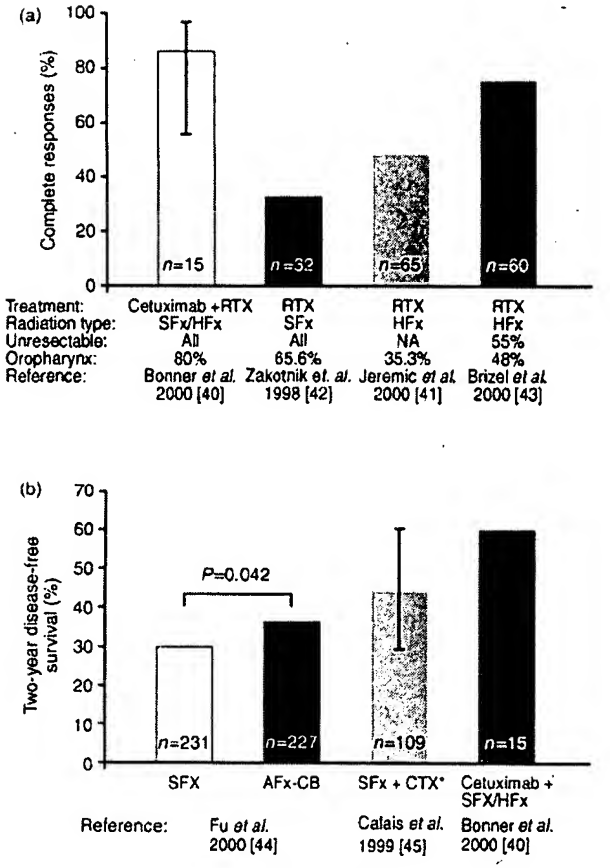

Fig. 4. Cetuximab plus radiotherapy (RTX) in squamous cell carcinoma of the head and neck (SCCHN)—response and survival rates compared with historical controls. (a) The complete response rate to cetuximab plus standard-fractionation (SFx) or hyperfractionation (HFx) RTX compared with past studies with RTX alone. Based on these encouraging results, phase III studies have been initiated to directly compare responses to cetuximab plus RTX versus RTX alone in SCCHN. Bar = confidence interval. NA, not available. (b) The 2-year disease-free survival rates of SCCHN patients treated with cetuximab plus RTX compare favourably with those of previous studies with SFx or accelerated fractionation with concomitant-boost (AFx-CB) RTX alone. *3-year disease-free survival (bar = 95% confidence interval).

5. Conclusion

Phase I/II trials with cetuximab have produced promising clinical results in SCCHN and CRC, particularly when cetuximab was administered in combination with CTX or RTX. Remarkably, complete responses were even observed in heavily pre-treated patients with particularly poor prognoses ([36,37,40]; ImClone Systems Inc., data on file]). In the light of these results, the clinical development of cetuximab is continuing with a number of phase II and III studies designed to determine whether cetuximab enhances the efficacy of conventional CTX or RTX in patients with SCCHN and CRC.

References

1. Klapper LN, Kirschbaum MH, Sela M, Yarden Y. Biochemical and clinical implications of the ErbB/HER signaling network of growth factor receptors. *Adv Cancer Res* 2000, **77**, 25–79.
2. Huang SM, Harari PM. Epidermal growth factor receptor inhibition in cancer therapy: biology, rationale and preliminary clinical results. *Invest New Drugs* 1999, **17**, 259–269.
3. Sato JD, Kawamoto T, Le AD, Mendelsohn J, Polikoff J, Sato GH. Biological effects in vitro of monoclonal antibodies to human epidermal growth factor receptors. *Mol Biol Med* 1983, **1**, 511–529.
4. Salomon DS, Bradt R, Ciardiello F, Normanno N. Epidermal growth factor-related peptides and their receptors in human malignancies. *Critical Rev Oncol/Hematol* 1995, **19**, 183–232.
5. Goldstein NI, Prewett M, Zuklys K, Rockwell P, Mendelsohn J. Biological efficacy of a chimeric antibody to the epidermal growth factor receptor in a human tumor xenograft model. *Clin Cancer Res* 1995, **1**, 1311–1318.
6. Baselga J, Cañadas M, Codony J, *et al.* Activated epidermal growth factor receptor: studies in head and neck tumors and tumor cell lines after exposure to ligand and receptor tyrosine-kinase inhibitors. *Proc Am Soc Clin Oncol* 1999 (abstr 2392).
7. Sunada H, Magun BE, Mendelsohn J, MacLeod CL. Monoclonal antibody against epidermal growth factor receptor is internalized without stimulating receptor phosphorylation. *Proc Natl Acad Sci USA* 1986, **83**, 3825–3829.
8. Klapper LN, Waterman H, Sela M, Yarden Y. Tumor-inhibitory antibodies to HER-2/ErbB-2 may act by recruiting c-Cbl and enhancing ubiquitination of HER-2. *Cancer Res* 2000, **60**, 3384–3388.
9. Wu X, Rubin M, Fan Z, *et al.* Involvement of p27Kip1 in G1 arrest mediated by an anti-epidermal growth factor receptor monoclonal antibody. *Oncogene* 1996, **12**, 1397–1403.
10. Peng D, Fan Z, Lu Y, DeBlasio T, Scher H, Mendelsohn J. Anti-epidermal growth factor receptor monoclonal antibody 225 up-regulates p27Kip1 and induces G1 arrest in prostatic cancer cell line DU145. *Cancer Res* 1996, **56**, 3666–3669.
11. Huang SM, Bock JM, Harari PM. Epidermal growth factor receptor blockade with C225 modulates proliferation, apoptosis, and radiosensitivity in squamous cell carcinomas of the head and neck. *Cancer Res* 1999, **59**, 1935–1940.
12. Mendelsohn J. Jeremiah Metzger Lecture. Targeted cancer therapy. *Trans Am Clin Climatol Assoc* 2000, **111**, 95–110.
13. Petit AMV, Rak J, Hung MC, *et al.* Neutralizing antibodies against epidermal growth factor and ErbB-2/neu receptor tyrosine kinases down-regulate vascular endothelial growth factor production by tumor cells in vitro and in vivo. *Am J Pathol* 1997, **151**, 1523–1530.
14. Perrotte P, Matsumoto T, Inoue K, *et al.* Anti-epidermal growth factor receptor antibody C225 inhibits angiogenesis in human transitional cell carcinoma growing orthotopically in nude mice. *Clin Cancer Res* 1999, **5**, 257–265.
15. Bruns CJ, Harbison MT, Davis DW, *et al.* Epidermal growth factor receptor blockade with C225 plus gemcitabine results in regression of human pancreatic carcinoma growing orthotopically in nude mice by antiangiogenic mechanisms. *Clin Cancer Res* 2000, **6**, 1936–1948.
16. O-Charoenrat P, Rhys-Evans P, Modjtahedi H, Court W, Box G, Eccles S. Overexpression of epidermal growth factor receptor in human head and neck squamous carcinoma cell lines correlates with matrix metalloproteinase-9 expression and in vitro invasion. *Int J Cancer* 2000, **86**, 307–317.
17. O-Charoenrat P, Rhys-Evans P, Court WJ, Box GM, Eccles SA. Differential modulation of proliferation, matrix metalloproteinase expression and invasion of human head and neck squamous carcinoma cells by c-erbB ligands. *Clin Exp Metastasis* 1999, **17**, 631–639.

18. Matsumoto T, Perrotte P, Bar-Eli M, *et al.* Blockade of EGF-R signaling with anti-EGFR monoclonal antibody (Mab) C225 inhibits matrix metalloproteinase-9 (MMP-9) expression and invasion of human transitional cell carcinoma (TCC) in vitro and in vivo. *Proc Am Assoc Cancer Res* 1998, **39**, 83.
19. Pepper C, Hoy T, Bentley DP. Bcl-2/Bax ratios in chronic lymphocytic leukaemia and their correlation with in vitro apoptosis and clinical resistance. *Br J Cancer* 1997, **76**, 935–938.
20. Wu X, Fan Z, Masui H, Rosen N, Mendelsohn J. Apoptosis induced by an anti-epidermal growth factor receptor monoclonal antibody in a human colorectal carcinoma cell line and its delay by insulin. *J Clin Invest* 1995, **95**, 1897–1905.
21. Mandal M, Adam L, Mendelsohn J, Kumar R. Nuclear targeting of Bax during apoptosis in human colorectal cancer cells. *Oncogene* 1998, **17**, 999–1007.
22. Liu B, Fang M, Schmidt M, Lu Y, Mendelsohn J, Fan Z. Induction of apoptosis and activation of the caspase cascade by anti-EGF receptor monoclonal antibodies in DiFi human colon cancer do not involve the c-jun N-terminal kinase activity. *Br J Cancer* 2000, **82**, 1991–1999.
23. Tortora G, Caputo R, Pomatico G, *et al.* Cooperative inhibitory effect of novel mixed backbone oligonucleotide targeting protein kinase A in combination with docetaxel and anti-epidermal growth factor-receptor antibody on human breast cancer cell growth. *Clin Cancer Res* 1999, **5**, 875–881.
24. Prewett M, Rockwell P, Rose C, Zuklys K, Goldstein NI. Altered cell cycle distribution and cyclin-CDK protein expression in A431 epidermoid carcinoma cells treated with doxorubicin and a chimeric monoclonal antibody to the epidermal growth factor receptor. *Molec Cell Differen* 1996, **4**, 167–186.
25. Ciardiello F, Bianco R, Damiano V, *et al.* Antitumor activity of sequential treatment with topotecan and anti-epidermal growth factor receptor monoclonal antibody C225. *Clin Cancer Res* 1999, **5**, 909–916.
26. Inoue K, Shuin T, Hicklin DJ, *et al.* Paclitaxel enhances the effect of treatment of metastatic human transitional cell carcinoma with the anti-epidermal growth factor receptor monoclonal antibody C225. *Proc Am Assoc Cancer Res* 2000, **41**, 529 (abstr 3372).
27. Aboud-Pirak E, Hurwitz E, Pirak ME, Bellot F, Schlessinger J, Sela M. Efficacy of antibodies to epidermal growth factor receptor against KB carcinoma in vitro and in nude mice. *J Natl Cancer Inst* 1988, **80**, 1605–1611.
28. Baselga J, Norton L, Masui H, *et al.* Antitumor effects of doxorubicin in combination with anti-epidermal growth factor receptor monoclonal antibodies. *J Natl Cancer Inst* 1993, **85**, 1327–1333.
29. Fan Z, Baselga J, Masui H, Mendelsohn J. Antitumor effect of anti-epidermal growth factor receptor monoclonal antibodies plus cis-diamminedichloroplatinum on well established A431 cell xenografts. *Cancer Res* 1993, **53**, 4637–4642.
30. Prewett MC, Overholser J, Hooper A, Waksal H, Hicklin DJ. Anti-EGF receptor monoclonal antibody IMC-C225 combined with docetaxel inhibits growth of renal cell carcinoma tumors in a nude mouse model. *Proc Am Assoc Cancer Res* 2000, **41**, 811 (abstr 5149).
31. Saleh MN, Raisch KP, Stackhouse MA, *et al.* Combined modality therapy of A431 human epidermoid cancer using anti-EGFr antibody C225 and radiation. *Cancer Biother Radiopharm* 1999, **14**, 451–463.
32. Milas L, Mason K, Hunter N, *et al.* In vivo enhancement of tumor radioresponse by C225 anti-epidermal growth factor receptor antibody. *Clin Cancer Res* 2000, **6**, 701–708.
33. Baselga J, Pfister D, Cooper MR, *et al.* Phase I studies of anti-epidermal growth factor receptor chimeric antibody C225 alone and in combination with cisplatin. *J Clin Oncol* 2000, **18**, 904–914.
34. Cohen RB, Falcey JW, Paulter VJ, Fetzer KM, Waksal HW. Safety profile of the monoclonal antibody (MOAB) IMC-C225, an anti-epidermal growth factor receptor (EGFR) used in the treatment of EGFR-positive tumors. *Proc Am Soc Clin Oncol* 2000 (abstr 1862).
35. Khazaeli MB, LoBuglio AF, Falcey JW, Paulter VJ, Fetzer MK, Waksal HW. Low immunogenicity of a chimeric monoclonal antibody (MOAB), IMC-C225, used to treat epidermal growth factor receptor-positive tumors. *Proc Am Soc Clin Oncol* 2000 (abstr 808).
36. Mendelsohn J, Shin DM, Donato N, *et al.* A phase I study of chimerized anti-epidermal growth factor receptor (EGFr) monoclonal antibody, C225, in combination with cisplatin (CDDP) in patients (PTS) with recurrent head and neck squamous cell carcinoma (SCC). *Proc Am Soc Clin Oncol* 1999, 18 (abstr 1502).
37. Rubin MS, Shin DM, Pasmantier M, *et al.* Monoclonal antibody (MOAB) IMC-C225, an anti-epidermal growth factor receptor (EGFR), for patients (PTS) with EGFR-positive tumors refractory to or in relapse from previous therapeutic regimens. *Proc Am Soc Clin Oncol* 2000, (abstr 1860).
38. Slovin SF, Kelly WK, Cohen R, *et al.* Epidermal growth factor receptor (EGFr) monoclonal antibody (MoAb) C225 and doxorubicin (DOC) in androgen-independent (AI) prostate cancer (PC): results of a phase Ib/IIa study. *Proc Am Soc Clin Oncol* 1997, 16, 311a (abstr 1108).
39. Grandis JR, Melhem MF, Gooding WE, *et al.* Levels of TGF-a and EGFR protein in head and neck squamous cell carcinoma and patient survival. *J Natl Cancer Ins* 1998, **90**, 824–832.
40. Bonner JA, Ezekiel MP, Robert F, Meredith RF, Spencer SA, Waksal HW. Continued response following treatment with IMC-C225, an EGFr MoAb, combined with RT in advanced head and neck malignancies. *Proc Am Soc Clin Oncol* 2000 (abstr 5F).
41. Jeremic B, Shibamoto Y, Milicic B, *et al.* Hyperfractionated radiation therapy with or without concurrent low-dose daily cisplatin in locally advanced squamous cell carcinoma of the head and neck: a prospective randomized trial. *J Clin Oncol* 2000, **18**, 1458–1464.
42. Zakotnik B, Smid L, Budihna M, *et al.* Concomitant radiotherapy with mitomycin C and bleomycin compared with radiotherapy alone in inoperable head and neck cancer. *Int J Radiat Oncol Biol Phys* 1998, **41**, 1121–1127.
43. Brizel DM, Wasserman TH, Henke M, *et al.* Phase III randomized trial of amifostine as a radioprotector in head and neck cancer. *J Clin Oncol* 2000, **18**, 3339–3345.
44. Fu KK, Pajak TF, Trotti A, *et al.* A Radiation Therapy Oncology Group (RTOG) phase III randomized study to compare hyperfractionation and two variants of accelerated fractionation to standard fractionation radiotherapy for head and neck squamous cell carcinomas: first report of RTOG 9003. *Int J Radiat Oncol Biol Phys* 2000, **48**, 7–16.
45. Calais G, Alfonsi M, Bardet E, *et al.* Randomized trial of radiation therapy versus concomitant chemotherapy and radiation therapy for advanced-stage oropharynx carcinoma. *J Natl Cancer Inst* 1999, **91**, 2081–2086.

UAB MEDIA RELATIONS

Finally, New Treatments Approved for Colon Cancer

Media Contact:
Hank Black
(205) 934-8938
E-mail:
hblack@uab.edu

HOME: UAB Media Relations

HEADLINE NEWS: Press Releases from UAB

HEADLINE NEWS ARCHIVE : Archived Press Releases from UAB

SEARCH: UAB Media Relations

STAFF: UAB Media Relations Contact Information

EXPERT LIST: Identify UAB Experts for Media Interviews

UAB NEWSWATCH: A Weekly Guide to News and Features

MEDIA: Contact Us

ABOUT UAB

REPORTER'S RESOURCES

VIDEO NEWS RELEASES: Streaming Video from UAB Broadcast News

UAB PEOPLE IN THE NEWS

LECTURES AT UAB

CALENDARS

UAB PUBLICATIONS

ATHLETICS at UAB

SITE MAP: UAB Media Relations

Posted on March 22, 2004 at 12:54 p.m.

Note to editors: UAB's Comprehensive Cancer Center played a major role in testing recently approved drugs for colon cancer. Dr. Albert F. LoBuglio is director of the Cancer Center.

By Albert F. LoBuglio, M.D.
Director, UAB Comprehensive Cancer Center
Evalina B. Spencer Professor of Oncology

BIRMINGHAM, AL — Colon cancer is the second leading cause of cancer death, claiming the lives of 57,000 Americans each year. Within the past month, the Food and Drug Administration (FDA) has approved two new drugs to treat patients with advanced stages of this disease — Erbitux and Avastin. What Alabamians may not know is that the UAB Comprehensive Cancer Center played an important role in the process that lead to approvals of these novel agents.

Before a drug receives FDA approval, it undergoes years of rigorous laboratory studies and patient trials. As the only comprehensive cancer center in a five-state area, the UAB Cancer Center is a national leader in such "bench-to-bedside" research, which provides our patients cutting-edge therapies unavailable elsewhere. The large number of patients enrolled in the studies of Erbitux and Avastin made the Cancer Center one of the major sites for both these pivotal clinical trials, which earned FDA approval for the drugs.

Because of our large contribution to the trials, the FDA carried out an intensive review of patient charts and research records at our Cancer Center. On February 12 Erbitux became the first monoclonal antibody approved for colon cancer. Avastin was approved February 26. (Avastin had another "first" — it's the only FDA-approved drug that works by preventing the formation of new blood vessels.) Today physicians across the United States are using these agents to shrink cancerous tumors. This is promising news for a population of patients who, until recent years, have had few treatment options.

It's no lucky break that the UAB Comprehensive Cancer Center has been an international leader in the development and research of the class of drugs to which Avastin and Eribitux belong. Called "monoclonal antibodies," such pharmaceutical agents are laboratory-produced molecules that bind to specific sites on tumor cells, interfering with tumor growth. Monoclonal antibody technology long has been one of the Cancer Center's priorities. Our investigators were the first in the world to administer the original monoclonal antibodies, and have worked for more than two decades designing and administering clinical trials using this approach.

In fact, the Cancer Center has been significantly involved with the study of every FDA-approved monoclonal antibody, including Rituxan and Zevalin, which are used to treat non-Hodgkin's lymphoma, and Herceptin, used to treat some types of breast cancer. We are currently developing several new promising monoclonal antibodies.

The success of the recent drug approvals, and all of our research endeavors, would not be possible without a dedicated team of physicians, scientists, nurses and staff working toward our common goal: improved quality-of-life and survival for patients with cancer. This goal extends throughout all of our research and patient care. It is our patients, and those treated elsewhere with these breakthrough drugs, who ultimately benefit from research at the UAB Comprehensive Cancer Center.

Albert F. LoBuglio, M.D.
Director, UAB Comprehensive Cancer Center
Evalina B. Spencer Professor of Oncology

FDA News

FOR IMMEDIATE RELEASE
P04-23
February 26, 2004

Media Inquiries: 301-827-6242
Consumer Inquiries: 888-INFO-FDA

FDA Approves First Angiogenesis Inhibitor to Treat Colorectal Cancer

FDA today approved Avastin (bevacizumab) as a first-line treatment for patients with metastatic colorectal cancer -- cancer that has spread to other parts of the body. Avastin, a monoclonal antibody, is the first product to be approved that works by preventing the formation of new blood vessels, a process known as angiogenesis. Avastin was shown to extend patients' lives by about five months when given intravenously as a combination treatment along with standard chemotherapy drugs for colon cancer (the "Saltz regimen" also known as IFL). IFL treatment includes ironotecan, 5-fluorouracil (5FU) and leucovorin.

Avastin is a genetically engineered version of a mouse antibody that contains both human and mouse components. (Antibodies are substances produced by the body's immune system to fight foreign substances.) Special technology also allows it to be produced in large quantities in the laboratory.

This new monoclonal antibody is believed to work by targeting and inhibiting the function of a natural protein called "vascular endothelial growth factor" (VEGF) that stimulates new blood vessel formation. When VEGF is targeted and bound to Avastin, it cannot stimulate the growth of blood vessels, thus denying tumors blood, oxygen and other nutrients needed for growth. Angiogenesis inhibitors such as Avastin have been studied, first in the laboratory and then in patients, for three decades with the hope they might prevent the growth of cancer. This is the first such product that has been proven to delay tumor growth and more importantly, significantly extend the lives of patients.

"The approval of Avastin is the result of many years of research and development exploring a promising new approach to fighting cancer, and it is one of a number of recent new treatments for colorectal cancer that taken together, have significantly improved the armamentarium for fighting this disease," said Mark B. McClellan, M.D., Ph.D., FDA Commissioner. "These medical achievements reflect the innovation of drug developers and the hard work of FDA's cancer review teams, and they are proof of the promise offered by biomedical innovation. The dedication of everyone involved in these efforts is making a real difference in the lives of cancer patients."

Colorectal cancer -- cancer of the colon or rectum -- is the third most common cancer affecting men and women in the U.S. and, according to the Centers for Disease Control and Prevention (CDC), is the second leading cause of cancer-related death. Colorectal cancer is also one of the most commonly diagnosed cancers in the U.S.; approximately 147,500 new cases were diagnosed in 2003.

The safety and efficacy of Avastin was primarily shown in a randomized, double-blind clinical trial of more than 800 patients with metastatic colorectal cancer designed to find out whether Avastin extended the lives of patients. Roughly half the patients received IFL, the standard chemotherapy combination, and the other half received Avastin once every two weeks in addition to IFL. Overall, patients given Avastin in combination with IFL survived about five months longer and the average time before tumors started regrowing or new tumors appeared was four months longer than patients receiving IFL alone. The overall response rate to the treatment was 45% compared to 35% for the control arm of the trial.

Serious, but uncommon, side-effects of Avastin include formation of holes in the colon (gastrointestinal perforation) generally requiring surgery and sometimes leading to intra-abdominal infections, impaired wound healing, and bleeding from the lungs or internally. Other, more common, side-effects are high blood pressure, tiredness, blood clots, diarrhea, decreased white blood cells (lowering immunity to diseases) headache, appetite loss and mouth sores.

Avastin is manufactured by Genentech, Inc., South San Francisco, Calif.

####

More information

1: Acta Pharmacol Sin. 2004 Oct;25(10):1292-8.

Links

Production of neutralizing monoclonal antibody against human vascular endothelial growth factor receptor II.

Li R, Xiong DS, Shao XF, Liu J, Xu YF, Xu YS, Liu HZ, Zhu ZP, Yang CZ.

State Key Laboratory of Experimental Hematology, Institute of Hematology, Chinese Academy of Medical Science and Peking Union Medical College,Tianjin 300020, China.

AIM: To prepare neutralizing monoclonal antibody (mAb) against extracellular immunoglobulin (Ig)-like domain III of vascular endothelial growth factor receptor KDR and study its biological activity. METHODS: Soluble KDR Ig domain III (KDR-III) fusion protein was expressed in E Coli and purified from the bacterial periplasmic extracts via an affinity chromatography. Monoclonal antibodies against KDR-III were prepared by hybridoma technique. ELISA and FACS analysis were used to identify its specificity. Immunoprecipitation and [3H]-thymidine incorporation assay were also used to detect the activity of anti-KDR mAb blocking the phosphorylation of KDR tyrosine kinase receptor and the influence on vascular endothelial growth factor-induced mitogenesis of human endothelial cells. RESULTS: A monoclonal antibody, Ycom1D3 (IgG1), was generated from a mouse immunized with the recombinant KDR-III protein. Ycom1D3 bound specifically to both the soluble KDR-III and the cell-surface expressed KDR. Ycom1D3 effectively blocked VEGF/KDR interaction and inhibited VEGF-stimulated KDR activation in human endothelial cells. Furthermore, the antibody efficiently neutralized VEGF-induced mitogenesis of human endothelial cells. CONCLUSION: Our results suggest that the anti-KDR mAb, Ycom1D3, has potential applications in the treatment of cancer and other diseases where pathological angiogenesis is involved. Copyright 2004 Acta Pharmacologica Sinica

PMID: 15456530 [PubMed - indexed for MEDLINE]

Acta Pharmacologica Sinica

A Phase I Study of Anti-Kinase Insert Domain-containing Receptor Antibody, IMC-1C11, in Patients with Liver Metastases from Colorectal Carcinoma[1]

James A. Posey,[2] Thian C. Ng, Baolian Yang, M. B. Khazaeli, Mark D. Carpenter, Floyd Fox, Mike Needle, Harlan Waksal, and Albert F. LoBuglio

Departments of Medicine and Radiation Oncology, Division of Hematology/Oncology, Comprehensive Cancer Center, University of Alabama at Birmingham, Birmingham, Alabama 35294-3300 [J. A. P., T. C. N., B. Y., M. B. K., M. D. C., A. F. L.], and Imclone Systems, Somerville, New Jersey 08876 [F. F., M. N., H. W.]

ABSTRACT

Purpose: **Angiogenesis plays an important role in colorectal cancer progression. Stimulation of vascular endothelial growth factor receptor (VEGFR), a transmembrane glycoprotein, results in endothelial mitogenesis. Within this family of receptors, VEGFR 2/kinase-insert-domain-containing receptor (KDR) appear to be principally upregulated during tumorigenesis. A chimeric anti-KDR antibody, IMC-1C11, blocks VEGFR-KDR interaction and inhibits VEGFR-induced endothelial cell proliferation. This trial seeks to assess the safety, tolerability and feasibility of targeting an important pathway in tumorigenesis.**

Experimental Design: **In a dose-escalation, single-agent study of IMC-1C11, we enrolled 14 patients with colorectal carcinoma and hepatic metastases. Safety-, pharmacokinetic-, immunogenicity-, and magnetic resonance imaging-assessed alteration of vascular effects of IMC-1C11 were evaluated in this trial. IMC-1C11 was infused weekly at 0.2 mg/kg (n = 3), 0.6 mg/kg (n = 4), 2.0 mg/kg (n = 3), and 4.0 mg/kg (n = 4) for 4 weeks, which constituted a cycle.**

Results: **No grade-3 or -4 IMC-1C11-related toxicities were observed. Minor grade-1 bleeding events were observed in four patients [0.2 mg/kg (n = 1) and 0.6 mg/kg (n = 3)]. Each resolved quickly and required no intervention. The starting dose of IMC-1C11 was selected to achieve a C_{max} of ~5 μg/ml. This concentration prevented KDR phosphorylation *in vitro*. Pharmacokinetic analysis demonstrated that the plasma $t_{1/2}$ and C_{max} were dose dependent with a plasma $t_{1/2}$ of 67 ± 3 h at the 4-mg/kg dose level. Human antichimeric antibodies were detected in 7 of 14 patients. The antibodies to IMC-1C11 inhibited the circulation of the agent in two patients. One patient had prolonged stable disease for seven cycles (28 weeks). The mean changes in tumor-influx volume-transfer constant k_{in} (min^{-1}) and enhancement factor after 4 weeks of therapy were significantly decreased compared with pretreatment values in 11 patients.**

Conclusion: **IMC-1C11 was both safe and well tolerated. Drug levels of IMC-1C11 were reliably predicted. Further clinical investigation of anti-VEGFR/KDR agents is warranted.**

INTRODUCTION

The inhibition of tumor-induced angiogenesis has become a major developmental strategy in cancer research (1, 2). Elucidation of the variety of molecular pathways involved in angiogenesis has provided targets for angiogenesis inhibition. Several potential angiogenic inhibitors against these therapeutic targets affect endothelial cell proliferation, migration, and survival (3–5). The inhibition of activated endothelial cells have been shown to abrogate tumor growth (6, 7).

VEGFR[3] is thought to be the predominant angiogenic factor in malignant disease and one of the major survival factors for endothelial cells (8, 9). It is frequently detected in tumors and its expression has been correlated with poor prognosis in colon, breast, renal, and other primary tumors (10–13). VEGFR overexpression is frequently observed in colorectal carcinoma, in which it may play a role in the progression of metastatic disease (14). It can be synthesized by both normal and malignant cells and mediates angiogenic signals through interaction with one or more of its tyrosine kinase receptors (15). VEGFR2, also known as Flk-1/KDR, has been reported to be the most important receptor in VEGFR-stimulated tumor angiogenesis. KDR is found primarily on vascular endothelium (16) and several tumor cell types (17). Inhibition of VEGFR or KDR is reported to inhibit tumor growth (18).

DC101, a rat antimouse monoclonal antibody that targets Flk-1 (the murine homologue of KDR), was shown to block VEGF-mediated endothelial cell signaling (19). Administration of DC101 produced dramatic antitumor effects in a variety of

Received 9/5/02; revised 11/7/02; accepted 11/8/02.
The costs of publication of this article were defrayed in part by the payment of page charges. This article must therefore be hereby marked *advertisement* in accordance with 18 U.S.C. Section 1734 solely to indicate this fact.
[1] Supported by Imclone Systems, Somerville, NJ, and National Cancer Institute Grant K23 RR16184.
[2] To whom requests for reprints should be addressed, at University of Alabama at Birmingham, Comprehensive Cancer Center, Wallace Tumor Institute 263, 1530 3rd Avenue South, Birmingham, AL 35294-3300, Phone: (205) 934-0916; Fax: (205) 934-1608; E-mail: James.Posey@ccc.uab.edu.

[3] The abbreviations used are: VEGFR, vascular endothelial growth factor receptor; KDR, kinase insert domain-containing receptor; ECOG, Eastern Cooperative Oncology Group; DLT, dose-limiting toxicity; ROI, region(s) of interest; HACA, human antichimeric antibody; MRI, magnetic resonance imaging; CT, computed tomography; scFv, single-chain FV.

human tumor xenograft models (20), as well as in a hepatic metastasis colon cancer model (21). Because DC101 does not cross-react with human KDR, a chimeric monoclonal antibody, IMC-1C11, was developed for human trials (22). IMC-1C11 binds specifically to the endothelial cell surface extracellular domain of KDR, blocks VEGFR-KDR interaction and prevents VEGFR activation of the intracellular tyrosine kinase pathway (23).

This report describes the initial Phase I trial of IMC-1C11 that was carried out in patients with colorectal carcinoma metastatic to the liver.

PATIENTS AND METHODS

Eligible patients met the following criteria: (*a*) pathologically confirmed adenocarcinoma of the colon/rectum that is metastatic to the liver and is not curable with available treatment; (*b*) at least one liver metastasis had to be bidimensionally measurable; (*c*) age greater than 19 years; (*d*) a median survival of at least 12 weeks; (*e*) ECOG performance status of ≤ 1; and (*f*) adequate hematopoietic function (hemoglobin >9.0 g/dl; total leukocyte count >3,000/mm^3; granulocytes >1,500/mm^3; platelet count >100,000/mm^3), hepatic function (alkaline phosphatase levels ≤ 4 times the upper limit of normal; bilirubin ≤ 1.5 upper limit of normal), and renal function (serum creatinine limit of normal). Patients may or may not have had extrahepatic sites of metastases. Major exclusion criteria included: (*a*) inability to assess vascular flow of hepatic metastatic lesion(s) by MRI; (*b*) therapy capable of inducing bleeding, such as warfarin, heparin or aspirin; (*c*) pregnancy or breast feeding; (*d*) major surgery, cytotoxic chemotherapy, or radiotherapy within the previous 4 weeks; (*e*) clinically significant cardiac disease; (*f*) inability to comply with or understand informed consent; and (*g*) brain metastases, uncontrolled seizure disorder, other active neurological disease, or serological evidence of chronic infection such as hepatitis or HIV. Signed informed consent was obtained from each patient before enrollment into the protocol. The protocol, informed consent, and informed consent procedures were reviewed and approved by the University of Alabama at Birmingham Institutional Review Board.

Treatment Plan. This study design was an open-label, single-arm Phase I trial designed to establish maximum tolerated dose and side effects of IMC-1C11 therapy. The study drug was infused in our outpatient General Clinical Research Center and patient were monitored with vital sign and symptom assessment for approximately one h post–infusion of IMC-1C11.

IMC-1C11 was given i.v. over ~1 h once a week for 4 weeks. This was considered a treatment cycle. Patients could continue treatment provided there was no evidence of disease progression or DLT. There were four cohorts of at least three evaluable patients per cohort. Patients were treated in cohorts of three to six patients at escalating doses of IMC-1C11 from 0.2 mg/kg to 4.0 mg/kg given weekly. Patients were enrolled at the next dose level 2 weeks after the last patient at the prior dose level completed a 4th week of IMC-1C11 in the absence of DLT. If one of the initial three patients in a cohort demonstrated a DLT, three more patients were entered into the cohort. The maximum tolerated dose was defined as one dose below the dose that induced a DLT in two or more patients in a cohort. Toxicity was evaluated according to the expanded National Cancer Institute Common Toxicity Criteria Version 2. A DLT was defined as any grade-3 or -4 toxicity excluding allergic reactions, nausea, vomiting, or alopecia. Patients underwent evaluation of measurable disease by CT scan after completing four weekly treatments and subsequent scan were repeated after four weekly infusions. Measurable disease must have been bidimensionally ≥ 2 cm for lesions that are palpable, ≥ 1 cm and for soft tissue lesions followed by CT scan, and ≥ 2 cm for lytic bone lesions followed by CT or MRI. Patients without DLT who had either stable disease (defined as no change, or tumor response that has not increased by 25% or decreased by 50%) or responding disease could go on to receive additional therapy. Two exceptions to allow a second cycle of therapy were granted to patients 7 and 10, who each had a decrease in parameters of tumor perfusion at week 5, had a modest level of progression (26 and 35%, respectively), were asymptomatic, and had no FDA-approved treatment options. Patients underwent MRI for vascular flow/diffusion measurements ~1 week before the initial dose of IMC-1C11 and the week after the fourth dose. For patients who had stable or responding disease by CT, additional dynamic MRI for vascular flow/diffusion was performed 1 week after each four-dose treatment cycle.

Production of IMC-1C11. A single-chain antibody phage display library was constructed from spleen cells of mice immunized with a soluble form of KDR. After two rounds of biopanning, >90% of the clones recovered were specifically reactive to KDR (23). Subsequent selection identified two clones that blocked VEGFR binding to KDR. These two clones were expressed in *Escherichia coli* and purified as soluble scFv antibodies. One scFv, p1C11, was shown to inhibit VEGFR-induced KDR phosphorylation and VEGFR-stimulated DNA synthesis in human umbilical vein endothelial cells (23). This led to the development of IMC-1C11, a chimeric anti-KDR antibody (IgG1κ; Ref. 19).

IMC-1C11 was developed by immunization of BALB/c mice with KDR-alkaline phosphatase fusion protein. Purified mRNA from splenocytes of these mice was used to construct a scFv antibody phage display library. The library was used to select against immobilized KDR protein. A clone was selected, expanded in cell culture, and frozen in liquid nitrogen. Clone p1C11 scFv was selected for its high-affinity binding to KDR and for its ability to block KDR/VEGFR interaction and to inhibit VEGFR-induced biological activity on human endothelial cells. The gene segments encoding p1C11 scFv variable domains were amplified and subcloned into an expression vector that contained human IgG1κ constant domains for the expression of a mouse/human chimeric antibody, IMC-1C11. The IMC-1C11 expression vector was used to transfect cells of Chinese-hamster-ovarian origin and a stable expressing cell line was established. The cell line was expanded in cell culture and was frozen in liquid nitrogen.

Pharmacokinetics. Five-ml samples of blood were obtained from each patient during the first cycle and before each subsequent cycle. The serum from each sample was stored at −20°C shortly after separation from the clotted blood. Blood was obtained preinfusion and at the end of infusion on day 1, and at 2, 6, 12, 24, 48, 96, and 168 h postinfusion. On days 8 and 15, blood samples were obtained preinfusion and 2 h postinfu-

sion. On day 22, samples were obtained preinfusion and at 2, 24, and 48 h postinfusion.

Briefly, 100 μl/well KDR-alkaline phosphatase [1 μg/ml in PBS (pH 7.2); ImClone Systems Incorporated, Somerville, NJ] was adsorbed to each well of a 96-well microtiter plate (Immulon 2, Dynatech) overnight at 2°C to 8°C. Plates were washed in washing buffer (PBS/0.05% Tween 20) and then were blocked for 2 h at room temperature with 10% HSBB [10% Horse Serum (Life Technologies, Inc.) in PBS/0.05% Tween 20]. The plates were washed with washing buffer, and a 100-μl volume of serum samples, standards, and internal controls were incubated in the wells for 2 h at room temperature. After washing with wash buffer, 100 μl of antihuman Fc-specific IgG1 horseradish peroxidase-conjugated antibody (Jackson ImmunoResearch) were added to each well. After a final washing, bound conjugate was then visualized by adding 100 μl of substrate tetramethylbenzidine (TMB) solution (Kirkegaard and Perry Laboratories). This gives a blue reaction product that turns yellow on the addition of the stopping solution (2 M H_2SO_4). The plates were read on a Molecular Devices Thermomax 340PC ELISA reader using a wavelength of 450 nm. IMC-1C11 was quantitated by comparing with a standard curve prepared from reference standard IMC-1C11.

Immunogenicity. Human antibody response to IMC-1C11 was determined by a double-antigen radiometric assay procedure (24). In brief, 6.4 mm of polystyrene beads were coated with 2 μg/bead IMC-1C11 antibody in PBS by gentle agitation at 80 rpm overnight at room temperature. The beads were washed three times with phosphate buffer containing EDTA (PBE), blocked with PBE for 1 h at room temperature, and stored in PBE at 4°C. Patient sera or standards in PBE were added to a glass culture tube. After the addition of a single antibody-coated bead to the tubes, the tubes were gently agitated at 140 rpm for 1 h at room temperature. Beads were washed by adding and aspirating 4 ml of PBS. ^{125}I-labeled IMC-1C11 antibody was added to the respective tubes and gently agitated at 140 rpm for 1 h at room temperature. Beads were washed again as above. The beads were transferred to clean tubes, then counted for 1 min to determine the ^{125}I antibody-bound radiation. The assay result was calculated from the ^{125}I antibody-bound radiation and known specific activity of ^{125}I-antibody. Results were expressed as ng of IMC-1C11 antibody-bound/ml of patient serum.

Assessment of Vascular Perfusion. Dynamic contrast-enhanced perfusion MRI using Gd-DTPA (0.2 mmol/kg, supplied by Magnevist, Berlex Lab, Inc.) was performed on a GE Signa 1.5 Tesla MRI scanner (General Electric, Milwaukee, WI). A torso phased-array receiving coil was used. The vest-like coil was centered over the upper abdomen to maximize the signal:noise ratio in the liver. Two sequences were used to localize the lesion(s) for subsequent perfusion analysis: axial T1-weighted spoiled gradient echo, and axial T2-weighted single-shot fast spin echo. Each of these sequences acquired images of the entire liver in a single breath hold. The orientation of the plane of choice (axial, coronal, or sagittal) was dependent on the size and location of the lesion, to reduce the likelihood that respiration would significantly alter the lesion position during serial scanning from a selected 5-mm slice. We used multiphase fast spoil gradient echo (SPGR) pulse sequence with acquisition parameters: TR/TE = 8/4 ms, flip angle = 70°, FOV = 40 × 40 cm^2, slice thickness = 5.0 mm, image matrix 256 × 256, the delay between different phases was 50 ms. One hundred twenty images were acquired and each phase (image) required 1.1 s. The image data were transferred to a personal computer and were processed according to a two-compartment model[4]:

$$k_{in}^{PSp} = \frac{\text{slope}}{T_{10} * A * C_p(0)}$$

where the slope is the initial rate of enhancement curve in the arterial phase (covers the first 20–35 images), A is the relaxivity and T_{10} = 1.433 s at 1.5 T and $C_p(0)$ = 8.77 D, D is the dose of Gd-DTPA, and the tumor influx volume transfer constant k_{in} is obtained. After the Gd-DTPA bolus injection, the nodules initial signal g is time point t_1 (set to 0 s) with signal height $S(0)$ and reaches a maximum intensity at ~15–30 time points (an image was acquired for each time point) t with signal $S(t)$. The maximum signal enhancement factor (EF) in arterial phase is defined as $S(t) - S(0)/S(0)$ with t = 15 time points (at ~16.5 s). Signal beyond 15 time points likely has more portal vein blood flow, thus complicating the kinetic model analysis. MRI assessment was carried out before therapy and 1 week after the fourth infusion of each treatment cycle.

Statistical Analysis. Because of the noncomparative nature of this study, descriptive statistics were used to summarize toxicities and laboratory data. The frequency of adverse events was tabulated, as well as the proportion of patients exhibiting each adverse event. Pharmacokinetic analysis was conducted on 14 patients. Compartmental models were fit to each patient's concentration profile using the nonlinear regression procedure in SAS (25). Pharmacokinetic parameters area under the curve (AUC), half-life ($t_{1/2}$), clearance (CL), and volume of steady state (V) were estimated using the fitted compartmental model. MRI assessments of vascular flow before and after treatment were examined, and the dose groups were compared descriptively. Comparisons were made before and after treatment overall, ignoring dose groups, using the paired t test and the signed-rank Wilcoxon test. For the dose group comparisons, the difference in vascular flow before and after therapy was computed for each patient, and the dose groups were compared using ANOVA and the nonparametric Kruskal-Wallis test. Spearman's correlation coefficients were computed between vascular parameters (EF and k_{in}) and tumor growth using the CORR procedure in SAS.

RESULTS

Patient Characteristics. The distribution of the fourteen patients among the four cohorts and their characteristics are listed in Table 1. There were six men and eight women, with an age range from 43 to 72 years. They all had excellent performance status, a median of two prior chemotherapy regimens, and five had liver as their only site of metastasis. Eight of the patients received one cycle of therapy (four infusions), whereas

[4] T. C. Ng *et al.*, Arterial phase Gd-enhanced MRI perfusion in liver metastasis from colorectal cancer, manuscript in preparation.

Table 1 Patient cohorts and characteristics

Patient no.	Dose (mg/kg)	Patient gender	Age	ECOG performance status	No. of prior therapies	No. of extrahepatic sites	Response[a]	No. of infusions
1	0.2	F	43	0	2	1	PD[b]	4
2	0.2	F	46	0	2	2	PD	4
3	0.2	M	57	0	2	0	PD	4
4	0.6	M	44	0	2	1	StD	8
5	0.6	M	58	0	1	1	PD	4
6	0.6	F	63	1	2	1	PD	4
7	0.6	F	60	1	3	2	PD	8
8	2.0	F	68	1	2	0	PD	4
9	2.0	F	55	1	2	0	PD	4
10	2.0	M	53	0	2	1	PD	8
11	4.0	F	64	1	3	1	StD	8
12	4.0	M	53	0	1	0	StD	28
13	4.0	M	47	0	1	0	StD	8
14	4.0	F	72	1	1	1	PD	4

[a] Response at initial evaluation (4 weeks).
[b] PD, progressive disease; StD, stable disease.

Table 2 Toxicity related to IMC-1C11 by dose level

	0.2 mg/kg $n = 3$		0.6 mg/kg $n = 4$		2.0 mg/kg $n = 3$		4.0 mg/kg $n = 4$	
	Gr[a] 1,2	Gr 3,4	Gr 1,2	Gr 3,4	Gr 1,2	Gr 3,4	Gr 1,2	Gr 3,4
Pain	1		2		2		1	
Bleeding	1		3					
GI	2		3				2	
Fever			2					
Asthenia	1						2	
Dizziness			1		1		1	
Stiffness	1							
Hypertension					1			
Cough							1	
Edema					1			

[a] Gr, grade; GI, gastrointestinal.

five received two cycles (eight infusions), and one received seven cycles (twenty-eight infusions).

Toxicity. The antibody treatment did not produce acute infusion symptoms and produced no grade-3 or -4 toxicity (Table 2). All of the grade-1 or -2 symptoms were sporadic, lasting 1–3 days, were not repetitive with each infusion, and did not increase in frequency with increasing dose cohorts. The four bleeding episodes, possibly related to IMC-1C11, included a patient with 3 days of brief and scanty epistaxis, two patients with 1 day of blood streaking of sputum, one of whom also had 1 day of blood streaking in his stool; and one patient (patient 7) who had gross hematuria on four occasions over 8 weeks of therapy and who was documented to have tumor infiltration of her right kidney. Bleeding episodes were reported as history data and were not active at the time of visits. Platelet counts before and after episodes remained within the normal range, and coagulation profiles were not done because the patients were not actively bleeding. Overall, the antibody infusions were well tolerated, and in most patients, symptoms were related to the underlying disease process.

Antibody Response to IMC-1C11. Human antibody response to IMC-1C11 is presented in Table 3 over the initial 42 days of the trial. A total of 7 of 14 patients had evidence of detectable antibody on more than one occasion; this was observed in the two low-dose cohorts. In addition, one patient (patient 10) had a single borderline value of 34 ng/ml on day 22. The two highest antibody responses were seen on day 22 in patients 3 and 6 and are discussed below regarding IMC-1C11 plasma kinetics.

Pharmacokinetics. Table 4 summarizes the pharmacokinetic parameters of the initial infusion of IMC-1C11 in patients from the four-dose cohorts. The kinetics were assessed using both a one-compartment and a noncompartmental analysis with similar results. The one-compartment results are presented here. The two lower-dose cohorts were characterized by a short plasma $t_{1/2}$, high plasma clearance rate (CL), and modest AUC. Multiple comparisons using ANOVA revealed significant differences between the dose cohorts ($P = 0.01$) for plasma $t_{1/2}$. The dose cohorts of 2 mg/kg and 4 mg/kg had much longer plasma $t_{1/2}$ (56 and 67 h) and lower plasma clearance rates (CL, 0.57 and 0.40 ml/h/kg), which were significantly different from the two low-dose cohorts. The two high-dose cohorts had much higher area under the curve (AUC) than the low-dose cohorts, reflecting both the larger dose administered and the longer

Table 3 Human antichimeric antibody response to IMC-1C11[a]

Patient no.	Dose (mg/kg)	Day 1 (ng/ml)	Day 22 (ng/ml)	Day 36 (ng/ml)	Day 42 (ng/ml)
1	0.2	16	77	117	133
2	0.2	6	13	15	
3	0.2	11	460	239	28
4	0.6	8	71	52	46
5	0.6	8	65	69	87
6	0.6	21	86	67	
7	0.6	17	37	41	26
8	2.0	6	8	7	51
9	2.0	4	22	20	16
10	2.0	6	34	11	13
11	4.0	4	5	5	7
12	4.0	7	8	7	11
13	4.0	10	13	11	10
14	4.0	6	7	6	7

[a] Normal sera (n = 27) 10 ± 6 ng/ml (× ± 1 SD) and a positive value was >28 ng/ml (>3 SD).

Table 4 IMC-1C11 pharmacokinetic parameters

Dose level (mg/kg)	Mean dose (mg)	*AUC*[a] (μg/ml·h)	C_{max} (μg/ml)	$t_{1/2}$ (hrs)	*CL* (ml/h/kg)	Volume (ml/kg)
0.2	22	209 ± 102	10.6 ± 8.3	16 ± 7	1.13 ± 0.57	26.1 ± 14.1
0.6	48	394 ± 116	20.6 ± 8.4	13 ± 5	1.66 ± 0.64	32.2 ± 10.1
2.0	141	3,674 ± 1,031	45.2 ± 3.4	56 ± 12	0.57 ± 0.14	44.4 ± 3.3
4.0	306	10,434 ± 2,266	107.3 ± 27.2	67 ± 3	0.40 ± 0.9	39.1 ± 9.5

[a] *AUC*, area under the curve; *CL*, clearance.

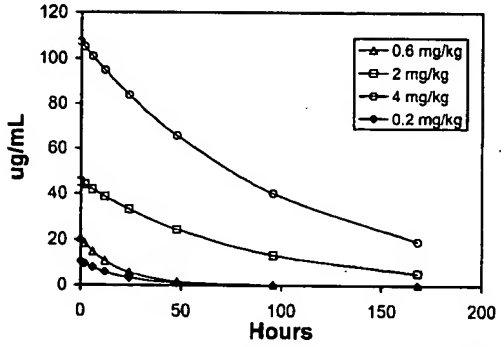

Fig. 1 Mean plasma IMC-1C11 levels expressed as percentage of C_{max} achieved at the four treatment dose levels based on a one-compartment model.

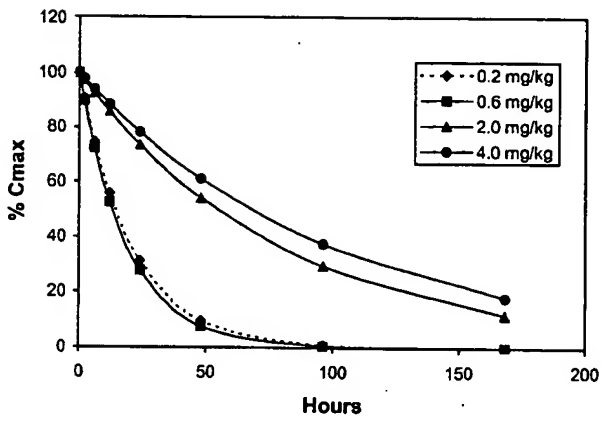

Fig. 2 Mean plasma concentrations (μg/ml) of the initial day 1 infusion of IMC-1C11 for each dose-group based on a one-compartment model.

plasma half-life. Fig. 1 provides the plasma IMC-1C11 disappearance curves plotted as the percentage of maximum IMC-1C11 concentration, demonstrating the substantial differences in plasma kinetics in the low-dose cohorts. Fig. 2 presents the plasma disappearance curves in terms of IMC-1C11 mean plasma concentrations depicting the inability of the low-dose cohorts to maintain plasma levels of IMC-1C11 beyond 48-h postinfusion and the mean levels generated in the higher-dose cohorts. The ability of four weekly infusions to maintain continuously circulating IMC-1C11 levels was evaluated over the initial 4 weeks of treatment. Nadir blood levels before repeat infusion were either 0 or <1 μg/ml in the two lower-dose groups. In patients receiving 2 mg/kg IMC-1C11, the mean nadir level was 7.7 ± 6.7 (range, 1–19) μg/ml, whereas patients in the 4-mg cohort had values of 43.9 ± 23.9, with a range of 9–94 μg/ml. The fourth infusion plasma concentrations and kinetics of IMC-1C11 were compared with each patient's initial infusion. In general, the fourth infusion had similar values as each patient's initial infusion with two exceptions. Patient 3 had a fourth infusion C_{max}, that was 28% of the first infusion C_{max}, and a 24-hour value that was below detection. This infusion took place on day 22 when he had an anti-IMC-1C11 level of 460

Table 5 MRI vascular parameters and tumor size change

Dose	Patient no.	K_{in}[a] (min^{-1}) Pre	Post	Δ	EF[a] Pre	Post	Δ	Tumor size change
0.2 mg/kg	3	0.29	0.19	−0.10	1.15	0.71	−0.44	+28%
0.6 mg/kg	4	0.44	0.05	−0.39	1.21	0.22	−0.99	+25%
	5	0.33	0.33	0	0.80	0.77	−0.03	+46%
	6	0.47	0.45	−0.02	1.25	0.80	−0.45	+10%
	7	0.45	0.25	−0.20	1.33	0.53	−0.80	+26%
2.0 mg/kg	8	0.40	0.46	+0.06	1.16	1.40	+0.34	+46%
	9	0.35	0.16	−0.19	1.50	1.10	−0.40	+65%
	10	0.26	0.21	−0.05	0.76	0.62	−0.14	+34%
4.0 mg/kg	12	0.24	0.11	−0.13	0.70	0.30	−0.40	−0.6%
	13	0.54	0.33	−0.21	1.63	1.21	−0.42	+18%
	14	0.58	0.36	−0.22	1.25	0.81	−0.44	+27%

[a] K_{in}, influx rate constant; EF, enhancement factor; Pre, pretreatment; Post, posttreatment.

ng/ml. Patient 6 had an undetectable C_{max} on his fourth infusion, when his anti-IMC-1C11 was 86 ng/ml.

Alteration in Vascular Parameters. Eleven of the 14 patients were evaluated for changes in vascular perfusion. Two parameters were measured before and after one cycle of treatment: the enhancement factor (*EF*) and tumor influx rate constant K_{in} (min^{-1}), both of which are proportional to perfusion. Patients 1, 2, and 11 were not evaluated secondary to technical difficulty with the procedure or data acquisition. On the computer-generated image slice, a ROI was placed around index liver lesion(s). A detailed analysis of these studies will be published separately, but Table 5 provides a summary of the measurements of *EF* and k_{in} for patients studied pre- and posttherapy with four weekly doses of IMC-1C11. Using paired *t* test and signed-rank Wilcoxon test, we observed a significant reduction in k_{in} (P = <0.007) and *EF* (P = 0.003) at the posttherapy interval. In four of five patients receiving additional cycles of therapy, vascular parameters (*EF* and k_{in}) exceeded the initial decline and tended to return to the baseline value (data not shown). Fig. 3 provides an example of the MRI dynamic flow before and after one cycle of therapy. The high vascular flow in the perimeter of the tumor with low flow in the interior is typical of human tumor flow studies (26). Fig. 4 provides a bar graph (derived from the images in Fig. 3) depicting the proportion of high and low vascular flow in the two tumor nodules before and after 4 weeks of therapy. A substantial increase in low flow and a decrease in high flow components are demonstrated. This patient had only a 10% increase in measurable disease with a change in *EF* from 1.25 to 0.80. We could not assess dose effects given limited patient numbers, especially with only one patient in the lowest dose cohort. Table 5 also lists the percentage of change in tumor size noted at the 4-week evaluation, which varied from −6% to +65%. There was a tendency for less tumor growth in patients with more inhibition of flow as judged by *EF* (Spearman correlation of 0.62 with P = 0.044), whereas no correlation was found between k_{in} and tumor growth.

IMC-1C11 Antitumor Efficacy. None of the patients had an objective response to therapy. Of the 14 patients, 4 had stable disease (≤25% increase in tumor measurements) at the 4-week assessment, and 3 of these patients were in the 4-mg/kg-dose cohort. Patient 12 was of particular interest in that he had a total of 28 infusions of IMC-1C11 over 28 weeks with stable disease. The measurements over the course of therapy for this patient are plotted in Fig. 5. This patient at study entry had a growing hepatic metastasis over the prior 3 months that remained stable over his 28-week treatment with IMC-1C11; however, an adrenal metastasis appeared and progressively grew. He was taken off study, because of the new lesion, whereas the hepatic tumor remained stable for an additional 8 weeks of observation.

DISCUSSION

Tumor-induced angiogenesis seems to be critical to the establishment and growth of primary and metastatic cancer cells (27). The vascular response and support of tumors represents an interplay of proangiogenic and antiangiogenic factors produced by tumor cells and surrounding normal cells (28). VEGFR has been reported to be one of the most important of the proangiogenic factors involved in murine tumor models (21) and patients (29, 30). As a result, several VEGFR-targeted therapeutic strategies have been developed and there are ongoing clinical trials to evaluate clinical benefit. VEGFR angiogenic activity is mediated through receptor tyrosine kinases that are present principally on endothelial cells. Two of the three identified VEGFR receptor family members are expressed on endothelial cells (VEGFR1 and VEGFR2), and the VEGFR2 (KDR/flk-1) has been shown to play the central role in tumor angiogenesis (31, 32).

Four VEGFR-targeted treatment strategies have entered the clinic to date. These include a humanized monoclonal antibody directed to VEGFR (Bevacizumab), a chimeric monoclonal antibody directed to the VEGFR2 (IMC-1C11), several small molecule inhibitors of the VEGFR2 tyrosine kinase, and a ribozyme (Angiozyme) specific for Flt-1/KDR mRNA. Although the two monoclonal antibody strategies would appear similar, *i.e.*, inhibition of ligand or inhibition of ligand receptor,

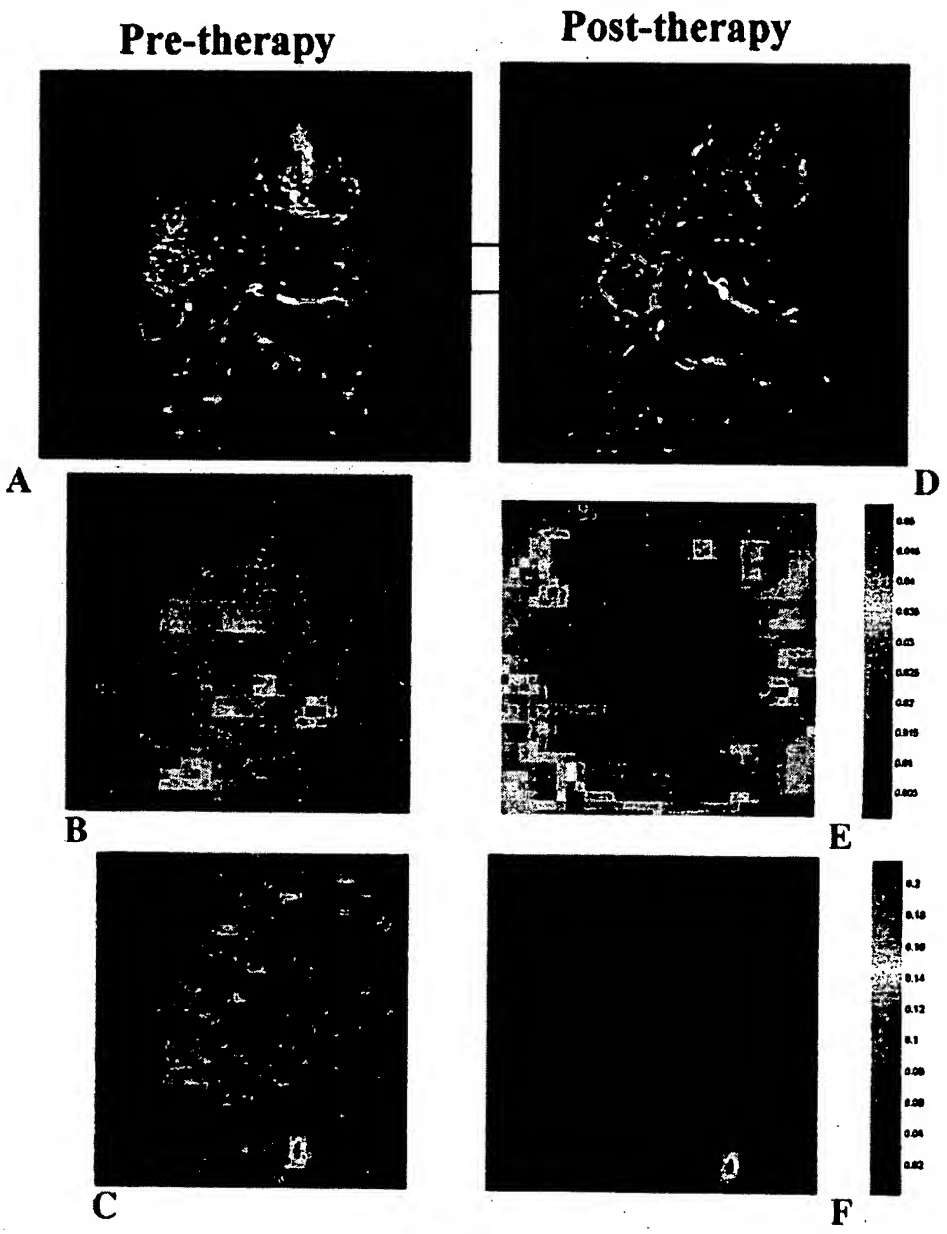

Fig. 3 Pre-therapy dynamic flow demonstrating two ROI in (*A*) with magnification of ROI (*B* and *C*). Post-therapy dynamic flow of the same ROI (*D*) with magnification views (*E* and *F*). *Flow color bar*, indicates intensity enhancement which is proportional to profusion.

they are likely to differ regarding alteration of different molecular pathways and possibly *in vivo* effects. It is clear that VEGFR can function as a ligand for a variety of receptors including three receptor/pathways in the VEGFR receptor family and at least one of two receptor/pathways in the neuropilin family (33). Thus, inhibition of VEGFR ligand has the potential to alter multiple signal transduction pathways in multiple cell types, whereas the targeting of the VEGFR2 (KDR) would be much more selective in that this receptor is found primarily on activated endothelial cells and some malignant cell types (34).

There are several parenteral and oral inhibitors of the VEGFR2 tyrosine kinase that are currently being examined in clinical trials, including SU5416, PTK 787, ZD6474, and CP547632 (35–38). These agents have been selected on the basis of relatively selective inhibition of the VEGFR2 ATP binding site. However, the large array of potential tyrosine kinase signaling elements in the human genome include many the functions of which are yet to be discovered. This may provide the potential for nonspecific (non-VEGFR2) effects that could account for side effects like refractory headaches, nausea, vomiting, and thrombotic events reported in early trials (39).

Thus, targeting the VEGFR2 (KDR) receptor represents a rather selective antiangiogenic strategy that has been demonstrated to have potent *in vivo* antitumor effects in murine models of multiple tumor types. This Phase I trial is the first clinical trial of a VEGFR2 (KDR)-specific monoclonal antibody, IMC-1C11. This reagent was very well tolerated over a dose range of 0.2–4.0 mg/kg weekly for a 4-week cycle, with total doses

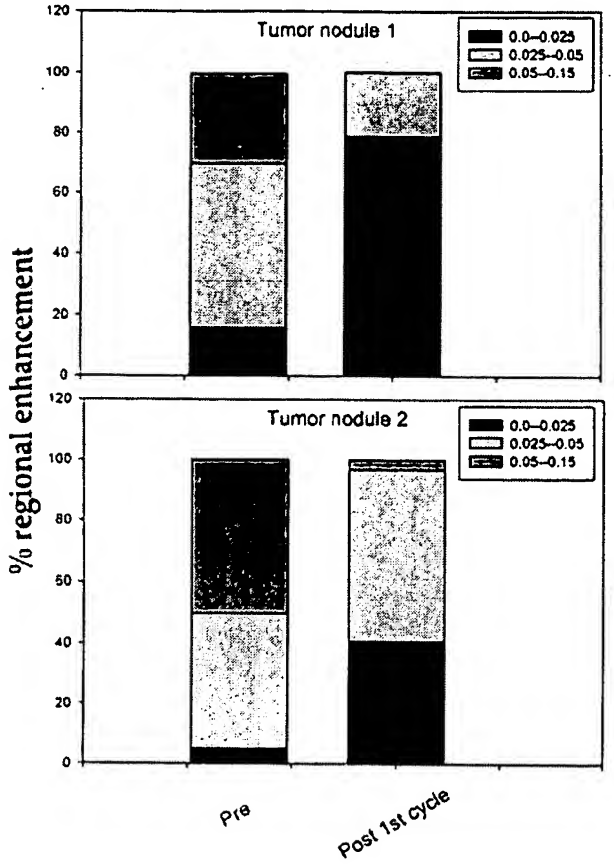

Fig. 4 From the nodules displayed in Fig. 3, this bar graph depicts the proportion of tumor nodule pixels that have high, intermediate, and low perfusion before (*Pre*) and after (*Post 1st cycle*) treatment.

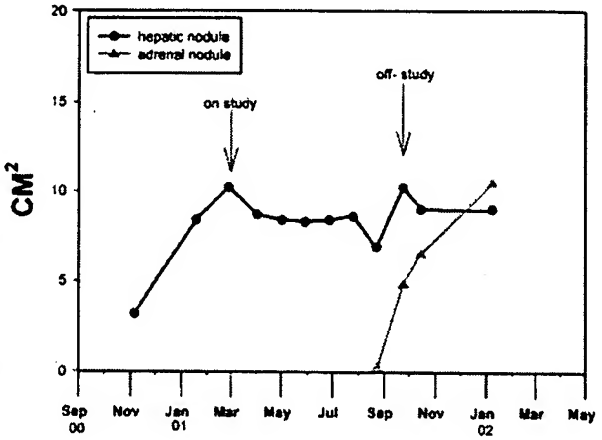

Fig. 5 The bidimensional tumor measurements of patient 12 treated at the 4-mg/kg dose level before, during, and after IMC-1C11 therapy that continued for 28 weeks.

administered at the highest-dose cohort of 920 to 1504 mg over 4 weeks. There were no DLTs, and most side effects reported were thought to be disease related. Several patients reported mild transient bleeding episodes (grade 1) with no particular pattern or dose effect. One patient had significant hematuria but had tumor invasion of the kidney as a contributing factor.

The pharmacokinetics of IMC-1C11 demonstrated a striking dose dependency with the two lower-dose cohorts (0.2 and 0.6 mg/kg) having a short plasma $t_{1/2}$, a high plasma clearance rate, and an inability to maintain circulating levels of antibody on a weekly infusion schedule. The two higher-dose cohorts were able to maintain circulating levels of IMC-1C11 on the weekly schedule, but the 4-mg/kg dose level was significantly better than the 2-mg/kg dose level. The plasma $t_{1/2}$ at 4 mg/kg was ~3 days, and, therefore, chronic schedules of administration could use weekly or biweekly schedules depending on the chosen target nadir levels. This pattern of dose dependence was also seen in our prior trial of anti-αvβ3 monoclonal antibody (Vitaxin), which also targeted an endothelial cell-expressed antigen. It may well be that endothelial cell antigens that are up-regulated on tumor neovasculature have a baseline low expression on normal endothelial cells representing an intravascular antigen sink requiring higher dose administration to achieve adequate pharmacokinetics similar to that seen with anti-CD20 in lymphoma patients ("B-cell sink") and anti-EGFR, (C225) with hepatic EGFR sink (40, 41).

Another characteristic of IMC-1C11 was its immunogenicity. Fifty percent of the patients developed a human antibody to chimera antibody (or HACA) response, primarily in the two low-dose cohorts. Two patients with the highest HACA response had an impairment of IMC-1C11 circulation at the time of their fourth infusion (day 22) when they had peak HACA levels. Some chimera mouse-human monoclonal reagents have had little or no immunogenicity in human trials, whereas others have induced significant HACA response. For example, C225 (anti-EGFR) has produced little or no HACA when assessed by the same HACA assay used in this trial (41).

Several of the antiangiogenesis trials have attempted to measure the vascular effects of antiangiogenesis strategies. This trial was our first experience with using dynamic contrast-enhanced perfusion MRI to assess the flow in hepatic metastases, and we were impressed with its potential. A detailed analysis of the data will be presented separately, but Table 5 provides a summary of the observations that demonstrated a significant decrease in two parameters (k_{in} and EF) associated with the four doses of IMC-1C11. These are the same parameters that were reported to have decreased in a recent trial of a small-molecule inhibitor of VEGFR-mediated receptor kinase activation (42). However, the decreases in these parameters were transient, returned to baseline by week 8, and were associated with progressive disease in 8 of 11 patients. Three of four patients receiving a second cycle of therapy had vascular flow parameters that returned to pretherapy levels. It is unknown at this stage of antiangiogenesis clinical trials, what represents a clinically important change in MRI parameters of tumor-blood perfusion or of the duration of therapy and/or duration of flow inhibition required to prevent tumor growth. This trial would suggest that 4 weeks of therapy and/or 4 weeks of reduced tumor flow via MRI parameters are insufficient to prevent tumor growth, although it was interesting that a decline in flow parameters tended toward a decreased degree of tumor growth,

which might suggest that therapy trials of antiangiogenic agents be designed for longer treatment periods than 4 weeks as suggested by others (43, 44).

Finally, none of our patients had objective tumor regressions, although one patient had a long-term tumor stabilization despite progression documented prior to the institution of IMC-1C11 therapy. This experience is similar to that seen with other single-agent antiangiogenesis trials (45), in which tumor regressions are infrequent. This may reflect the need for long-term chronic treatment regimens to alter tumor growth rates or the need for combining antiangiogenesis strategies with other treatment modalities. The antimurine VEGFR receptor reagent, DC101, has shown striking ability to enhance radiation (46) and chemotherapy (47) antitumor efficacy in animal models. Similar trials in human cancer are indicated.

This study provides evidence of the safety and low toxicity for an antibody blockade of VEGFR2, as well as insight into dose and schedule requirements. A fully human anti-VEGFR2 agent has been produced as a second-generation agent, which is anticipated to be nonimmunogenic for chronic administration as a single agent and in combination with chemotherapy or radiation.

ACKNOWLEDGMENTS

Special thanks to Sharon Garrison and Sherron Thornton for manuscript preparation.

REFERENCES

1. Ellis, L. M., Liu, W., Fan, F., Jung, Y. D., Reinmuth, N., Stoeltzing, O., Takeda, A., Akagi, M., Parikh, A. A., and Ahmad, S. Synopsis of angiogenesis inhibitors in oncology. Oncology, *16* (Suppl. 4): 14–22, 2002.

2. Folkman, J. Angiogenesis and angiogenesis inhibition: an overview. EXS (Basel), *79:* 1–8, 1997.

3. Verheul, H. M., and Pinedo, H. M. The role of vascular endothelial growth factor (VEGF) in tumor angiogenesis and early clinical development of VEGF-receptor kinase inhibitors. Clin. Breast Cancer, (Suppl. 1): S80–S84, 2000.

4. Posey, J. A., Khazaeli, M. B., DelGrosso, A., Saleh, M. N., Lin, C. Y., Huse, W., and LoBuglio, A. F. A pilot trial of Vitaxin, a humanized anti-vitronectin receptor (anti-$\alpha_v\beta_3$) antibody in patients with metastatic cancer. Cancer Biother. Radiopharm., *16:* 125–132, 2001.

5. Shaheen, R. M., Davis, D. W., Liu, W., Zebrowski, B. K., Wilson, M. R., Bucana, C. D., McConkey, D. J., McMahon, G., and Ellis, L. M. Antiangiogenic therapy targeting the tyrosine kinase receptor for vascular endothelial growth factor receptor inhibits the growth of colon cancer liver metastasis and induces tumor and endothelial cell apoptosis. Cancer Res., *59:* 5412–5416, 1999.

6. Liu, W., Ahmad, S. A., Reinmuth, N., Shaheen, R. M., Jung, Y. D., Fan, F., and Ellis, L. M. Endothelial cell survival and apoptosis in the tumor vasculature. Apoptosis, *5:* 323–328, 2000.

7. Chavakis, E., and Dimmeler, S. Regulation of endothelial cell survival and apoptosis during angiogenesis. Arterioscler. Thromb. Vasc. Biol., *22:* 887–893, 2002.

8. Harmey, J. H., and Bouchier-Hayes, D. Vascular endothelial growth factor (VEGF), a survival factor for tumor cells: implications for anti-angiogenic therapy. Bioessays, *24:* 280–283, 2002.

9. Farrara, N. The role of vascular endothelial growth factor in pathological angiogenesis. Breast Cancer Res. Treat., *36:* 127–137, 1995.

10. Giatromanolaki, A. Prognostic role of angiogenesis in non-small cell lung cancer. Anticancer Res., *21:* 4373–4382, 2001.

11. Harada, Y., Ogata, Y., and Shirouzu, K. Expression of vascular endothelial growth factor and its receptor KDR (kinase domain-containing receptor)/Flk-1 (fetal liver kinase-1) as prognostic factors in human colorectal cancer. Int. J. Clin. Oncol., *6:* 221–228, 2001.

12. MacConmara, M., O'Hanlon, D. M., Kiely, M. J., Connolly, Y., Jeffers, M., and Keane, F. B. An evaluation of the prognostic significance of vascular endothelial growth factor in node positive primary breast carcinoma. Int. J. Oncol., *20:* 717–721, 2002.

13. Song, K. H., Song, J., Jeong, G. B., Kim, J. M., Jung, S. H., and Song, J. Vascular endothelial growth factor—its relation to neovascularization and their significance as prognostic factors in renal cell carcinoma. Yonsei Med. J., *42:* 539–546, 2001.

14. Lee, J. C., Chow, N. H., Wang, S. T., and Huang, S. M. Prognostic value of vascular endothelial growth factor expression in colorectal cancer patients. Eur. J. Cancer, *36:* 748–753, 2000.

15. Masood, R., Cai, J., Zheng, T., Smith, D. L., Hinton, D. R., and Gill, P. S. Vascular endothelial growth factor (VEGF) is an autocrine growth factor for VEGF receptor-positive human tumors. Blood, *98:* 1904–1913, 2001.

16. Brekken, R. A., and Thorpe, P. E. Vascular endothelial growth factor and vascular targeting of solid tumors. Anticancer Res., *21:* 4221–4229, 2001.

17. Herold-Mende, C., Steiner, H. H., Andl, T., Riede, D., Buttler, A., Reisser, C., Fusenig, N. E., and Mueller, M. M. Expression and functional significance of vascular endothelial growth factor receptors in human tumor cells. Lab. Investig., *79:* 1573–1582, 1999.

18. Witte, L., Hicklin, D. J., Zhu, Z., Pytowski, B., Kotanides, H., Rockwell, P., and Bohlen, P. Monoclonal antibodies targeting the VEGFR receptor-2 (Flkl/KDR) as an anti-angiogenic therapeutic strategy. Cancer Metastasis Rev., *17:* 155–161, 1998.

19. Zhu, Z., and Witte, L. Inhibition of tumor growth and metastasis by targeting tumor-associated angiogenesis with antagonists to the receptors of vascular endothelial growth factor. Investig. New Drugs, *17:* 195–212, 1999.

20. Prewett, M., Huber, J., Li, Y., Santiago, A., O'Connor, W., King, K., Overholser, J., Hooper, A., Pytowski, B., Witte, L., Bohlen, P., and Hicklin, D. J. Antivascular endothelial growth factor receptor (fetal liver kinase 1) monoclonal antibody inhibits tumor angiogenesis and growth of several mouse and human tumors. Cancer Res., *59:* 5209–5218, 1999.

21. Bruns, C. J., Liu, W., Davis, D. W., Shaheen, R. M., McConkey, D. J., Wilson, M. R., Bucana, C. D., Hicklin, D. J., and Ellis, L. M. Vascular endothelial growth factor is an *in vivo* survival factor for tumor endothelium in a murine model of colorectal carcinoma liver metastases. Cancer (Phila.), *89:* 488–499, 2000.

22. Lu, D., Kussie, P., Pytowski, B., Persaud, K., Bohlen, P., Witte, L., Zhu, Z. Identification of the residues in the extracellular region of KDR important for interaction with endothelial growth factor and neutralizing anti-KDR antibodies. J. Biol. Chem., *19:* 14321–14330, 2000.

23. Zhu, Z., Rockwell, P., Lu, D., Kotanides, H., Pytowski, B., Hicklin, D. J., Bohlen, P., and Witte, L. Inhibition of vascular endothelial growth factor-induced receptor activation with anti-kinase insert domain-containing receptor single-chain antibodies from a phage display library. Cancer Res., *58:* 3209–3214, 1998.

24. Khazaeli, M. B., Conry, R. M., and LoBuglio, A. F. Human immune response to monoclonal antibodies. J. Immunother., *15:* 42–52, 1994.

25. SAS/STAT User's Guide, Version 6, Ed. 4, Vols. 1–2. Cary, NC: SAS Institute, Inc., 1989.

26. Thomas, A., Morgan, B., Drevs, J., Jivan, A., Buchert, M., Horsfield, M., Hennig, J., Mross, K., Henry, A., Ball, H., Peng, B., Fuxius, S., Unger, C., O'Byrne, K., Laurent, D., Dugan, M., and Steward, W. Pharmacodynamic results using dynamic contrast enhanced magnetic resonance imaging, of 2 Phase 1 studies of the VEGF inhibitor PTK787/ZK 222584 in patients with liver metastases from colorectal cancer. ASCO 37th Annual Meeting, May 12–15, 2001. Proc. Am. Soc. Clin. Oncol., 2001.

27. Folkman, J. Incipient angiogenesis. J. Natl. Cancer Inst. (Bethesda), *92:* 94–95, 2000.

28. Crowther, M., Brown, N. J., Bishop, E. T., and Lewis, C. E. Microenvironmental influence on macrophage regulation of angiogenesis in wounds and malignant tumors. J. Leukoc. Biol., *70:* 478–490, 2001.

29. George, M. L., Eccles, S. A., Tutton, M. G., Abulafi, A. M., and Swift, R. I. Correlation of plasma and serum vascular endothelial growth factor levels with platelet count in colorectal cancer: clinical evidence of platelet scavenging? Clin. Cancer Res., *6:* 3147–3152, 2000.

30. Ishigami, S. I., Arii, S., Furutani, M., Niwano, M., Harada, T., Mizumoto, M., Mori, A., Onodera, H., and Imamura, M. Predictive value of vascular endothelial growth factor (VEGF) in metastasis and prognosis of human colorectal cancer. Br. J. Cancer, *78:* 1379–1384, 1998.

31. Li, Y., Wang, M. N., Li, H., King, K. D., Bassi, R., Sun, H., Santiago, A., Hooper, A. T., Bohlen, P., and Hicklin, D. J. Active immunization against the vascular endothelial growth factor receptor flk1 inhibits tumor angiogenesis and metastasis. J. Exp. Med., *195:* 1575–1584, 2002.

32. Millauer, B., Longhi, M. P., Plate, K. H., Shawver, L. K., Risau, W., Ullrich, A., and Strawn, L. M. Dominant-negative inhibition of Flk-1 suppresses the growth of many tumor types *in vivo.* Cancer Res., *56:* 1615–1620, 1996.

33. Oh, H., Takagi, H., Otani, A., Koyama, S., Kemmochi, S., Uemura, A., and Honda, Y. Selective induction of neuropilin-1 by vascular endothelial growth factor (VEGF): a mechanism contributing to VEGFR-induced angiogenesis. Proc. Natl. Acad. Sci. USA, *99:* 383–388, 2002.

34. Neufeld, G., Cohen, T., Gengrinovitch, S., and Poltorak, Z. Vascular endothelial growth factor (VEGF) and its receptors. FASEB J., *13:* 9–22, 1999.

35. Rosen, L. S. Clinical experience with angiogenesis signaling inhibitors: focus on vascular endothelial growth factor (VEGF) blockers. Cancer Control, *9* (Suppl. 2)*:* 36–44, 2002.

36. Drevs, J., Mross, K., Fuxius, S., Muller, M., Dugan, M., Peng, B., Chong, J., Henry, A., Laurent, D., Putz, B., Marme, D., and Unger, C. A Phase-1 dose escalating and pharmacokinetic (PK) study of the VEGF-receptor-inhibitor PTK787/ZK222584 (PTK/ZK) in patients with liver metastasis of advanced cancer. Proc. Am. Soc. Clin. Oncol., *20:* 100, 2001.

37. Hurwitz, H., Holden, S. N., Eckhardt, S. G., Rosenthal, M., de Boer, R., Rischin, D., Green, M., and Basser, R. Clinical evaluation of ZD6474, an orally active inhibitor of VEGFR signaling, in patients with solid tumors. Proc. Am. Soc. Clin. Oncol., *21:* 82, 2002.

38. Tolcher, A., Karp, D. D., O'Leary, J. J., DeBono, J. S., Caulkins, J. D., Molpus, K., Sutula, K., Ferrante, K. J., Gualberto, A., Noe, D. A., Huberman, M., Rowinsky, E. K., and Healey, D. A Phase I and biologic correlative study of an oral vascular endothelial growth factor receptor-2 (VEGF-2) tyrosine kinase inhibitor, CP-547, 632, in patients (pts) with advanced solid tumors. Proc. Am. Soc. Clin. Oncol., *21:* 84, 2002.

39. Rosen, L. S. Angiogenesis inhibition in solid tumors. Cancer J., *7* (Suppl. 3)*:* S120–S128, 2001.

40. Maloney, D. G., Liles, T. M., Czerwinski, D. K., Waldichuk, C., Rosenberg, J., Grillo-Lopez, A., and Levy, R. Phase I clinical trial using escalating single-dose infusion of chimeric anti-CD20 monoclonal antibody (IDEC-C2B8) in patients with recurrent B-cell lymphoma. Blood, *84:* 2457–2466, 1994.

41. Robert, F., Ezekiel, M. P., Spencer, S. A., Meredith, R. F., Bonner, J. A., Khazaeli, M. B., Saleh, M. N., Carey, D., LoBuglio, A. F., Wheeler, R. H., Cooper, M. R., and Waksal, H. W. Phase I study of anti-epidermal growth factor receptor antibody Cetuximab in combination with radiation therapy in patients with advanced head and neck cancer. J. Clin. Oncol., *19:* 3234–3243, 2001.

42. Deplanque, G., and Harris, A. L. Anti-angiogenic agents: clinical trial design and therapies in development. Eur. J. Cancer, *36* (13 Spec No)*:* 1713–1724, 2000.

43. Hayes, C., Padhani, A. R., Leach, M. O. Assessing changes in tumor vascular function using dynamic contrast-enhanced magnetic resonance imaging. NMR Biomed., *2:* 154–162, 2002.

44. Kozin, S. V., Boucher, Y., Hicklin, D. J., Bohlen, P., Jain, R. K., and Suit, H. D. Vascular endothelial growth factor receptor-2-blocking antibody potentiates radiation-induced long-term control of human tumor xenografts. Cancer Res., *61:* 39–44, 2001.

45. Zhang, L., Yu, D., Hicklin, D. J., Hannay, J. A., Ellis, L. M., and Pollock, R. E. Combined anti-fetal liver kinase 1 monoclonal antibody and continuous low-dose doxorubicin inhibits angiogenesis and growth of human soft tissue sarcoma zenografts by induction of endothelial cell apoptosis. Cancer Res., *62:* 2034–2042, 2002.

46. Pluda, J. M. Tumor-associated angiogenesis: mechanisms, clinical implications, and therapeutic strategies. Semin. Oncol., *2:* 203–218, 1997.

47. Harris, S. R., and Thorgeirsson, U. P. Tumor angiogenesis: biology and therapeutic prospects. In Vivo, *6:* 563–570, 1998.

Experimental Dermatology 2004: 13: 671–681
Blackwell Munksgaard . Printed in Denmark

EXPERIMENTAL DERMATOLOGY
ISSN 0906–6705

Anti-vascular endothelial growth factor receptor-2 (Flk-1/KDR) antibody suppresses contact hypersensitivity

Watanabe H, Mamelak AJ, Wang B, Howell BG, Freed I, Esche C, Nakayama M, Nagasaki G, Hicklin DJ, Kerbel RS, Sauder DN. Anti-vascular endothelial growth factor receptor-2 (Flk-1/KDR) antibody suppresses contact hypersensitivity.
Exp Dermatol 2004: 13: 671–681. © Blackwell Munksgaard, 2004

Abstract: The angiogenic mediator vascular endothelial growth factor (VEGF) and its receptors (VEGFRs) have been studied extensively in neoplastic disease and some inflammatory conditions. Contact hypersensitivity (CHS) is a prototypic Langerhans' cell-dependent, T-helper (Th) 1 cell-mediated inflammatory skin disease that is now also thought to involve angiogenic mediators. The purpose of our study was to examine the role of angiogenesis and VEGF in CHS. We demonstrated that VEGF production is up-regulated in murine skin after challenge with dinitrofluorobenzene. Administration of a monoclonal antibody directed against the VEGFR-2 (DC101) resulted in a 28.8% decrease in CHS response ($P < 0.001$). Examination of the DC101-treated mouse skin 24 h after challenge revealed decreases in dermal inflammatory cellular infiltrates and total vessel area. Furthermore, mRNA and protein of the Th1-type cytokine interferon (IFN)-γ was significantly down-regulated in skin of DC101-treated animals 24 h after challenge. The results of the study demonstrate that VEGFR-2 blockade significantly reduces vascular enlargement and edema formation and effects IFN-γ expression in the skin during challenge in CHS. Our findings suggest that DC101 could function by reducing inflammatory cell migration and hence IFN-γ expression during the CHS response.

Hideaki Watanabe[1], Adam J. Mamelak[1], Binghe Wang[1], Brandon G. Howell[1], Irwin Freed[1], Clemens Esche[1], Masashi Nakayama[2], Go Nagasaki[3], Daniel J. Hicklin[4], Robert S. Kerbel[5] and Daniel N. Sauder[1]

[1]Department of Dermatology, Johns Hopkins University, Baltimore, MD, USA
[2]Department of Pathology, Johns Hopkins University, Baltimore, MD, USA
[3]Department of Anesthesiology, Johns Hopkins University, Baltimore, MD, USA
[4]ImClone Systems Inc., New York, NY, USA
[5]Division of Cancer Biology Research, Sunnybrook and Women's College Health Science Centre, Toronto, ON, Canada

Key words: angiogenesis – antibodies – contact hypersensitivity – cytokines – inflammation

Dr Daniel N. Sauder
Professor and Chairman
Department of Dermatology
Johns Hopkins University
601 N. Caroline Street
JHOC 6068
Baltimore
MD 21287-0900
USA
Tel.: + 410 955 6943
Fax: + 410 955 8645
e-mail: dsauder@jhmi.edu

Accepted for publication 25 June 2004

Introduction

Contact hypersensitivity (CHS) is a delayed-type immune response that can be separated into two distinct immunologic phases. In the sensitization phase, skin is exposed to haptenated proteins that are recognized and captured by Langerhans' cells (LCs). Uptake of hapten by LC, the major dendritic cells (DCs) in the skin (1), triggers these cells' maturation and migration from the epidermis to the skin-draining lymph nodes (DLNs). Depending on the allergen, LC can either bind haptens directly to major histocompatibility (MHC) molecules on their surface or process the hapten internally into antigenic peptides that are then expressed on the surface with the MHC. In the DLN, LCs present the antigen to naïve T cells (2,3). T cells become activated and polarize toward a type-1 cytokine

Abbreviations: CHS, contact hypersensitivity; DC, dendritic cell(s); DLN, skin-draining lymph nodes; DNFB, 2,4-dinitrofluorobenzene; ELISA, enzyme-linked immunosorbant assay; FITC, fluorescein isothiocyanate; Flt-1, Fms-like tyrosine kinase; IFN, interferon; IL, interleukin; KDR, kinase insert domain containing receptor; LC, Langerhans' cell(s); MHC, major histocompatibility complex; PAF, platelet-activating factor; Th, T-helper cells; TNF, tumor necrosis factor; VEGF, vascular endothelial growth factor; VEGFR, vascular endothelial growth factor receptor.

expression pattern. When the skin is re-exposed to the same hapten, the elicitation phase is initiated. The hapten is again taken up and presented by LC [and other antigen-presenting cells (APCs)] to hapten-specific T cells. The T cells are induced to produce Th1 type cytokines (e.g. IFN-γ) and the cutaneous inflammatory reaction ensues (4). CHS is thus a prototypic DC-dependent, T-cell-mediated, Th1 type cytokine inflammatory skin reaction (4–6).

Recently, other mechanisms beyond cytokine signaling and this classic cellular pathway have also been implicated in CHS. In particular, angiogenesis and its mediators are now thought to play a critical role in this immune reaction (7,8). For example, vascular endothelial growth factor (VEGF), a major regulator of vascular endothelial cells and new blood vessel formation, has been shown to stimulate LC migration from the skin to the DLN (9). Brown et al. (8) observed that VEGF was overexpressed in keratinocytes and dermal-infiltrating mononuclear cells in CHS. Furthermore, mRNAs of VEGFR-1 and VEGFR-2, two key VEGFRs, were strongly expressed by the endothelial cells of the vessels in these skin lesions (8). Others have also observed VEGF overexpression in inflammatory skin diseases (10) and recently, Reinders et al. (11,12) noted VEGF may have an effect on leukocyte recruitment in inflammation. In general, interfering with certain angiogenic pathways has been shown to have direct consequences on the CHS response (7,13,14).

Extensive investigations over the past 10 years on the VEGF signaling pathway have implicated this system to be directly involved in both vasculogenesis and angiogenesis (15). It is for this reason that VEGF and VEGFRs have been examined in diseases characterized by aberrant or pathologic angiogenesis. For example, VEGF expression has been documented in many human solid tumors (16), wounds (17), diabetic retinopathy (18), rheumatoid arthritis (19), and psoriasis (10). Whether discussing angiogenesis in its traditional sense, as the growth of new capillaries from preexisting vessels (20), or as the more recently observed enlargement and elongation of preexisting vessels (7,21), endothelial cell proliferation and vascular hyperpermeability is a shared feature of this process. Interestingly, enlarged and hyperpermeable dermal microvessels are also a consistent feature of skin inflammation associated with CHS reactions (13).

In this study, we utilized an established murine CHS model (22) to analyze VEGF and cytokine production over a 96-h period following elicitation of CHS. Furthermore, we utilized the neutralizing monoclonal antibody DC101, specific for the murine VEGFR-2 homolog that effectively inhibits angiogenesis and suppresses solid tumor growth (23–25), to determine the effect of anti-angiogenic therapy on cell-mediated immunity *in vivo*. Histological findings 24 h after challenge showed remarkable decreases in edema, perivascular infiltration, and vascular enlargement, with a decrease in total vessel areas. Our results improve the understanding of allergic skin disease by giving further insights into the mechanism underlying the inflammatory process as well as suggest a potential novel therapeutic approach to patients suffering from these types of disorders.

Materials and methods

Animals

Female BALB/c mice were obtained from the Charles River Breeding Laboratory (Wilmington, MA, USA) and used at 6–10 weeks of age. Four to six mice were used in each experimental group. Each experiment was repeated at least three times. The animal protocol was approved by the institutional Animal Care and Use Committee.

Reagents

2,4-dinitrofluorobenzene (DNFB), glutaraldehyde, and paraformaldehyde were purchased from Sigma-Aldrich (St. Louis, MO, USA). Fluorescein-*Lycopersicon esculentum* lectin was purchased from Vector Laboratories (Burlingame, CA, USA). The DC101 rat monoclonal antibody directed against murine VEGFR-2 was graciously provided by ImClone Systems Inc., (New York, NY, USA). A control monoclonal rat immunoglobulin (Ig)G1 antibody was purchased from Southern BiotechnologyAssociates, Inc., (Birmingham, AL, USA).

CHS assay

Induction of CHS was conducted as previously described (6,13,26). Briefly, the abdomens of the mice were shaved, and 25 μl of 0.5% DNFB in acetone/olive oil (4:1) was applied to their shaved skin for sensitization. Five days later, mice were challenged by applying 10 μl of 0.2% DNFB to the dorsal surface of the right ear. As a control, the left ear was painted with an identical amount of vehicle alone. The ear thickness was measured at 6, 12, 24, 48, 72, and 96 h after challenge using a Peacock spring-loaded micrometer (Ozaki Co., Tokyo, Japan). Results were expressed as net ear swelling which was calculated by subtracting the thickness of the vehicle-treated ear from the thickness of the hapten-challenged ear.

VEGF protein production on CHS

Ear tissue samples, collected at 6, 12, 24, 48, 72, and 96 h following challenge with DNFB or DNFB vehicle, were prepared as previously described with minor modification (27). Briefly, ear tissue samples were finely chopped on ice, weighed and homogenized in RPMI-1640 culture medium supplemented with 5% fetal calf serum (FCS), 2 mM glutamine, 200 units/ml of penicillin, and 200 μg/ml of streptomysin (RPMI-FCS). The homogenates were snap frozen in liquid nitrogen, brought rapidly to room temperature, and sonicated for 15 s (50 Hz). Supernatants were collected after centrifugation (2000 × *g*, 5 min) and stored at −70°C until analysis. A murine VEGF ELISA kit (R&D

Systems, Minneapolis, MN, USA) was used to quantify the amounts of VEGF protein. Each supernatant was analyzed in duplicate. Results were expressed as VEGF concentration in ng/g tissue for homogenates (28,29).

VEGFR-2 antibody treatment

Previous reports demonstrated that overexpression of VEGF in skin results in increased inflammation (12). As well, injection of VEGF increases vascular hypermeability in the skin (13). We therefore examined the effect of DC101 on the CHS inflammatory response. 800 μg of DC101, the documented effective dose in cancer therapy (24,25,30,31), was administered intraperitoneally (IP) at both 24 h and immediately prior to sensitization with DNFB (32). The same volume of phosphate-buffered saline (PBS) (DC101 vehicle) was administered in the same fashion to another control group.

To determine the effect of DC101 on the elicitation phase, 800 μg of DC101 was administered at both 24 h and immediately prior to challenge. Our treatment regime was based on previous studies (32,33) and our own observation of increased VEGF levels following DNFB challenge (see Results). A control group was injected with the same volume of PBS at the same time intervals for comparison.

PBS was selected because previous DC101 treatment studies demonstrated no statistical difference between PBS-treated animals and non-specific IgG antibody-treated animals (24,25,34). Furthermore, non-specific rat IgG does not effect ear swelling or CHS regulation (28,32,33). Prior to initiating this study, we confirmed that same 800-μg dose of a control monoclonal rat IgG1 antibody (Southern BiotechnologyAssociates, Inc.,) injected IP did not effect the CHS response, similar to PBS (Fig. 1). No overt signs of toxicity were observed in the mice with DC101 treatment (35).

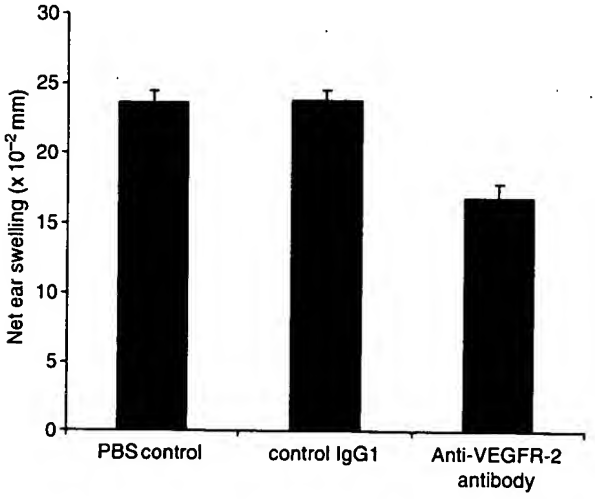

Figure 1. Administration of DC101 prior to challenge suppressed the contact hypersensitivity (CHS) response. BALB/c mice were sensitized by 0.5% 2,4-dinitrofluorobenzene (DNFB) and 5 days later challenged with 0.2% DNFB on the ears. Mice were treated with 800 μg DC101, immunoglobulin (Ig)G1 rat isotype control, or phosphate-buffered saline (PBS) (DC101 control vehicle) intraperitoneally at 24 h and immediately before challenge and ear swelling responses were measured 24 h after challenge. The CHS response was significantly decreased by 28.8 and 29.1% in the DC101-treated mice compared to the PBS control mice and IgG1 control, respectively. The data represents the mean ± SEM ($n = 15$; $P < 0.001$). VEGFR, vascular endothelial growth factor receptor.

Histologic examination

Ear tissue from the DC101-treated and control mice was collected 24 h after challenge and fixed in 10% formalin. Slides were prepared for routine histology and stained with hematoxylin and eosin. The slides were examined by light microscopy, and the histological changes including the density of dermal infiltration were compared between the groups. A cell count was performed on each slide in 10 random high-power fields with a ×40 objective (net magnification ×400) in order to calculate the mean dermal cellular infiltrate in areas of each ear.

Intravascular fluorescein isothiocyanate (FITC)-lectin injection and quantification of blood vessel formation

Vascular perfusions and morphometric analysis of blood vessels were conducted as previously described with slight modification (7,36). DC101 ($n = 3$) and PBS ($n = 3$) prior-to-challenge-treated mice were anesthetized with pentobarbital sodium (50 mg/kg IP; Abbott Laboratories; Abbott Park, IL, USA) 24 h after elicitation, and Fluorescein-*Lycopersicon esculentum* lectin was injected into the tail veins. Five minutes later, the animals' chests were opened and the tissues were fixed by perfusion of 0.5% glutaraldehyde and 1% paraformaldehyde in PBS using a left ventricle intravenous catheter. The right atrium of heart was cut and washed free of blood. Ear tissue samples were taken and rinsed in PBS, and then rinsed in 15% sucrose in PBS.

The tissue was placed on glass slides and visualized using confocal microscopy (Zeiss LSM 410 confocal microscope). Tagged image file format (TIFF) images were obtained and analyzed using Image Pro-Plus 5.1® software (Media Cybernetics, Silver Spring, MA, USA) (37,38). Briefly, the FITC-lectin histochemistry evaluation was made through the Color Segmentation analysis, which extracts objects by locating all vessels of the specified color(s) and setting everything else to black. In this way, we measured the total area of the blood vessels. Because of lectin's specificity for endothelial glycoproteins, our measurements do not reflect vascular hyperpermeability or any fluorescein that may have extravasated into the extravascular space (36,39). We counted three different fields in each of the three sample examined, and the total blood vessels area in 1.4 million μm^2 of each ear was determined.

Quantitative reverse-transcription and real time polymerase chain reaction (PCR)

Ear tissue from the DC101-treated and control mice were collected 24 h following epicutaneous hapten challenge. Total RNA was isolated from each ear specimen with an acid guanidinium thiocyanate-phenol-chloroform method and immediately treated with DNAse to remove traces of genomic DNA. First-strand cDNA was prepared from the isolated total RNA using AncT oligo primer [dT_{20}VN] (Invitrogen, CA, USA) and Superscript RNase H$^-$ reverse transcriptase (Gibco-BRL, Gaithersburg, MD, USA). Quantitative real-time PCR with SYBR ®Green I (Molecular Probes Inc., Eugene, OR, USA) was performed using i-Cycler IQ™ Real-Time Detection System instrument and soft ware (Bio-Rad Laboratories, Inc., Hercules, CA, USA). Relative expressions of IFN-γ, interleukin (IL)-4 and IL-10 target genes to the β-actin control housekeeping gene were measured using a threshold cycle number. The primer sequences were as follows: IFN-γ, upstream 5′-ATGAACGCTACACACTGAT-3′, downstream 5′-TTCAGACTTTCTAGGCTTTC-3′; IL-4, upstream 5′-ATGGGTCTCAACCCCCAGCT-3′, downstream 5′-ATGATCTCTCTCAAGTGATT-3′; IL-10, upstream 5′-GTCATCG ATTTCTCCCCTGTG-3′; downstream 5′-ATGGCCTTGTA GACACCTTGG-3′; β-actin, upstream 5′-ATGGGTCAGAAG

GACTCCTA-3', downstream 5'-TCCCAGTTGGTAACAAT-GCC-3'. Each PCR mixture contained a final concentration of 1 × PCR buffer, 200 μM each of dNTPs, 2 μM of each forward and reverse primer, 2.5 units Ampli Platinum Taq polymerase (Invitrogen), 3.5 mM $MgCl_2$, and 1/100 000 SYBR Green® I. The two-step PCR conditions included an initial 5 min at 94°C, followed by 40 cycles of 15 s at 94°C and 60 s at 65°C. A melting curve was performed upon the completion of the 40 cycles to validate amplification product specificity. Furthermore, PCR products were confirmed 3% agarose gel electrophoresis. cDNA amplification was carried out in a 96-well reaction plate, and all PCRs were performed in triplicate.

Quantitation of IFN-γ protein by enzyme-linked immunosorbent assay (ELISA)

Ear skin lysates were collected from DC101-treated and control mice 24 h after challenge for IFN-γ quantification. IFN-γ protein was quantified using a sandwich ELISA method with a murine IFN-γ ELISA kit (R&D Systems). Each supernatant was analyzed in duplicate. Results were expressed as IFN-γ concentration in ng/g tissue for homogenates (28,29).

Statistical analysis

Data are expressed as the mean ± SEM. The statistical significance of differences between the means was determined by applying the Student's *t*-test. Statistical significance was defined by $P < 0.05$.

Results

VEGF protein levels increase during the elicitation phase of CHS

Mice were sensitized with 0.5% DNFB and challenged 5 days later with 0.2% DNFB. The CHS response, measured by ear swelling, was recorded at 6, 12, 24, 48, 72, and 96 h after challenge. Ear swelling peaked between 24 and 48 h following challenge. The response then weakened and gradually disappeared by 96 h (Fig. 2a).

We obtained skin lysates at the same time intervals from both challenged and unchallenged ears after ear swelling measurements and analyzed VEGF protein levels during the CHS elicitation phase. VEGF protein was detected at 6 h and peaked between 24 and 48 h after challenge. The production of VEGF gradually decreased from 48 to 96 h after challenge (Fig. 2b). No VEGF was detected in the unchallenged skin tissue during this time (data not shown).

In general, the CHS response is characterized by a rapid increase in inflammatory mediators and cellular infiltration that peak between 24 and 48 h after challenge (2,40). After 24 h, the negative regulatory effects of the Th2/Tc2 cells are thought to be responsible for intensifying and modulating the inflammatory reaction (41–43). The inflammatory mediators gradually decrease and dissipate from the challenged site over the subsequent 48–72 h. Our studies demonstrated that the protein levels of VEGF follow this same paradigm during the elicitation phase of CHS.

VEGF levels were not measured in animals that received DC101 treatment prior to CHS sensitization or in unsensitized DNFB ear-challenged mice because no significant difference was observed in CHS response compared to vehicle-treated control groups.

CHS is reduced in animals treated with DC101 prior to the elicitation phase

To investigate whether VEGF is functionally relevant to the elicitation of CHS, VEGF signaling was neutralized by anti-VEGFR-2 antibody (DC101) administration. When DC101 was injected 24 h

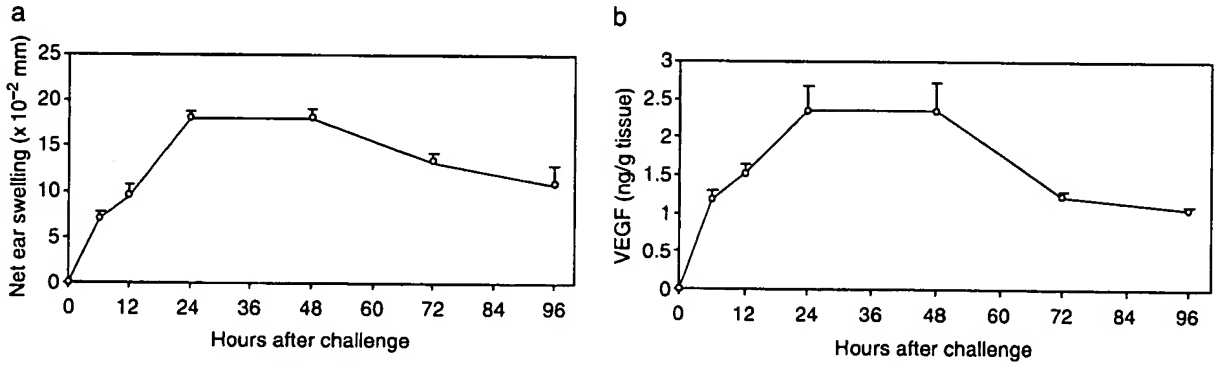

Figure 2. Protein levels of vascular endothelial growth factor (VEGF) increase during the elicitation phase of contact hypersensitivity. BALB/c mice were sensitized with 0.5% 2,4-dinitrofluorobenzene (DNFB) and 5 days later were challenged with 0.2% DNFB on the ears. (a) Ear-swelling responses determined at various time points following challenge. Results are expressed as net ear swelling, calculated by subtracting the thickness of the vehicle-treated ear from the thickness of the hapten-challenged ear. (b) VEGF protein concentrations in challenged ear skin at each time point as measured by enzyme-linked immunosorbant assay analysis. VEGF protein levels increase over the first 24–48 h after challenge and gradually decrease by 96 h. No VEGF was detected in the skin tissue exact from unchallenged mice during this time.

and immediately before elicitation, ear-swelling responses 24 h after challenge to DNFB were suppressed by 28.8 and 29.1% compared to the PBS-control group and isotype-matched antibody-treated group, respectively ($P < 0.001$) (Fig. 1). The effects of DC101 treatment at 48 h after challenge were not evaluated in this study.

We examined the effect of DC101 administration prior to CHS sensitization. However, when DC101 was injected prior to sensitization, ear-swelling responses 24 h after challenge were not significantly suppressed (data not shown). We also examined the animals' ear-swelling response to DNFB challenge without prior sensitization, as the challenge dose used could potentially induce a considerable amount of inflammation. Ear swelling measured at 24 h after challenge was no different that the vehicle-treated ear (data not shown).

DC101 suppresses the inflammatory histopathologic changes observed in CHS

To further confirm the functional relevance of DC101 treatment in CHS, we examined the histopathology of the ear tissue following challenge. At 24 h after challenge, ear samples were taken from both DC101- and PBS-treated mice. The control tissue showed marked mononuclear cell infiltrates, pronounced edema, and enhanced vascular enlargement. Histological examination revealed that the infiltrate was primarily composed of mononuclear cells. Injection of DC101 before challenge led to a significant inhibition in the above findings (Fig. 3). This data suggest that VEGFR-2 signaling may contribute to the mechanisms of edema formation and cellular infiltration in this inflammatory reaction.

DC101 treatment decreases inflammatory cell infiltration

The dermal infiltrate was quantified by examining 10 randomly selected high-power fields (net magnification ×400) in representative areas of each ear. The number of infiltrated cells in the dermis was significantly reduced (DC101: 381 ± 23.6; control: 244 ± 9.03; mean ± SEM; $P < 0.001$) by DC101 treatment, suggesting DC101 could function by prohibiting the extravasations of inflammatory cells (11).

Total vessel area is decreased in DC101-treated mice

The total area of the vessels in the ear skin was examined to determine the effect of DC101 therapy on the vasculature in CHS. Intravascular FITC-lectin injection was utilized to compare the blood vessel architecture with and without treatment. When injected into the circulation via the tail vein, the lectins non-specifically bind to glycoprotein on the surface of endothelial cells allowing for the direct visualization of the vasculature. Upon examination, the vessels in the DC101-treated animals appeared smaller and shorter 24 h after challenge with DNFB compared to the control group (Fig. 4a–d). The total vessel area was decreased when quantified using the Image Pro-Plus 5.1® software (Fig. 4e), indicating a reduction in angiogenesis in the DC101-treated, inflamed tissue. The vessel areas in the unchallenged and vehicle-challenged ears were comparable to the DC101-treated ears.

Relative expression of IFN-γ, IL-4, and IL-10 mRNA to β-actin

IFN-γ is recognized as the main effector cytokine in CHS, while IL-4 and IL-10 have been implicated in CHS inhibition (4,6). Total RNA was extracted from the skin tissue 24 h after challenge with DNFB. The relative expression of IFN-γ mRNA to β-actin was significantly decreased in the ear skin of mice treated with DC101 prior to challenge compared to the control group when examined using quantitative reverse transcription real time PCR. We observed no significant difference in the relative expressions of IL-4 and IL-10 mRNA to β-actin between the two groups (Table 1).

IFN-γ protein levels are decreased in the elicitation phase of CHS

Similar to mRNA levels, the IFN-γ protein level was decreased at 24 h after challenge in the ear skin of the DC101-treated mice compared to the control mice when measured by ELISA (Fig. 5). These findings demonstrate that the level of IFN-γ message correlates well with the IFN-γ protein level.

Discussion

VEGF (now denoted VEGF-A) was originally described as a vascular permeability factor (44) and as an endothelial cell mitogen (45). The VEGF family currently includes VEGF-A, -B, -C, -D, -E, and placenta growth factor (PlGF) (46). VEGF can be produced by a variety of cell types, including different tumor cells and activated macrophages (47). These VEGF family proteins bind in a distinct pattern to three structurally related receptor tyrosine kinases denoted VEGF receptor-1, -2, -3 (46). While VEGFR-1 and VEGFR-2 are expressed on endothelial cells,

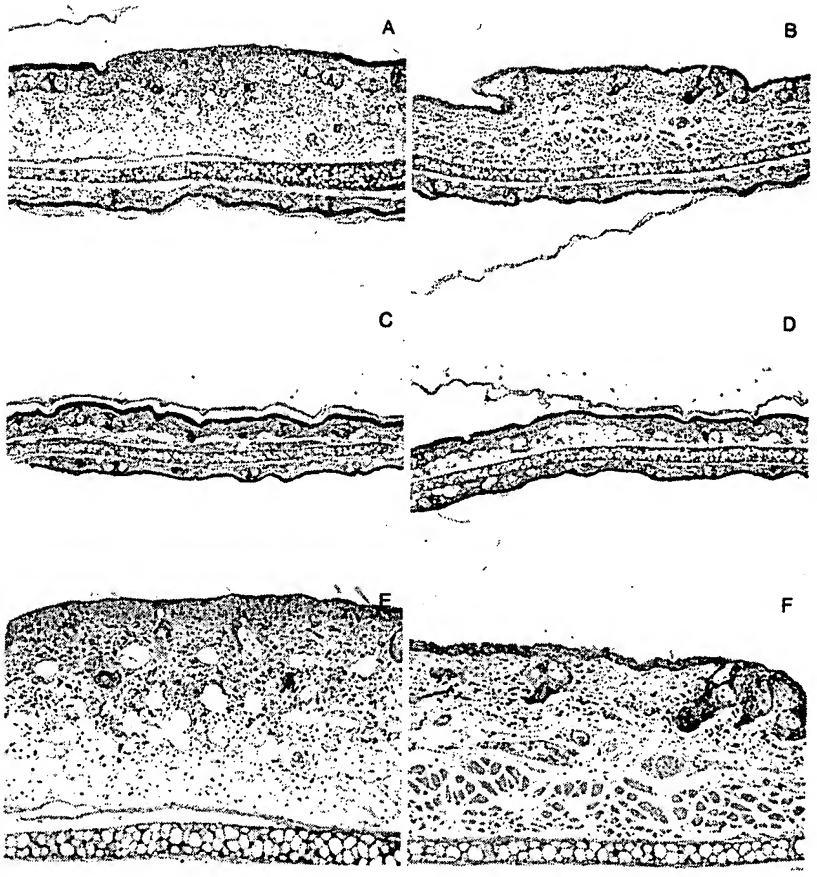

Figure 3. DC101 treatment induces changes in the hisopathologic features typically observed in contact hypersensitivity. (a) Hematoxylin and eosin-stained ear tissue sections obtained 24 h after dinitrofluorobenzene (DNFB) challenge from a phosphate-buffered saline (PBS) control-treated mouse and (b) from a mouse treated with DC101 prior to the elicitation phase. (a) Marked inflammatory infiltration, pronounced edema, vascular enlargement, and exocytosis are typical histopathologic features observed in the epidermis following epicutaneous hapten challenge. (b) With DC101, decreased edema and inflammatory infiltration results. The left ear painted with an identical amount of DNFB vehicle in a (c) PBS-treated mouse and (d) DC101-treated mouse. Both show no remarkable changes. Net magnification: (a–d) (×100). High magnification of hematoxylin and eosin-stained ear tissue sections obtained 24 h after DNFB challenge from a (e) PBS control-treated mouse and (f) mouse treated with DC101 prior to the elicitation phase. (e) High magnification of panel Fig. 3(a). (f) High magnification of panel Fig. 3(b). Hematoxylin/eosin stains were used to produce panels a–f. Net magnification: (e, f) (×200).

monocytes, and hematopoietic precursors, VEGFR-3 is only expressed on the endothelial cells of lymphatic vessels (46). The levels of VEGFR-1 and VEGFR-2 mRNA are significantly increased in the vessels feeding tumors compared to the vessels of normal tissues surrounding the malignancies. Furthermore, a similar pattern of expression appears to be present in non-tumorigenic diseases (46,48).

VEGF activity and signaling through VEGFRs is mediated in a paracrine fashion (46). In general, the VEGF proteins are poor mitogens. Binding of VEGF-A to VEGFR-2 has been shown to increase survival, and stimulate migration and differentiation of endothelial cells, as well as mediate vascular permeability. VEGFR-1, on the other hand, may act either as a decoy receptor or by suppressing signaling through VEGFR-2 (30,46). Although VEGFR-1 and -2 have been shown to be important in the regulation of vasculogenesis and physiological angiogenesis, signaling through VEGFR-2 is thought to be more important because it is essential for the induction of the full spectrum of VEGF functions (46).

The hypothesis that VEGF might be involved in the pathogenesis of CHS initially arose from a number of observations suggesting a close interrelationship between chronic inflammation and the angiogenic process (49). A number of growth factors, cytokines, and inflammatory mediators were noted to promote migration and proliferation of endothelial cells (44,45,50), while several other inflammatory cytokines including IL-1, IL-6, tumor necrosis factor (TNF)-α were also able to stimulate VEGF expression (51–53). VEGF, in turn, stimulates the synthesis of platelet-activating factors (PAF) in endothelial cells in the skin leading to enhanced angiogenesis (54).

Further evidence of an angiogenesis-CHS relationship was presented by Brown et al. (8,9) who proposed a direct contribution for VEGF and VEGFRs in this immune response. Recently, two other angiogenetic factors, thrombospondin-2 and PlGF, have also been implicated in CHS (7,13). Clearly, the mounting evidence points to a role of angiogenesis and its mediators in the CHS response. Further clarifying these mechanisms will be essential in providing useful framework for understanding this disease and other inflammatory conditions as well as potentially identifying new targets for therapeutic intervention (4).

Therefore, to clarify the role of VEGF in this delayed-type immune response, we examined the

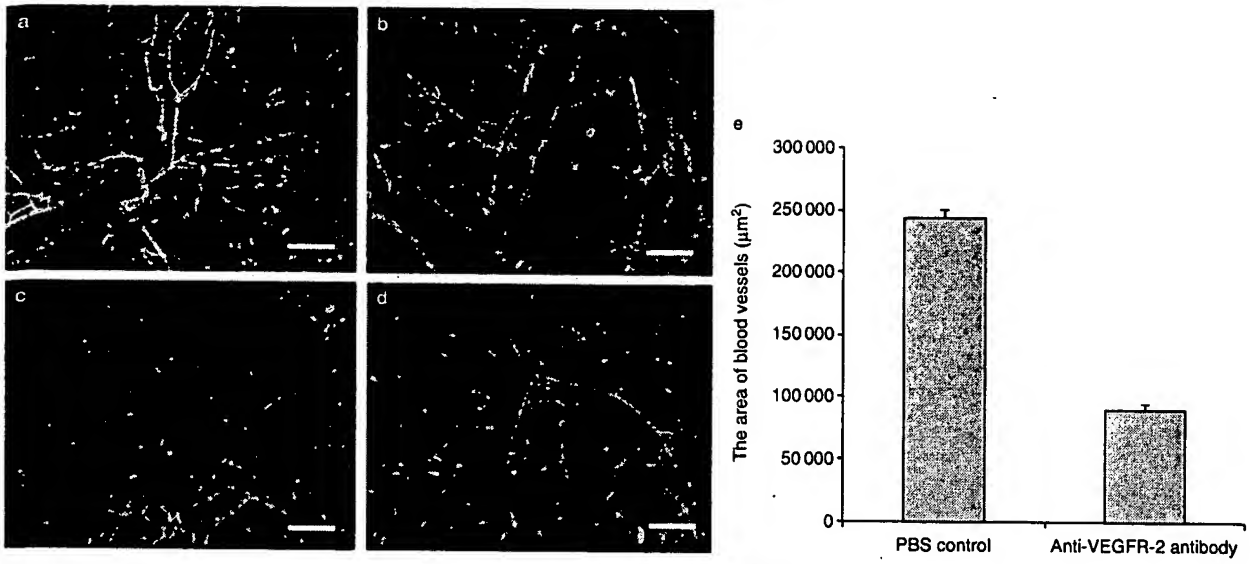

Figure 4. Angiogenesis was suppressed by the injection of DC101. Fluorescein-*Lycopersicon esculentum lectin* was injected into phosphate-buffered saline (PBS)- and DC101-treated mice, and blood vessel formation was visualized by confocal microscopy. Vascular enlargement and elongation were decreased in (b) DC101-treated mice compared to the (a) PBS-control group. (c) Unchallenged ears from the PBS-treated mice and (d) unchallenged ears from the DC101-treated mice, both showed no remarkable changes. Scale Bar = 183 μm. (e) The total blood vessel area was decreased by 63.5% in DC101-treated mice compared to the PBS-control group following challenge. The fluorescein isothiocyanate-lectin histochemistry evaluation was made by color segmenta- tion analysis using Image Pro-Plus 5.1® software. Three different fields in three samples were examined from each group, and the total blood vessel area in 1.4 million μm^2 of each ear was measured ($P < 0.001$). VEGFR, vascular endothelial growth factor receptor.

direct effect of anti-VEGFR-2 antibody (DC101) treatment on CHS. CHS is a DC-dependent, T-cell-derived, cytokine-mediated inflammatory skin disease (4). CHS assays were performed in an established murine model that closely resembles the analogous human process (6,13,26). We demonstrated that DC101 significantly reduced CHS by 28.8% at 24 h after challenge when administered prior to the elicitation phase. Kunstfeld et al. (55) demonstrated that the administration of both anti-VEGFR-1 antibody and anti-VEGFR-2 antibody before sensitization and every three days thereafter inhibited the CHS reaction. These findings suggest that both VEGFR-1 and VEGFR-2 are necessary for sensitization. In general, it is thought that APCs predominantly express VEGFR-1, not VEGFR-2 (46). DC101 treatment was ineffective in modulating the CHS response when administered prior to sensitization. Our findings suggest that VEGFR-2 signaling plays a role in the infiltration of inflammatory cells in the elicitation phase.

Histopathologic examination confirmed that the pronounced edema and inflammatory cell infiltration normally present in the CHS response was decreased in the challenged skin of the DC101-treated animals. Our findings reflect a decrease in vascular permeability and further indicated that VEGF-VEGFR-2 system is involved in edema formation and cutaneous inflammation in the CHS response. VEGF induces the formation of fenestrations in blood vessels (56,57) and the formation of vesiculo-vascuolar organelles that form channels through which blood-borne proteins can extravasate (58). This leads to the formation of an extravascular fibrin gel that provides a matrix to support the growth of endothelial cells (59). Oura et al. (13) demonstrated a significant increase of vascular permeability after intradermal injection of VEGF into mouse ears compared to PBS control-treated tissue. These observations support the idea that a marked increase in vascular leakage in inflamed skin could contribute to edema formation. Blocking VEGFR-2 could therefore prevent the formation of blood vessel fenestrations and the vesiculo-vascuolar organelles that form channels. The result, as we observed in our CHS study using anti-VEGFR-2 antibody, would be a decrease in permeability with less inflammatory swelling and edema.

When FITC-lectin was injected intravascularly and tissue sections analyzed by confocal microscopy, we observed a decrease in total area of vessels in the challenged tissue of DC101-treated animals. This suggests that VEGFR-2 signaling is involved in angiogenesis and the regulation of inflammatory vascular remodeling. As stated, angiogenesis is defined as both the growth of new capillaries from preexisting vessels (20) and the

Table 1. Interferon (IFN)-γ mRNA expression was down-regulated in the challenged ear skin of DC101-treated animals. No significant difference in interleukin (IL)-4 and IL-10 mRNA expression was noted. The level of mRNA for IFN-γ, IL-4, and IL-10 was measured by real time reverse trandcriptase polymerse chain reaction and expressed as a ratio relative to β-actin mRNA in each sample. The data is expressed as the mean ± SEM of eight experiments performed in triplicate.

	Analyzed	IFN-γ	IL-4	IL-10
DC101-treated group	8	0.651 ± 0.219*	0.06 ± 0.018	0.068 ± 0.016
Control group	8	1.799 ± 0.462*	0.128 ± 0.045	0.148 ± 0.038

*$P < 0.05$.

enlargement and elongation of preexisting vessels (7,21). VEGFR-2 blockade could prevent vascular enlargement as well as the vascular abnormalities usually present in inflammation and the CHS response (21), although a vasoconstrictive effect cannot be excluded (13,60). Our findings also support the recent observation that increases in vessel size are more sensitive target for angiogenesis inhibition than vessel density (i.e. number of vessels) or sprouting in inflammatory disorders (7,61).

Previous reports explained that the recruitment of leukocytes from the blood into tissues requires a cascade of molecular events that mediate leukocyte rolling, adhesion, and extravasation in postcapillary venules (62). Overexpression of VEGF in the skin is known to enhance leukocyte rolling and adhesion in postcapillary venules. VEGF has, therefore, been considered important in recruiting leukocytes to sites of inflammation (12). Recently, Reinders et al. (11) demonstrated that VEGF effects the trafficking of human T cells into skin allografts *in vivo*. They provided evidence that early VEGF expression promotes T-cell and monocyte recruitment. This finding is consistent with our results that DC101 could prevent mononuclear cell infiltration. Accordingly, blocking VEGFR-2 may not only alter vessel permeability but also prevents specific cell adhesion, and chemotactic mechanisms leading to decreased recruitment and hence, inflammation.

On the other hand, VEGFR-1 has also been implicated in cell recruitment. VEGF is able to stimulate monocyte/macrophage migration through endothelial monolayers using VEGFR-1 signaling (63). Recently, VEGFR-1's importance was again recognized when Luttun et al. (64) reported anti-VEGFR-1 antibody inhibited angiogenesis in tumors and inflammatory disorders. In our study, DC101 treatment appears to affect the dermal vasculature in the challenge site by decreasing vascular enlargement and permeability. Furthermore, VEGFR-2 blockade may also be inhibiting the leukocyte recruitment that is important in the CHS response (11). Further research will clarify the roles of VEGFR-1 and VEGFR-2 in leukocytes migration.

The Th1 cytokine, IFN-γ is a main effector cytokine in the elicitation of CHS, while the Th2 cytokines, IL-4 and IL-10 have been shown to negatively regulate these reactions (4,6). As such, CHS can theoretically be suppressed by down-regulating IFN-γ expression and augmenting IL-4 and IL-10 activity. We demonstrated that DC101 treatment prior to elicitation suppressed the relative expression of IFN-γ mRNA and protein quantity in the ear skin following challenge. Administration of DC101 could function by reducing inflammatory cell migration and hence IFN-γ expression during the CHS response.

Although a wide range of cytokines including TNF-α, transforming growth factor-β, IL-1β, and IL-6 is also known to stimulate the expression of VEGF-A (in some cases through increased VEGF-A mRNA stability) (51,53,65,66), the literature on IFN-γ's role in angiogenesis is controversial and mainly purported from observations in *in vitro* studies (53,67,68). Most likely, the decrease in IFN-γ corresponds to a decreased source of this pro-inflammatory cytokine's production, with a decreased inflammatory infiltrate following DC101 treatment.

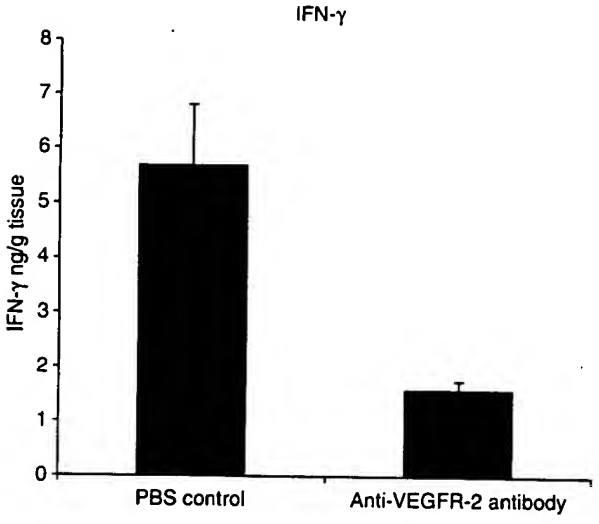

Figure 5. Administration of DC101 inhibits interferon (IFN)-γ protein production. Challenged ear skin lysates from DC101-treated and control mice were obtained, and IFN-γ concentration was measured using a specific murine ELISA kit. DC101 treatment suppressed protein production by 72.1% when measure at 24 h following challenge with dinitrofluorobenzene. The data are expressed as the mean ± SEM obtained from two groups of five mice ($P < 0.01$). PBS, Phosphate-buffered saline; VEGFR, vascular endothelial growth factor receptor.

In summary, the present study demonstrates anti-VEGFR-2 antibody significantly reduces the formation of angiogenesis and prevents cellular infiltration and edema formation in CHS at 24 h after challenge when administered prior to the elicitation phase. DC101 seems to alter the dermal vasculature in the challenge site, affecting both vascular permeability and enlargement, and interfering with the migration of inflammatory cells that are important to the immune response. Hence, levels of the main effector cytokine, IFN-γ, were also decreased in CHS with anti-VEGFR-2 antibody treatment. Further elucidation of the VEGF-VEGFR systems in the body will lead to the development of new strategies for suppressing and controlling major diseases in humans. Studies using antisense VEGF mRNA, neutralizing monoclonal VEGF antibodies, neutralizing soluble VEGF receptors, and Flk-1/KDR kinase inhibitors have already been performed and demonstrated their ability to inhibit angiogenesis (15,16,23). The precise molecular mechanisms targeted by these agents in blocking the VEGF-VEGFR system differ. Future research will focus on matching the treatment to the disease and determine which approach is most appropriate to control pathogenic angiogenesis in specific settings (15).

Acknowledgements

We thank Shan Man, Helen Santana, Naoko Sakamoto, and Hiroyuki Nambu for additional excellent technical advice and assistance with our study.

References

1. Bell D, Young J W, Banchereau J. Dendritic cells. Adv Immunol 1999: 72: 255–324.
2. Belsito D V. Allergic Contact Dermatitis. In: Freedberg I M, Eisen A Z, Wolff K, Austen K F, Goldsmith L A, Katz S I, Fitzpatrick T B, eds. Fitzpatrick's dermatology in general medicine. 5th edn. McGraw-Hill, USA, 2001: 1447–1461.
3. Wang B, Feliciani C, Howell B G et al. Contribution of Langerhans cell-derived IL-18 to contact hypersensitivity. J Immunol 2002: 168: 3303–3308.
4. Watanabe H, Unger M, Tuvel B, Wang B, Sauder D N. Review: contact hypersensitivity: the mechanism of immune responses and T cell balance. J Interferon Cytokine Res 2002: 22: 407–412.
5. Grabbe S, Schwarz T. Immunoregulatory mechanisms involved in elicitation of allergic contact hypersensitivity. Immunol Today 1998: 19: 37–44.
6. Wang B, Fujisawa H, Zhuang L et al. $CD4^+$ Th1 and $CD8^+$ type 1 cytotoxic T cells both play a crucial role in the full development of contact hypersensitivity. J Immunol 2000: 165: 6783–6790.
7. Lange-Asschenfeldt B, Weninger W, Velasco P et al. Increased and prolonged inflammation and angiogenesis in delayed-type hypersensitivity reactions elicited in the skin of thrombospondin-2 – deficient mice. Blood 2002: 99: 538–545.
8. Brown L F, Olbricht S M, Berse B et al. Overexpression of vascular permeability factor (VPF/VEGF) and its endothelial cell receptors in delayed hypersensitivity skin reactions. J Immunol 1995: 154: 2801–2807.
9. Staquet M J, Godefroy S, Jacquet C, Viac J, Schmitt D. Vascular endothelial growth factor (VEGF) induces human Langerhans cell migration. Arch Dermatol Res 2001: 293: 26–28.
10. Detmar M, Brown L F, Claffey K P et al. Overexpression of vascular permeability factor/vascular endothelial growth factor and its receptors in psoriasis. J Exp Med 1994: 180: 1141–1146.
11. Reinders M E, Sho M, Izawa A et al. Proinflammatory functions of vascular endothelial growth factor in alloimmunity. J Clin Invest 2003: 112: 1655–1665.
12. Detmar M, Brown L F, Schon M P et al. Increased microvascular density and enhanced leukocyte rolling and adhesion in the skin of VEGF transgenic mice. J Invest Dermatol 1998: 111: 1–6.
13. Oura H, Bertoncini J, Velasco P, Brown L F, Carmeliet P, Detmar M. A critical role of placental growth factor in the induction of inflammation and edema formation. Blood 2003: 101: 560–567.
14. Dupont E, Wang B, Mamelak A J et al. Modulation of the contact hypersensitivity response by AE-941 (Neovastat), a novel antiangiogenic agent. J Cutan Med Surg 2003: 7: 208–216.
15. Shibuya M. Structure and function of VEGF/VEGF-receptor system involved in angiogenesis. Cell Struct Funct 2001: 26: 25–35.
16. Kim K J, Li B, Winer J et al. Inhibition of vascular endothelial growth factor-induced angiogenesis suppresses tumour growth in vivo. Nature 1993: 362: 841–844.
17. Brown L F, Yeo K T, Berse B et al. Expression of vascular permeability factor (vascular endothelial growth factor) by epidermal keratinocytes during wound healing. J Exp Med 1992: 176: 1375–1379.
18. Aiello L P, Avery R L, Arrigg P G et al. Vascular endothelial growth factor in ocular fluid of patients with diabetic retinopathy and other retinal disorders. N Engl J Med 1994: 331: 1480–1487.
19. Kasama T, Shiozawa F, Kobayashi K et al. Vascular endothelial growth factor expression by activated synovial leukocytes in rheumatoid arthritis: critical involvement of the interaction with synovial fibroblasts. Arthritis Rheum 2001: 44: 2512–2524.
20. Risau W. Mechanisms of angiogenesis. Nature 1997: 386: 671–674.
21. Carmeliet P. Mechanisms of angiogenesis and arteriogenesis. Nat Med 2000: 6: 389–395.
22. Galli S J, Hammel I. Unequivocal delayed hypersensitivity in mast cell-deficient and beige mice. Science 1984: 226: 710–713.
23. Prewett M, Huber J, Li Y et al. Antivascular endothelial growth factor receptor (fetal liver kinase 1) monoclonal antibody inhibits tumor angiogenesis and growth of several mouse and human tumors. Cancer Res 1999: 59: 5209–5218.
24. Klement G, Baruchel S, Rak J et al. Continuous low-dose therapy with vinblastine and VEGF receptor-2 antibody induces sustained tumor regression without overt toxicity. J Clin Invest 2000: 105: R15–R24.
25. Jung Y D, Mansfield P F, Akagi M et al. Effects of combination anti-vascular endothelial growth factor

receptor and anti-epidermal growth factor receptor therapies on the growth of gastric cancer in a nude mouse model. Eur J Cancer 2002: 38: 1133–1140.
26. Gaspari A A, Katz S I. Contact Hypersensitivity. In: Coligan J E, Kruisbeek A M, Margulies D H, Shevach E M, Strober W, eds. Current Protocols in Immunology. John Wiley & Sons, Inc., USA, 1998: 4.2.1–4.2.5.
27. Kermani F, Flint M S, Hotchkiss S A. Induction and localization of cutaneous interleukin-1 beta mRNA during contact sensitization. Toxicol Appl Pharmacol 2000: 169: 231–237.
28. Ferguson T A, Dube P, Griffith T S. Regulation of contact hypersensitivity by interleukin-10. J Exp Med 1994: 179: 1597–1604.
29. Kitagaki H, Ono N, Hayakawa K, Kitazawa T, Watanabe K, Shiohara T. Repeated elicitation of contact hypersensitivity induces a shift in cutaneous cytokine milieu from a T helper cell type 1 to a T helper cell type 2 profile. J Immunol 1997: 159: 2484–2491.
30. Kunkel P, Ulbricht U, Bohlen P et al. Inhibition of glioma angiogenesis and growth in vivo by systemic treatment with a monoclonal antibody against vascular endothelial growth factor receptor-2. Cancer Res 2001: 61: 6624–6628.
31. Shaheen R M, Ahmad S A, Liu W et al. Inhibited growth of colon cancer carcinomatosis by antibodies to vascular endothelial and epidermal growth factor receptors. Br J Cancer 2001: 85: 584–589.
32. Kondo S, Pastore S, Fujisawa H et al. Interleukin-1 receptor antagonist suppresses contact hypersensitivity. J Invest Dermatol 1995: 105: 334–338.
33. Schwarz A, Grabbe S, Riemann H et al. In vivo effects of interleukin-10 on contact hypersensitivity and delayed-type hypersensitivity reactions. J Invest Dermatol 1994: 103: 211–216.
34. Bruns C J, Liu W, Davis D W et al. Vascular endothelial growth factor is an in vivo survival factor for tumor endothelium in a murine model of colorectal carcinoma liver metastases. Cancer 2000: 89: 488–499.
35. Witte L, Hicklin D J, Zhu Z et al. Monoclonal antibodies targeting the VEGF receptor-2 (Flk1/KDR) as an anti-angiogenic therapeutic strategy. Cancer Metastasis Rev 1998: 17: 155–161.
36. Thurston G, Murphy T J, Baluk P, Lindsey J R, McDonald D M. Angiogenesis in mice with chronic airway inflammation: strain-dependent differences. Am J Pathol 1998: 153: 1099–1112.
37. Mori K, Duh E, Gehlbach P et al. Pigment epithelium-derived factor inhibits retinal and choroidal neovascularization. J Cell Physiol 2001: 188: 253–263.
38. Ando A, Yang A, Nambu H, Campochiaro P A. Blockade of nitric-oxide synthase reduces choroidal neovascularization. Mol Pharmacol 2002: 62: 539–544.
39. Thurston G, Baluk P, Hirata A, McDonald D M. Permeability-related changes revealed at endothelial cell borders in inflamed venules by lectin binding. Am J Physiol 1996: 271: H2547–H2562.
40. Cohen L M, Skopicki D K, Harrist T J, Clark Jr, W H. Noninfectious Vesiculobullous and Vesiculopustular diseases. In: Elder D, Elenitsas R, Jaworsky C, Johnson B Jr, eds. Lever's Histopathology of the Skin. 8th edn. Lippincott-Raven Publishers, Philadelphia. 1997: 209–252.
41. Weigmann B, Schwing J, Huber H et al. Diminished contact hypersensitivity response in IL-4 deficient mice at a late phase of the elicitation reaction. Scand J Immunol 1997: 45: 308–314.
42. Yokozeki H, Ghoreishi M, Takagawa S et al. Signal transducer and activator of transcription 6 is essential in the induction of contact hypersensitivity. J Exp Med 2000: 191: 995–1004.
43. Yokozeki H, Wu M H, Sumi K et al. Th2 cytokines, IgE and mast cells play a crucial role in the induction of para-phenylenediamine-induced contact hypersensitivity in mice. Clin Exp Immunol 2003: 132: 385–392.
44. Senger D R, Galli S J, Dvorak A M, Perruzzi C A, Harvey V S, Dvorak H F. Tumor cells secrete a vascular permeability factor that promotes accumulation of ascites fluid. Science 1983: 219: 983–985.
45. Ferrara N, Henzel W J. Pituitary follicular cells secrete a novel heparin-binding growth factor specific for vascular endothelial cells. Biochem Biophys Res Commun 1989: 161: 851–858.
46. Matsumoto T, Claesson-Welsh L. VEGF receptor signal transduction. Sci STKE 2001: 2001: RE21.
47. Yano S, Herbst R S, Shinohara H et al. Treatment for malignant pleural effusion of human lung adenocarcinoma by inhibition of vascular endothelial growth factor receptor tyrosine kinase phosphorylation. Clin Cancer Res 2000: 6: 957–965.
48. Sato K, Yamazaki K, Shizume K et al. Stimulation by thyroid-stimulating hormone and Grave's immunoglobulin G of vascular endothelial growth factor mRNA expression in human thyroid follicles in vitro and flt mRNA expression in the rat thyroid in vivo. J Clin Invest 1995: 96: 1295–1302.
49. Jackson J R, Seed M P, Kircher C H, Willoughby D A, Winkler J D. The codependence of angiogenesis and chronic inflammation. FASEB J 1997: 11: 457–465.
50. Oberg C, Waltenberger J, Claesson-Welsh L, Welsh M. Expression of protein tyrosine kinases in islet cells: possible role of the Flk-1 receptor for beta-cell maturation from duct cells. Growth Factors 1994: 10: 115–126.
51. Cohen T, Nahari D, Cerem L W, Neufeld G, Levi B Z. Interleukin-6 induces the expression of vascular endothelial growth factor. J Biol Chem 1996: 271: 736–741.
52. Ben-Av P, Crofford L J, Wilder R L, Hla T. Induction of vascular endothelial growth factor expression in synovial fibroblasts by prostaglandin E and interleukin-1: a potential mechanism for inflammatory angiogenesis. FEBS Lett 1995: 372: 83–87.
53. Trompezinski S, Denis A, Vinche A, Schmitt D, Viac J. IL-4 and interferon-gamma differentially modulate vascular endothelial growth factor release from normal human keratinocytes and fibroblasts. Exp Dermatol 2002: 11: 224–231.
54. Montrucchio G, Lupia E, Battaglia E et al. Platelet-activating factor enhances vascular endothelial growth factor-induced endothelial cell motility and neoangiogenesis in a murine matrigel model. Arterioscler Thromb Vasc Biol 2000: 20: 80–88.
55. Kunstfeld R, Hirakawa S, Hong Y K et al. Induction of cutaneous delayed-type hypersensitivity reactions in VEGF-A transgenic mice results in chronic skin inflammation associated with persistent lymphatic hyperplasia. Blood 2004.
56. Esser S, Wolburg K, Wolburg H, Breier G, Kurzchalia T, Risau W. Vascular endothelial growth factor induces endothelial fenestrations in vitro. J Cell Biol 1998: 140: 947–959.
57. Roberts W G, Palade G E. Neovasculature induced by vascular endothelial growth factor is fenestrated. Cancer Res 1997: 57: 765–772.

58. Dvorak A M, Kohn S, Morgan E S, Fox P, Nagy J A, Dvorak H F. The vesiculo-vacuolar organelle (VVO): a distinct endothelial cell structure that provides a transcellular pathway for macromolecular extravasation. J Leukoc Biol 1996: 59: 100–115.
59. Neufeld G, Cohen T, Gengrinovitch S, Poltorak Z. Vascular endothelial growth factor (VEGF) and its receptors. FASEB J 1999: 13: 9–22.
60. Detmar M. The role of VEGF and thrombospondins in skin angiogenesis. J Dermatol Sci 2000: 24 (Suppl. 1): S78–S84.
61. Yuan F, Chen Y, Dellian M, Safabakhsh N, Ferrara N, Jain R K. Time-dependent vascular regression and permeability changes in established human tumor xenografts induced by an anti-vascular endothelial growth factor/vascular permeability factor antibody. Proc Natl Acad Sci USA 1996: 93: 14765–14770.
62. von Andrian U H, Mackay C R. T-cell function and migration. Two sides of the same coin. N Engl J Med 2000: 343: 1020–1034.
63. Barleon B, Sozzani S, Zhou D, Weich H A, Mantovani A, Marme D. Migration of human monocytes in response to vascular endothelial growth factor (VEGF) is mediated via the VEGF receptor flt-1. Blood 1996: 87: 3336–3343.
64. Luttun A, Tjwa M, Moons L et al. Revascularization of ischemic tissues by PlGF treatment, and inhibition of tumor angiogenesis, arthritis and atherosclerosis by anti-Flt1. Nat Med 2002: 8: 831–840.
65. Pertovaara L, Kaipainen A, Mustonen T et al. Vascular endothelial growth factor is induced in response to transforming growth factor-beta in fibroblastic and epithelial cells. J Biol Chem 1994: 269: 6271–6274.
66. Li J, Perrella M A, Tsai J C et al. Induction of vascular endothelial growth factor gene expression by interleukin-1 beta in rat aortic smooth muscle cells. J Biol Chem 1995: 270: 308–312.
67. Sato N, Nariuchi H, Tsuruoka N et al. Actions of TNF and IFN-gamma on angiogenesis in vitro. J Invest Dermatol 1990: 95: 85S–89S.
68. Voest E E, Kenyon B M, O'Reilly M S, Truitt G, D'Amato R J, Folkman J. Inhibition of angiogenesis in vivo by interleukin-12. J Natl Cancer Inst 1995: 87: 581–586.

JOURNAL OF VIROLOGY, July 1998, p. 6131–6137
0022-538X/98/$04.00+0

Vol. 72, No. 7

Human Immunodeficiency Virus Tat Modulates the Flk-1/KDR Receptor, Mitogen-Activated Protein Kinases, and Components of Focal Adhesion in Kaposi's Sarcoma Cells†

RAMESH K. GANJU,[1] NERU MUNSHI,[1] B. C. NAIR,[2] ZHONG-YING LIU,[1] PARKASH GILL,[3] AND JEROME E. GROOPMAN[1]*

Divisions of Experimental Medicine and Hematology/Oncology, Beth Israel Deaconess Medical Center, Harvard Institutes of Medicine, Boston, Massachusetts 02115[1]; Advanced Bioscience Laboratories, Inc., Kensington, Maryland 20895[2]; and Division of Hematology/Oncology, Norris Cancer Center, University of Southern California, Los Angeles, California 90033[3]

Received 24 November 1997/Accepted 9 April 1998

Kaposi's sarcoma (KS) spindle cell growth and spread have been reported to be modulated by various cytokines as well as the human immunodeficiency virus (HIV) gene product Tat. Recently, HIV-1 Tat has been shown to act like a cytokine and bind to the Flk-1/KDR receptor for the vascular endothelial growth factor A (VEGF-A), which is expressed by KS cells. We have characterized signal transduction pathways stimulated by HIV-1 Tat upon its binding to surface receptors on KS cells. We observed that stimulation in KS 38 spindle cells resulted in tyrosine phosphorylation and activation of the Flk-1/KDR receptor. We also report that HIV-1 Tat treatment enhanced the phosphorylation and association of proteins found in focal adhesions, such as the related adhesion focal tyrosine kinase RAFTK, paxillin, and p130^{cas}. Further characterization revealed the activation of mitogen-activated protein kinase, c-Jun amino-terminal kinase (JNK), and Src kinase. HIV-1 Tat contains a basic domain which can interact with growth factor tyrosine kinase receptors and a classical RGD sequence which may bind to and activate the surface integrin receptors for fibronectin and vitronectin. We observed that stimulation of KS cells with basic as well as RGD sequence-containing Tat peptides resulted in enhanced phosphorylation of RAFTK and activation of MAP kinase. These studies reveal that Tat stimulation activates a number of signal transduction pathways that are associated with cell growth and migration.

Kaposi's sarcoma (KS) is the major neoplastic manifestation of AIDS (30, 37, 42, 55). Its pathogenesis has been the focus of considerable study. Several different cytokines including vascular endothelial growth factor A (VEGF-A), platelet-derived growth factor, interleukin-6, the KS virus-encoded homolog of the chemokine MIP1, and tumor necrosis factor alpha have been reported to modulate KS cell growth (17, 20, 24, 25, 38, 43, 47, 52, 56, 62). These cytokines have been postulated to be released in a paracrine fashion (by neighboring leukocytes and endothelial cells) or in an autocrine-paracrine fashion (by spindle cells themselves). Recent results suggest that the Tat protein of human immunodeficiency virus type 1 (HIV), known to be a transcriptional regulator of virus, potentiates KS cell growth in vitro and in in vivo animal models (2, 7, 11, 18). HIV Tat has been reported to act synergistically with inflammatory cytokines and basic fibroblast growth factor in promoting KS proliferation and migration (19).

HIV Tat is a protein of 86 to 104 amino acids encoded by two exons and is essential for viral replication. Tat can be divided into five distinct domains termed N terminal, cysteine rich, core, basic, and C terminal. The C-terminal domain contains an Arg-Gly-Asp (RGD) sequence, which represents the major cell attachment moiety recognized by integrin receptors. This Tat domain can bind with high affinity to the integrins $\alpha_5\beta_1$, and $\alpha_5\beta_3$, receptors for fibronectin and vitronectin, respectively (8, 60). The basic sequence of Tat (amino acids 42 to 64) is similar to the basic sequence of several growth factors (fibroblast growth factor, VEGF-A, hepatocyte growth factor, and heparin-binding epidermal growth factor) (12, 46, 57). The basic sequence of Tat has also been shown to bind to a novel integrin, $\alpha_v\beta_5$ (60). Because Tat can be released by infected cells during HIV infection and can act extracellularly in the microenvironment, it may function in a paracrine fashion as a protocytokine in KS pathogenesis (14, 21). Recently, another link between Tat and a cytokine-based model of KS pathogenesis was made by demonstrating that HIV Tat specifically binds with high affinity to the mitogenic Flk-1 (but not the Flt-1) receptor, also known as VEGFR-2, for VEGF-A (3). Moreover, VEGF-A was recently shown to act as a potent growth stimulator in KS cells (38).

Despite the increasingly prominent role of Tat in the induction of cell proliferation and migration of KS cells, relatively little is known about the signal transduction pathways which mediate these effects (41). In the present study, we observed that Tat treatment activates the Flk-1 receptor (VEGFR-2). Further characterization of downstream molecules revealed increased phosphorylation of various components of focal adhesions, structures which mediate adherent contacts with the extracellular matrix. These components included the related adhesion focal tyrosine kinase (RAFTK), paxillin, and p130^{cas}. Tat treatment also activated various members of the mitogen-activated protein (MAP) kinase family and Src kinases. Our studies identify activation of specific signaling molecules that may participate in the Tat-induced growth and migration of KS cells.

* Corresponding author. Mailing address: Divisions of Experimental Medicine and Hematology/Oncology, Beth Israel Deaconess Medical Center, Harvard Institutes of Medicine, 4 Blackfan Circle, 3rd Floor, Boston, MA 02115. Phone: (617) 667-0070. Fax: (617) 975-5244. E-mail: jgroopma@west.bidmc.harvard.edu.

† Dedicated to Ronald Ansin for his continuing support of our research program.

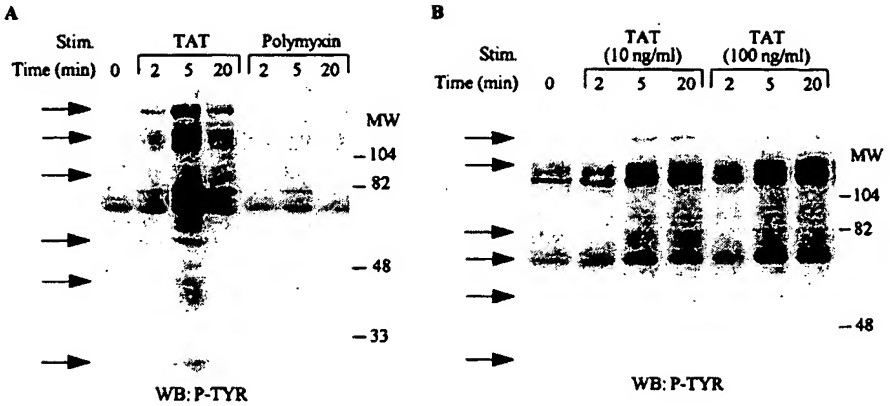

FIG. 1. Tyrosine phosphorylation of cellular proteins in KS cells after HIV Tat stimulation. Serum-starved KS cells were stimulated with either Tat at 100 ng/ml or polymixin at 100 ng/ml (A) or Tat at 10 ng/ml or 100 ng/ml (B) for the indicated times. Total-cell lysates (100 μg) obtained after cell lysis were fractionated on 10% polyacrylamide gels and subjected to Western blot (WB) analysis with the antiphosphotyrosine antibody 4G10. The arrows indicate the protein bands which show increased tyrosine phosphorylation after Tat treatment. MW, molecular weight in thousands. P-TYR, phosphotyrosine.

MATERIALS AND METHODS

Cells and cell culture. The KS cell line, KS 38, was derived from a biopsy specimen of a cutaneous lesion from an AIDS patient (13, 28, 39, 40). The cell line possesses many characteristics of primary KS cells, including endothelial markers and smooth muscle markers (13, 49), and has been used as a model for cytokine-mediated signaling studies (34). The cells were grown in flasks coated with 1.5% gelatin as described previously (34) and were suspended in RPMI 1640 containing 15% fetal calf serum, 2 mM glutamine, 1 mM MEM sodium pyruvate, 0.05 mM minimal essential medium (MEM) nonessential amino acids, 1× MEM amino acids, 1% Nutridoma-HU (Boehringer Mannheim Biochemicals, Indianapolis, Ind.), 50 μg of penicillin per ml, and 50 μg of streptomycin per ml. Cells were grown to confluence before being used in the signaling studies described below.

Reagents and antibodies. RAFTK antibodies were generated as described previously (33). Antibodies to the VEGF receptor Flk-1 (VEGFR-2), c-Src, JNK, ERK-1, ERK-2, and p38 MAP kinase were obtained from Santa Cruz Biotechnology (Santa Cruz, Calif.). The monoclonal antibodies against $p130^{cas}$ and paxillin were obtained from Transduction Laboratories, Inc. (Lexington, Ky.). Antiphosphotyrosine antibody (4G10) was a generous gift from Brian Druker (Oregon Health Sciences University). Electrophoresis reagents were obtained from Bio-Rad Laboratories (Hercules, Calif.). The protease inhibitors leupeptin and aprotinin and all other reagents were obtained from Sigma Chemical Co. (St. Louis, Mo.). The nitrocellulose membrane was obtained from Bio-Rad Laboratories. HIV Tat (1 to 86 amino acids) was expressed in *Escherichia coli* and purified by heparin affinity chromatography. Further purification was done by high-performance liquid chromatography (data not shown). The protein was found to be homogenous by sodium dodecyl sulfate-polyacrylamide gel electrophoresis (SDS-PAGE) with Coomassie blue stain. The purified Tat preparation (500 ng/ml) was found to be endotoxin free by the timed gel formation method with the *Limulus* amoebocyte lysate reagent as recommended by the manufacturer (Sigma). It was found to be biologically active as assessed by the HIV rescue assay with a cell line (HLM-1) containing an integrated nonreversible Tat-defective provirus. The Tat protein was lyophilized and reconstituted in Tat buffer (phosphate-buffered saline containing 1 mg of bovine serum albumin and 0.1 mM per ml dithiothreitol and was used for further studies.

Stimulation of cells. KS 38 cells, grown to confluence, were serum starved for 16 to 18 h and washed twice with Hanks' balanced salt solution (Gibco BRL, Gaithersburg, Md.) before Tat treatment. The cells were treated with 100 ng of Tat per ml, and 10 IU of heparin per ml was added in each case. The addition of heparin enhanced the Tat-mediated effects. Tat protein was added to cell cultures singly for different periods in vitro. Controls included media with 10 IU of heparin per ml in the absence of Tat. The cell lysates were prepared directly within the culture dish by lysis in 500 μl of modified RIPA buffer (50 mM Tris-HCl [pH 7.4], 1% Nonidet P-40, 0.25% sodium deoxycholate, 150 mM NaCl, 1 mM phenylmethylsulfonyl fluoride, 10 μg of aprotinin per ml, 10 μg of leupeptin per ml, 10 μg of pepstatin per ml, 10 mM sodium vanadate, 10 mM sodium fluoride, 10 mM sodium pyrophosphate) per dish at various time points. Total-cell lysates were clarified by centrifugation at 10,000 × *g* for 10 min. Protein concentrations were determined by the protein assay (Bio-Rad Laboratories).

Immunoprecipitation and Western blot analysis. For the immunoprecipitation studies, identical amounts of protein from each sample were clarified by incubation with protein A-Sepharose or Gamma Bind Sepharose (Pharmacia Biotech, Piscataway, N.J.) for 1 h at 4°C followed by a brief centrifugation. The solution was incubated for 4 h with different primary antibodies for each experiment or clarified overnight at 4°C. The antibody-antigen complexes were immunoprecipitated by incubation for 2 h at 4°C with 50 μl of the protein A-Sepharose or Gamma Bind sepharose (10% suspension). Nonspecific proteins were removed by washing the Sepharose beads three times with the modified RIPA buffer and once with phosphate-buffered saline. Bound proteins were solubilized in 40 μl of 2× Laemmli buffer and further analyzed by immunoblotting. Samples were separated by SDS-PAGE (8% polyacrylamide) and then transferred to nitrocellulose membranes. The membranes were blocked with 5% nonfat milk protein and probed with primary antibody for 2 h at room temperature (RT) or overnight at 4°C. Immunoreactive bands were visualized by using horseradish peroxidase-conjugated secondary antibody and the enhanced chemiluminescence system (Amersham Corp., Arlington Heights, Ill.).

MAP and JNK kinase assays. Cell lysates were immunoprecipitated with ERK-1, ERK-2 (1:1) (for MAP kinase), or JNK antibodies (for JNK kinase) (Santa Cruz Biotechnology). The immune complexes were washed twice with RIPA buffer and twice with kinase buffer (50 mM HEPES [pH 7.4], 10 mM $MgCl_2$, 20 μM ATP). The complex was then incubated for 30 min at RT with the substrates myelin basic protein (MBP) (7 μg) or glutathione *S*-transferase (GST)–c-Jun (4 μg) for MAP and JNK kinase, respectively, and 5 μCi [γ-^{32}P]ATP. The reaction was stopped by adding 2× SDS sample buffer and boiling the sample for 5 min at 100°C. Proteins were separated by SDS-PAGE (12 or 15% polyacrylamide) and detected by autoradiography.

c-Src kinase assay. The c-Src kinase assay was carried out as described previously (23). Briefly, the immunoprecipitated complexes obtained by immunoprecipitating cell lysates with the c-Src antiserum were washed twice with RIPA buffer and once with kinase buffer (10 mM HEPES [pH 7.4], 5 mM $MnCl_2$, 10 μM Na_3VO_4). For in vitro kinase assays, the immune complex was incubated for 30 min at RT in kinase buffer containing acid-denatured rabbit muscle enolase (Sigma Chemical Co.) and 5 μCi of [γ-^{32}P]ATP. The reaction was stopped by adding 2× SDS sample buffer and boiling the samples for 5 min. The samples were subjected to SDS-PAGE (10% polyacrylamide) and detected by autoradiography.

Autophosphorylation assay. The autophosphorylation assay was done as described by Albini et al. (3). The Flk-1/KDR immunoprecipitates were incubated in kinase buffer (50 mM HEPES [pH 7.4], 10 mM $MnCl_2$, 10 mM $MgCl_2$, 1 mM dithiothreitol, 20 μM ATP) plus 5 μCi [γ-^{32}P]ATP for 30 min at 25°C. The reaction was stopped by adding 2× SDS sample buffer. The samples were then subjected to SDS-PAGE (8% polyacrylamide), and the proteins were detected by autoradiography.

RESULTS

HIV Tat induces tyrosine phosphorylation of cellular proteins in KS cells. Signal transduction by the binding of ligands to cognate surface receptors involves the tyrosine phosphorylation of an array of targets. Since HIV Tat has been shown to bind to the Flk-1/KDR receptor (3) and to integrin receptors (8, 60), we analyzed the spectrum of substrates phosphorylated after its stimulation of KS cells. As shown in Fig. 1A, Tat stimulation resulted in the increased tyrosine phosphorylation of several different proteins with approximate molecular

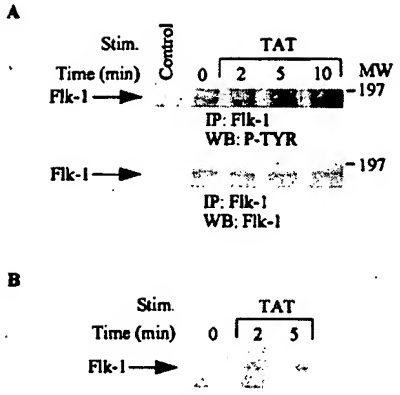

FIG. 2. Activation of the Flk-1/KDR receptor after HIV Tat treatments. KS cells were serum starved and treated with HIV Tat (100 ng/ml) for 2, 5, or 10 min. Total-cell lysates (1 mg) from treated or untreated cells were immunoprecipitated (IP) with anti-Flk-1/KDR receptor antibody. (A) Immunoprecipitates were separated by SDS-PAGE (8% polyacrylamide) and subjected to serial Western blotting (WB) with antiphosphotyrosine antibody (top) and anti-Flk-1/KDR receptor antibody (bottom). (B) Immunoprecipitates were subjected to autokinase assay, and ^{32}P-incorporated proteins were resolved by SDS-PAGE (7.5% polyacrylamide) followed by autoradiography. Control lane represents immunoprecipitates of antibody alone. MW, molecular weight in thousands. P-TYR, phosphotyrosine.

masses of 180, 120, 110, 100, 85, 70, 55, and 40 kDa. However, polymixin B treatment did not induce any increase in tyrosine phosphorylation of the various proteins. Furthermore, we found that Tat at 100 ng/ml had a slightly greater effect than Tat at 10 ng/ml (Fig. 1B). These results indicate that HIV-Tat can transduce signals by binding to surface receptors that result in induction of the tyrosine phosphorylation of a number of proteins.

HIV Tat induces tyrosine phosphorylation and activation of the Flk-1/KDR receptor in KS cells. HIV Tat binds and activates the Flk-1/KDR receptor (VEGFR-2) in vascular endothelial cells (3). We have previously shown that the Flk-1/KDR receptor is expressed in KS cells (34). We therefore investigated whether HIV Tat activates the Flk-1/KDR receptor (VEGFR-2) in these cells. As shown in Fig. 2, Tat stimulation resulted in an increase in tyrosine phosphorylation of this receptor (Fig. 2A, top). Equivalent amounts of receptor protein were present in each lane, as confirmed by stripping and reprobing the membrane with anti-Flk-1/KDR antibody (Fig. 2A, bottom). The autokinase activity of the Flk-1/KDR receptor was also activated upon Tat stimulation (Fig. 2B).

RAFTK is tyrosine phosphorylated upon HIV Tat stimulation. RAFTK is a novel signaling molecule of the focal adhesion kinase family that has been shown to link surface signals from integrins, cytokines, and T-cell receptors to the cytoskeleton and downstream to the MAP kinase pathway in certain cell types (4, 6, 26, 32, 33, 53). RAFTK was recently shown to be phosphorylated upon VEGF stimulation in KS cells (34). We therefore investigated whether HIV Tat phosphorylates RAFTK. HIV Tat treatment of KS cells resulted in rapid tyrosine phosphorylation of RAFTK (Fig. 3, top). Equivalent amounts of RAFTK protein were present in these experiments (Fig. 3, bottom).

HIV Tat stimulates tyrosine phosphorylation of paxillin and its association with RAFTK. Cytoskeletal proteins such as paxillin have been shown to be modulated during cell functions related to migration and adhesion (35). Paxillin is a focal adhesion protein that serves as a binding site for a number of important signaling molecules including crk, Src, and RAFTK/

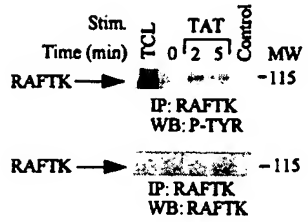

FIG. 3. Tyrosine phosphorylation of RAFTK by HIV Tat stimulation. Unstimulated KS cells or KS cells stimulated with HIV Tat (100 ng/ml) were lysed in RIPA buffer. Total-cell lysates (1 mg) were immunoprecipitated (IP) with RAFTK polyclonal antibody. Immunoprecipitates were size-fractionated on 7.5% polyacrylamide gels, transferred to a nitrocellulose membrane, and then subjected to serial Western blotting (WB) with antiphosphotyrosine antibody (4G10; top) and anti-RAFTK antibody (bottom). Control lane represents immunoprecipitates of antibody alone, and TCL lane represents 50 μg of total-cell lysates. MW, molecular weight in thousands. P-TYR, phosphotyrosine.

Pyk2 (9, 10, 35, 50, 51, 54). Thus, we sought to investigate whether HIV Tat treatment of KS 38 cells resulted in changes in the phosphorylation state of paxillin and its association with other proteins. As shown in Fig. 4A (top), HIV Tat stimulation resulted in enhanced tyrosine phosphorylation of paxillin. Equivalent amounts of paxillin were present in each lane (Fig. 4A, bottom). Furthermore, we observed that paxillin was associated with RAFTK and that this association was enhanced upon HIV Tat treatment (Fig. 4B).

p130^{cas} is tyrosine phosphorylated upon HIV Tat treatment. p130^{cas}, which is a component of focal adhesions, is essential for many functions including the regulation of cell shape and adhesive properties (36). We observed that HIV Tat treatment also resulted in enhanced tyrosine phosphorylation of p130^{cas} (Fig. 5, top). The blots were stripped and blotted with anti-p130^{cas} antibody (Fig. 5, bottom).

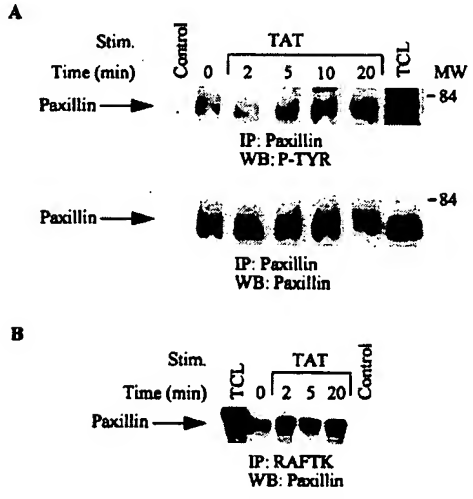

FIG. 4. Phosphorylation of paxillin and its association with RAFTK. KS cells were stimulated with HIV Tat (100 ng/ml) for various times, and stimulated or unstimulated cell lysates were immunoprecipitated (IP) with anti-paxillin antibody. (A) The immunoprecipitates were then run on SDS-PAGE and subjected to Western blotting (WB) with antiphosphotyrosine antibody (top) and anti-paxillin antibody (bottom). (B) The cell lysates were immunoprecipitated with anti-RAFTK antibody run on SDS-PAGE (7.5% polyacrylamide) and blotted with paxillin antibody. Control lane represents immunoprecipitates of antibody alone, and TCL lane represents 50 μg of total-cell lysates. MW, molecular weight in thousands. P-TYR, phosphotyrosine.

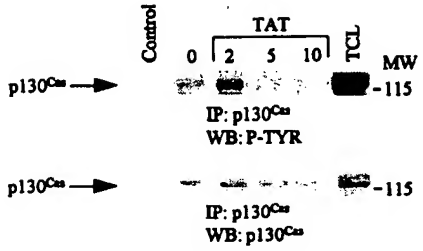

FIG. 5. HIV Tat treatment of KS cells stimulates tyrosine phosphorylation of $p130^{Cas}$. Unstimulated or HIV Tat-stimulated KS cell lysates were immunoprecipitated (IP) with anti-$p130^{Cas}$. The immunoprecipitates were subjected to SDS-PAGE (7.5% polyacrylamide), transferred to a nitrocellulose membrane, and Western blotted (WB) with antiphosphotyrosine antibody 4G10 (top). The same blots were stripped and blotted with anti-$p130^{Cas}$ antibody (bottom). Control lane represents immunoprecipitates of antibody alone, and TCL lane represents 50 μg of total-cell lysates. MW, molecular weight in thousands. P-TYR, phosphotyrosine.

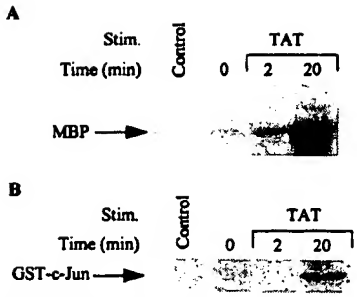

FIG. 7. Activation of MAP kinase and JNK upon Tat stimulation. (A) KS cells were stimulated with Tat (100 ng/ml) and immunoprecipitated with ERK-1 or ERK-2 antibody and then subjected to an in vitro kinase assay with MBP (7 μg) as a substrate. (B) Stimulated KS cells were immunoprecipitated with JNK antibody and subjected to an in vitro kinase assay with GST–c-Jun (1 to 79 amino acids) as the substrate. The ^{32}P-labeled proteins were subjected to SDS-PAGE (12% polyacrylamide) followed by autoradiography. Control lane represents immunoprecipitates of antibody alone.

HIV Tat stimulates tyrosine phosphorylation and activation of c-Src kinase. The Src family kinases have been shown to be activated by various growth factors and act to transmit growth signals downstream via adaptor molecules, RAFTK/Pyk2, and other substrates (15, 16, 61). KS 38 cells express c-Src kinase (data not shown). HIV Tat treatment of KS 38 cells resulted in rapid tyrosine phosphorylation of c-Src kinase (Fig. 6A, top). Equivalent amounts of c-Src were present in each lane (Fig. 6A, bottom). An in vitro kinase assay in which enolase was used as an exogenous substrate demonstrated that HIV Tat stimulation of KS cells resulted in the activation of the intrinsic kinase activity of c-Src (Fig. 6B).

Activation of the MAP pathway in KS cells after HIV Tat treatment. ERK and JNK kinases are important members of the MAP kinase family and have been shown to act as downstream mediators of the RAFTK/Pyk2 signaling pathway in PC12 neuronal cells (32, 59). We examined whether Tat treatment, which activated RAFTK, was also able to activate various members of the MAP kinase pathway. As shown in Fig. 7, HIV Tat stimulation of KS 38 cells resulted in activation of ERK and JNK kinases as determined by the phosphorylation of MBP and GST–c-Jun, respectively. p38 MAP kinase activity was not enhanced under these conditions (data not shown).

Tat basic and RGD peptides activate RAFTK and the MAP kinase pathway. Tat contains several functional domains, including a basic domain spanning amino acids 46 to 60 and an RGD-containing domain spanning the carboxyl terminus of the molecule (amino acids 65 to 80). Having observed that full-length Tat stimulation resulted in phosphorylation of RAFTK and activation of the MAP kinase pathway, we studied whether treatment with basic or RGD-containing Tat peptides also resulted in activation of these kinases. As seen in Fig. 8, stimulation with both basic and RGD-containing peptides re-

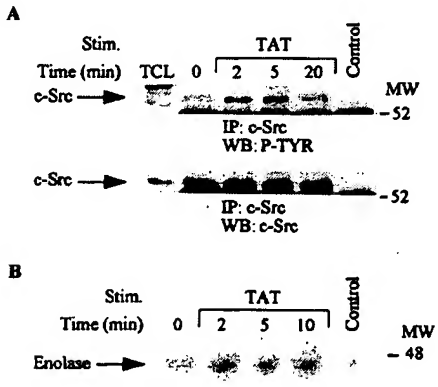

FIG. 6. Activation of Src kinases upon HIV Tat stimulation. Total-cell lysates (500 μg) from unstimulated or HIV Tat-stimulated cell lysates were immunoprecipitated (IP) with anti-Src antibody. The immune complexes were subjected to Western blotting (WB) with antiphosphotyrosine antibody (top) followed by c-Src antibody (bottom) (A) or an in vitro kinase assay with enolase as the substrate. The ^{32}P-incorporated proteins were resolved by SDS-PAGE (7.5% polyacrylamide) followed by autoradiography. Control lane represents immunoprecipitates of antibody alone, and TCL lane represents 50 μg of total-cell lysates. MW, molecular weight in thousands. P-TYR, phosphotyrosine.

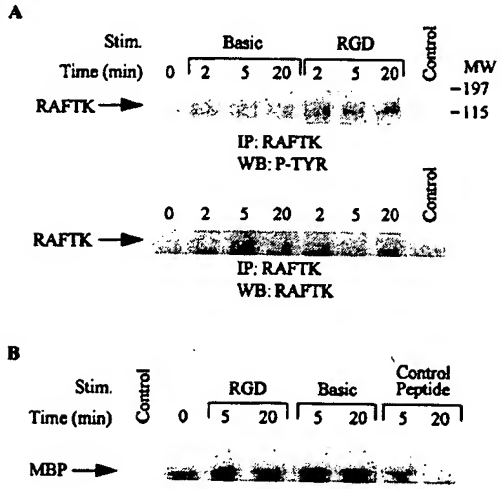

FIG. 8. Phosphorylation of RAFTK and activation of MAP kinase by basic and RGD domain-containing peptides of Tat. KS cells were stimulated with peptides containing either the basic or RGD domain of Tat or a control peptide. (A) The cell lysates were immunoprecipitated (IP) with RAFTK antibody, and immune complexes were subjected to SDS-PAGE (7.5% polyacrylamide) and subjected to Western blotting (WB) with antiphosphotyrosine antibody followed by anti-RAFTK antibody. (B) The cell lysates were immunoprecipitated with ERK-1 or ERK-2 antibody, and immune complexes were subjected to an in vitro kinase assay with MBP as the substrate. The samples were subjected to SDS-PAGE (12% polyacrylamide) followed by autoradiography. Control lane represents immunoprecipitates of antibody alone. MW, molecular weight in thousands. P-TYR, phosphotyrosine.

sulted in phosphorylation of RAFTK (Fig. 8A) and activation of MAP kinase (Fig. 8B). However, a control 15-amino-acid unrelated peptide did not activate MAP kinase under similar conditions (Fig. 8B).

DISCUSSION

Various etiological factors implicated in KS include the recently discovered human herpesvirus 8 (HHV-8)/Kaposi's sarcoma herpesvirus (KSHV) (45, 48), cytokines, and HIV Tat (2, 11, 17, 19, 25, 52). There is an extensive literature supporting a role for HIV Tat in regulating the growth and spread of KS cells and chemotaxis in monocytes (31, 44). However, relatively little is known about the signaling pathways used by HIV Tat that mediate these effects within KS cells or other monocytes (44). Tat can be released by HIV-infected cells (14, 21), and the protein might either be taken up by the target cells and *trans*-activate growth-related genes (11) or act as a paracrine growth factor by binding to cell surface receptors and leading to the generation of intracellular signals that modulate KS spindle cell growth and spread (3, 8, 19, 60). We observed that HIV Tat treatment of KS cells activated the Flk-1/KDR receptor (VEGFR-2) for VEGF-A. This effect may be mediated by direct binding of Tat to the Flk-1 receptor through its basic domain, since HIV Tat has recently been reported to bind to this receptor in endothelial cells (3). Moreover, VEGF-A has been shown to act as an autocrine growth factor for KS and therefore may play an important role in KS pathogenesis (38).

Since HIV Tat has been shown to affect cell migration, which involves alteration in cytoskeletal elements, we analyzed the phosphorylation of RAFTK, paxillin, and p130^{cas}, components of focal adhesions. We observed that Tat stimulation resulted in the tyrosine phosphorylation of all three components of focal adhesions. RAFTK, which is also known as Pyk2 or Cak-β, is a novel member of the focal adhesion kinase family and has previously been shown to be activated upon VEGF-A stimulation in KS cells (34) and integrin stimulation in megakaryocytes and B cells (4, 33). RAFTK has been shown to act as a "platform kinase" and to link growth factor and stress signals (such as UV and osmotic shock) to the nucleus and cytoskeleton in neuronal and hematopoietic cells (4, 26, 32). Paxillin and p130^{cas} have also been shown to participate in integrin- and VEGF-mediated signal transduction pathways (1, 4, 5, 36, 54). Our data revealed that Tat induces a rapid tyrosine phosphorylation of RAFTK, which reaches a maximum around 2 min and declines thereafter. However, paxillin tyrosine phosphorylation reaches a maximum after 5 min. This suggests that tyrosine phosphorylation of RAFTK leads to its activation and that activated RAFTK may phosphorylate paxillin. RAFTK has been shown to phosphorylate paxillin in hematopoietic cells (29, 50). We also observed that there was an enhanced association of paxillin with RAFTK upon Tat stimulation. Paxillin has previously been shown to be associated with RAFTK and FAK in various cell types through the proline-rich COOH terminus (9, 26, 27, 50). Phosphorylation of RAFTK, p130^{cas}, and paxillin and association of RAFTK with paxillin may result in the formation of a cytoskeletal complex, which contributes to chemotaxis.

c-Src, MAP, and JNK kinases are also activated upon Tat treatment in KS cells. These kinases are thought to play important roles in regulating cellular proliferation (22, 58). Furthermore, c-Src also plays a role in regulating adhesion, since v-Src-transformed cells have morphologically abnormal focal adhesions and are defective in cell substrate adhesion (22, 58). Recent studies also indicate that RAFTK mediates G-protein-coupled activation of Src and MAP kinases in PC12 cells (16).

Both the basic and RGD Tat peptides resulted in the activation of KS cells, with phosphorylation of RAFTK and activation of MAP kinase. The basic-domain-containing peptide may mediate its effect by binding to the Flk-1/KDR receptor (VEGFR-2). Recently, Albini et al. (3) showed that Tat basic peptide can induce tyrosine phosphorylation of the Flk-1/KDR receptor (VEGFR-2) whereas the RGD-containing peptide does not activate the Flk-1/KDR receptor. However, the RGD-containing peptide may induce signaling by binding to integrin receptors. RAFTK has been shown to participate in both Flk-1- and integrin-mediated signaling pathways in hematopoietic and other cells (4, 34, 36).

Our data provide new information on HIV-Tat-induced signal transduction pathways in KS cells and demonstrate how Tat may act at a molecular level to modulate chemotaxis and cell proliferation in these cells. Tat has previously been shown to activate phosphatidylinositol 3-kinase in PC12 neuronal cells (41). We add to this report data on Tat stimulation and subsequent activation of the Flk-1 receptor and phosphorylation of the recently identified focal adhesion components RAFTK and p130^{cas}. The characterization of the Tat-induced signal transduction pathway in KS may provide insights into developing targeted therapies to inhibit its growth and spread.

ACKNOWLEDGMENTS

The first two authors contributed equally to this work.

This work was supported in part by NIH grants HL 55187, HL 53745, HL 43510, and CA76950.

We thank Hava and Shalom Avraham for the generous gift of RAFTK antibody. We also thank our colleagues Stephanie Brubaker for technical assistance, Janet Delahanty for editing and preparation of figures, and Nancy DesRosiers for assistance with the figures. We are grateful to Delroy Heath for facilitating receipt of needed reagents and to Tee Trac for typing the manuscript.

REFERENCES

1. **Abedi, H., and I. Zachary.** 1997. Vascular endothelial growth factor stimulates tyrosine phosphorylation and recruitment to new focal adhesions of focal adhesion kinase and paxillin in endothelial cells. J. Biol. Chem. 272: 15442–15451.
2. **Albini, A., G. Barillari, R. Benelli, R. C. Gallo, and B. Ensoli.** 1995. Angiogenic properties of human immunodeficiency virus type 1 Tat protein. Proc. Natl. Acad. Sci. USA 92:4838–4842.
3. **Albini, A., R. Soldi, D. Giunciuglio, E. Giraudo, R. Benelli, L. Primo, D. Noonan, M. Salio, G. Camussi, W. Rockl, and F. Bussolino.** 1996. The angiogenesis induced by HIV-1 tat protein is mediated by the Flk-1/KDR receptor on vascular endothelial cells. Nat. Med. 2:1371–1375.
4. **Astier, A., H. Avraham, S. N. Manie, J. E. Groopman, T. Canty, S. Avraham, and A. S. Freedman.** 1997. The related adhesion focal tyrosine kinase is tyrosine-phosphorylated after B1-integrin stimulation in B cells and binds to p130cas. J. Biol. Chem. 272:228–232.
5. **Astier, A., S. N. Manie, H. Avraham, H. Hirai, S. F. Law, Y. Zhang, E. A. Golemis, Y. Fu, B. J. Druker, N. Haghayeghi, A. S. Freedman, and S. Avraham.** 1997. The related adhesion focal tyrosine kinase differentially phosphorylated p130cas and the cas-like protein, p105HEF1. J. Biol. Chem. 272:19719–19724.
6. **Avraham, S., R. London, Y. Fu, S. Ota, D. Hiregowdara, J. Li, S. Jiang, L. M. Pasztor, R. A. White, J. E. Groopman, and H. Avraham.** 1995. Identification and characterization of a novel related adhesion focal tyrosine kinase (RAFTK) from megakaryocytes and brain. J. Biol. Chem. 270:27742–27751.
7. **Barillari, G., L. Buonaguro, V. Fiorelli, J. Hoffman, F. Michaels, R. C. Gallo, and B. Ensoli.** 1992. Effects of cytokines from activated immune cells on vascular cell growth and HIV-1 gene expression. Implications for AIDS-Kaposi's sarcoma pathogenesis. Immunology 149:3727–3734.
8. **Barillari, G., R. Gendelman, R. C. Gallo, and B. Ensoli.** 1993. The Tat protein of human immunodeficiency virus type 1, a growth factor for AIDS Kaposi sarcoma and cytokine-activated vascular cells, induces adhesion of the same cell types by using integrin receptors recognizing the RGD amino acid sequence. Proc. Natl. Acad. Sci. USA 90:7941–7945.
9. **Bellis, S. L., J. T. Miller, and C. E. Turner.** 1995. Characterization of tyrosine phosphorylation of paxillin *in vitro* by focal adhesion kinase. J. Biol. Chem. 270:17437–17441.
10. **Birge, R. B., J. E. Fajardo, C. Reichman, S. E. Shoelson, Z. Songyang, L. C.**

Cantley, and H. Hanafusa. 1993. Identification and characterization of a high-affinity interaction between v-Crk and tyrosine-phosphorylated paxillin in CT10-transformed fibroblasts. Mol. Cell. Biol. 13:4648–4656.
11. Buonaguro, L., G. Barillari, H. K. Chang, C. A. Bohan, V. Kao, R. Morgan, R. C. Gallo, and B. Ensoli. 1992. Effects of the human immunodeficiency virus type 1 Tat protein on the expression of inflammatory cytokines. J. Virol. 66:7159–7167.
12. Bussolino, F., M. Arese, G. Montrucchio, L. Barra, L. Primo, R. Benelli, F. Sanavio, M. Aglietta, D. Ghigo, M. Rola-Pleszczynski, A. Bosia, A. Albini, and G. Camussi. 1995. Platelet activating factor produced in vitro by Kaposi's sarcoma cells induces and sustains in vivo angiogenesis. J. Clin. Invest. 96:940–952.
13. Cai, J., P. S. Gill, R. Masood, P. Chandrasoma, B. Jung, R. E. Law, and S. F. Radka. 1994. Oncostatin-M is an autocrine growth factor in Kaposi's sarcoma. Am. J. Pathol. 145:74–79.
14. Chang, H. C., F. Samaniego, B. C. Nair, L. Buonaguro, and B. Ensoli. 1997. HIV-1 Tat protein exits from cells via a leaderless secretory pathway and binds to extracellular matrix-associated heparin sulfate proteoglycans through its basic region. AIDS 11:1421–1431.
15. Cooper, J. A., and B. Howell. 1993. The when and how of Src regulation. Cell. 73:1051–1054.
16. Dikic, I., G. Tokiwa, S. Lev, S. A. Courtneidge, and J. Schlessinger. 1996. A role for Pyk2 and Src in linking G-protein-coupled receptors with MAP kinase activation. Nature 383:547–550.
17. Ensoli, B., G. Barillari, and R. C. Gallo. 1992. Cytokines and growth factors in the pathogenesis of AIDS-associated Kaposi's sarcoma. Immunol. Rev. 127:147–155.
18. Ensoli, B., G. Barillari, S. Z. Salahuddin, R. C. Gallo, and F. Wong-Staal. 1990. Tat protein of HIV-1 stimulates growth of cells derived from Kaposi's sarcoma lesions of AIDS patients. Nature 345:84–86.
19. Ensoli, B., R. Gendelman, P. Markham, V. Fiorelli, S. Colombini, M. Raffeld, A. Cafaro, H. K. Chang, J. N. Brady, and R. C. Gallo. 1994. Synergy between basic fibroblast growth factor and HIV-1 Tat protein in induction of Kaposi's sarcoma. Nature 371:674–680.
20. Ensoli, B., S. Nakamura, S. Z. Salahuddin, P. Biberfeld, L. Larsson, B. Beaver, F. Wong-Staal, and R. C. Gallo. 1989. AIDS-Kaposi's sarcoma-derived cells express cytokines with autocrine and paracrine growth effects. Science 243:223–226.
21. Ensoli, B., L. Buonaguro, G. Barillari, V. Fiorelli, R. Gendelman, R. A. Morgan, P. Wingfield, and R. C. Gallo. 1993. Release, uptake, and effects of extracellular human immunodeficiency virus type 1 Tat protein on cell growth and viral transactivation. J. Virol. 67:277–287.
22. Erpel, T., and S. A. Courtneidge. 1995. Src family protein tyrosine kinases and cellular signal transduction pathways. Curr. Opin. Cell Biol. 7:176–182.
23. Feder, D., and J. M. Bishop. 1990. Purification and enzymatic characterization of pp60c-src from human platelets. J. Biol. Chem. 265:8205–8211.
24. Fiorelli, V., R. Gendelman, F. Samaniego, P. D. Markham, and B. Ensoli. 1995. Cytokines from activated T cells induce normal endothelial cells to acquire the phenotypic and functional features of AIDS-Kaposi's sarcoma spindle cells. J. Clin. Invest. 95:1723–1734.
25. Ganem, D. 1995. AIDS. Viruses, cytokines and Kaposi's sarcoma. Curr. Biol. 5:469–471.
26. Ganju, R. K., W. C. Hatch, H. Avraham, M. A. Ona, B. Druker, S. Avraham, and J. E. Groopman. 1997. RAFTK, a novel member of the focal adhesion kinase family, is phosphorylated and associates with signaling molecules upon activation of mature T lymphocytes. J. Exp. Med. 185:1–9.
27. Ganju, R. K., P. Dutt, L. Wu, W. Newman, H. Avraham, S. Avraham, and J. E. Groopman. 1998. β-Chemokine receptor CCR5 signals via the novel tyrosine kinase RAFTK. Blood 91:791–797.
28. Guo, W., T. Antakly, M. Cadotte, Z. Kachra, L. Kindel, R. Masood, and P. Gill. 1996. Expression and cytokine regulation of glucocorticoid receptors in Kaposi's sarcoma. Am. J. Pathol. 148:1999–2007.
29. Hiregowdara, D., H. Avraham, Y. Fu, R. London, and S. Avraham. 1997. Tyrosine phosphorylation of the related adhesion focal tyrosine kinase in megakaryocytes upon stem cell factor and phorbol myristate acetate stimulation and its association with paxillin. J. Biol. Chem. 272:10804–10810.
30. Karp, J. E., J. M. Pluda, and R. Yarchoan. 1996. AIDS-related Kaposi's sarcoma. A template for the translation of molecular pathogenesis into targeted therapeutic approaches. Hematol. Oncol. Clin. North Am. 10:1031–1049.
31. Lafrenie, R. M., L. M. Wahl, J. S. Epstein, I. K. Hewlett, K. M. Yamada, and S. Dhawan. 1996. HIV-1-tat protein promotes chemotaxis and invasive behavior by monocytes. J. Immunol. 157:974–977.
32. Lev, S., H. Moreno, R. Martinez, P. Canoll, E. Peles, J. M. Musacchio, G. D. Plowman, B. Rudy, and J. Schlessinger. 1995. Protein tyrosine kinase PYK2 involved in Ca(2+)-induced regulation of ion channel and MAP kinase functions. Nature 376:737–745.
33. Li, J., H. Avraham, R. Rogers, S. Raja, and S. Avraham. 1996. Characterization of RAFTK, a novel focal adhesion kinase, and its integrin-dependent phosphorylation and activation in megakaryocytes. Blood 88:417–428.
34. Liu, Y., R. Ganju, M. Ona, W. Hatch, J. Wang, T. Zheng, P. Gill, S. Avraham, and J. Groopman. 1997. Cytokine signaling through the novel tyrosine kinase RAFTK in Kaposi's sarcoma cells. J. Clin. Invest. 99:1798–1804.
35. Lo, S. H., and L. B. Chen. 1994. Focal adhesion as a signal transduction organelle. Can. Metas. Rev. 13:9–24.
36. Manie, S. N., A. Astier, N. Haghayeghi, T. Canty, B. J. Druker, H. Hirai, and A. S. Freedman. 1997. Regulation of integrin-mediated p130cas tyrosine phosphorylation in human B cells. J. Biol. Chem. 272:15636–15641.
37. Masood, R., J. Cai, R. Law, and P. Gill. 1993. AIDS-associated Kaposi's sarcoma pathogenesis, clinical features, and treatment. J. Opin. Oncol. 5:831–834.
38. Masood, R., J. Cai, T. Zheng, D. L. Smith, Y. Naidu, and P. S. Gill. 1997. Vascular endothelial growth factor/vascular permeability factor is an autocrine growth factor for AIDS-Kaposi sarcoma. Proc. Natl. Acad. Sci. USA 94:974–984.
39. Masood, R., S. R. Husain, A. Rahman, and P. Gill. 1993. Potentiation of cytotoxicity of Kaposi's sarcoma related to immunodeficiency syndrome (AIDS) by liposome-encapsulated doxorubicin. AIDS Res. Hum. Retroviruses 9:741–746.
40. Masood, R., Y. Lunardi-Iskandar, L. Jean, J. Murphy, C. Waters, R. Gallo, and P. Gill. 1994. Inhibition of AIDS-associated Kaposi's sarcoma cell growth by DAB389-interleukin 6. AIDS Res. Hum. Retroviruses 10:969–975.
41. Milani, D., M. Mazzoni, P. Borgatti, G. Zauli, L. Cantley, and S. Capitani. 1996. Extracellular human immunodeficiency virus type-1 tat protein activates phosphatidylinositol 3-kinase in PC12 neuronal cells. J. Biol. Chem. 271:22961–22964.
42. Miles, S. A. 1994. Pathogenesis of HIV-related Kaposi's sarcoma. J. Opin. Oncol. 6:497–502.
43. Miles, S. A., A. R. Rezai, J. F. Salazar-Gonzalez, M. Vander Meyden, R. H. Stevens, D. M. Logan, R. T. Mitsuyasu, T. Taga, T. Hirano, T. Kishimoto, and O. Martinez-Maza. 1990. AIDS Kaposi sarcoma-derived cells produce and respond to interleukin 6. Proc. Natl. Acad. Sci. USA 87:4068–4072.
44. Mitola, S., S. Sozzani, W. Luini, L. Primo, A. Borsatti, H. Weich, and F. Bussolino. 1997. Tat-human immunodeficiency virus-1 induces human monocyte chemotaxis by activation of vascular endothelial growth factor receptor-1. Blood 90:1365–1372.
45. Moore, P. S., C. Boshoff, R. A. Weiss, and Y. Chang. 1996. Molecular mimicry of human cytokine and cytokine response pathway genes by KSHV. Science 274:1739–1744.
46. Naidu, Y. M., E. M. Rosen, R. Zitnick, I. Goldberg, M. Park, M. Naujokas, P. J. Polverini, and B. J. Nickoloff. 1994. Role of scatter factor in the pathogenesis of AIDS-related Kaposi sarcoma. Proc. Natl. Acad. Sci. USA 91:5281–5285.
47. Nair, B. C., A. L. DeVico, S. Nakamura, T. D. Copeland, Y. Chen, A. Patel, T. O'Neil, S. Oroszlan, R. C. Gallo, and M. G. Sarngadharan. 1992. Identification of a major growth factor for AIDS-Kaposi's sarcoma cells as oncostatin M. Science 255:1430–1432.
48. Nicholas, J., V. R. Ruvolo, W. H. Burns, G. Sandford, X. Wan, D. Ciufo, S. B. Hendrickson, H.-G. Guo, G. S. Hayward, and M. S. Reitz. 1997. Kaposi's sarcoma-associated human herpesvirus-8 encodes homologues of macrophage inflammatory protein-1 and interleukin-6. Nat. Med. 3:287–292.
49. Rabkin, C. S., S. Janz, A. Lash, A. E. Coleman, E. Musaba, L. Liotta, R. Biggar, and Z. Zhuang. 1997. Monoclonal origin of multicentric Kaposi's sarcoma lesions. N. Engl. J. Med. 336:988–993.
50. Salgia, R., H. Avraham, E. Pisick, J.-L. Li, S. Raja, E. Greenfield, M. Sattler, H. Avraham, and J. Griffin. 1996. The related adhesion focal tyrosine kinase forms a complex with paxillin in hematopoietic cells. J. Biol. Chem. 271: 31222–31226.
51. Salgia, R., N. Uemura, K. Okuda, J. L. Li, E. Pisick, M. Sattler, R. de Jong, B. Druker, N. Heisterkamp, L. B. Chen, J. Groffen, and J. D. Griffin. 1995. CRKL links $p210^{BCR/ABL}$ with paxillin in chronic myelogenous leukemia cells. J. Biol. Chem. 270:29145–29150.
52. Samaniego, F., P. D. Markham, R. C. Gallo, and B. Ensoli. 1995. Inflammatory cytokines induce AIDS-Kaposi's sarcoma-derived spindle cells to produce and release basic fibroblast growth factor and enhance Kaposi's sarcoma-like lesion formation in nude mice. J. Immunol. 154:3582–3592.
53. Sasaki, H., K. Nagura, M. Ishino, H. Tobioka, K. Kotani, and T. Sasaki. 1995. Cloning and characterization of cell adhesion kinase beta, a novel protein-tyrosine kinase of the focal adhesion kinase subfamily. J. Biol. Chem. 270:21206–21219.
54. Schaller, M. D., and J. T. Parsons. 1995. $pp125^{fak}$-dependent tyrosine phosphorylation of paxillin creates a high-affinity binding site for Crk. Mol. Cell. Biol. 15:2635–2645.
55. Schwartz, R. A. 1996. Kaposi's sarcoma: advances and perspectives. J. Am. Acad. Dermatol. 34:804–814.
56. Sturzl, M., W. K. Roth, N. H. Brockmeyer, C. Zietz, B. Speiser, and P. H. Hofschneider. 1992. Expression of platelet-derived growth factor and its receptor in AIDS-related Kaposi sarcoma in vivo suggests paracrine and autocrine mechanisms of tumor maintenance. Proc. Natl. Acad. Sci. USA 89:7046–7050.
57. Sturzl, M., H. Brandstetter, C. Zietz, B. Eisenburg, G. Raivich, D. P. Gearing, N. H. Brockmeyer, and P. H. Hofschneider. 1995. Identification of interleukin-1 and platelet-derived growth factor-B as major mitogens for the

spindle cells of Kaposi's sarcoma: a combined in vitro and in vivo analysis. Oncogene **10**:2007–2016.
58. **Superti-Furga, G., and S. A. Courtneidge.** 1995. Structure-function relationships in Src family and related protein tyrosine kinases. Bioessays **17**:321–330.
59. **Tokiwa, G., I. Dikic, S. Lev, and J. Schlessinger.** 1996. Activation of Pyk2 by stress signals and coupling with JNK signaling pathway. Science **273**:792–794.
60. **Vogel, B. E., S. J. Lee, A. Hildebrand, W. Craig, M. D. Pierschbacher, F. Wong-Staal, and E. Ruoslahti.** 1993. A novel integrin specificity exemplified by binding of the alpha v beta 5 integrin to the basic domain of the HIV Tat protein and vitronectin. J. Cell Biol. **121**:461–468.
61. **Xu, W., S. C. Harrison, and M. J. Eck.** 1997. Three-dimensional structure of the tyrosine kinase c-Src. Nature **385**:595–602.
62. **Yang, J., Y. Xu, C. Zhu, M. K. Hagan, T. Lawley, and M. K. Offermann.** 1994. Regulation of adhesion molecule expression in Kaposi's sarcoma cells. J. Immunol. **152**:361–373.

MOLECULAR AND CELLULAR BIOLOGY, Feb. 1992, p. 491–498
0270-7306/92/020491-08$02.00/0

Vol. 12, No. 2

Anti-Oncogenic Activity of Signalling-Defective Epidermal Growth Factor Receptor Mutants

NORBERT REDEMANN,[1] BERNHARD HOLZMANN,[1] THOMAS VON RÜDEN,[2] ERWIN F. WAGNER,[2] JOSEPH SCHLESSINGER,[3] AND AXEL ULLRICH[1]*

Department of Molecular Biology, Max-Planck-Institut für Biochemie, Am Klopferspitz 18A, 8033 Martinsried, Germany[1]; Institute of Molecular Pathology, 1030 Vienna, Austria[2]; and Department of Pharmacology, New York University Medical Center, New York, New York 10016[3]

Received 21 June 1991/Accepted 1 November 1991

Overexpression and autocrine activation of the epidermal growth factor receptor (EGF-R) cause transformation of cultured cells and correlate with tumor progression in cancer patients. Dimerization and transphosphorylation are crucial events in the process by which receptors with tyrosine kinase activity generate normal and transforming cellular signals. Interruption of this process by inactive receptor mutants offers the potential to inhibit ligand-induced cellular responses. Using recombinant retroviruses, we have examined the effects of signalling-incompetent EGF-R mutants on the growth-promoting and transforming potential of ligand-activated, overexpressed wild-type EGF-R and the v-*erb*B oncogene product. Expression of a soluble extracellular EGF-R domain had little if any effect on the growth and transformation of NIH 3T3 cells by either tyrosine kinase. However, both a kinase-negative EGF-R point mutant (HERK721A) and an EGF-R lacking 533 C-terminal amino acids efficiently inhibited wild-type EGF-R-mediated, de novo DNA synthesis and cell transformation in a dose-dependent manner. Furthermore, coexpression with the v-*erb*BES4 oncogene product in NIH 3T3 cells resulted in transphosphorylation of the HERK721A mutant receptor and reduced soft-agar colony growth but had no effect in a focus formation assay. These results demonstrate that signalling-defective receptor tyrosine kinase mutants differentially interfere with oncogenic signals generated by either overexpressed EGF-R or the retroviral v-*erb*BES4 oncogene product.

The epidermal growth factor receptor (EGF-R) is a 170-kDa glycoprotein with intrinsic protein tyrosine kinase activity (47). Ligand-induced receptor dimerization is thought to generate an allosteric signal that is transmitted across the plasma membrane and translated into stimulation of the kinase activity (for a review, see reference 48). While EGF normally generates a mitogenic response in fibroblasts, hyperstimulation of the EGF-R signalling pathway by ligand-activated, overexpressed receptors or the structurally altered retroviral v-*erb*B oncogene product leads to transformation of mouse NIH 3T3 cells (8, 39) or chicken embryo fibroblasts, respectively (8, 23, 39). Indeed, v-*erb*B expression after avian erythroblastosis virus infection causes erythroleukemia and fibrosarcomas in chicks (12–14). Moreover, EGF-R is overexpressed in many types of human cancer tumors, in most cases accompanied by transforming growth factor alpha (TGFα) expression, suggesting the involvement of an autocrine activation mechanism in oncogenesis (7, 9). Overexpression of a structurally related growth factor receptor-type tyrosine kinase, the EGF-R-like proto-oncogene product, $p185^{HER2/neu}$ (or $p185^{c\text{-}erbB2}$), also results in NIH 3T3 cell transformation and tumorigenesis in nude mice (8, 19). Extensive clinical evidence strongly supports the role of the EGF-R and $p185^{HER2/neu}$ in the progression of human breast, ovarian, squamous, gastric, and non-small-cell lung carcinomas, as well as various types of brain cancers (2, 15, 22, 28, 40, 42, 43, 52). Knowledge of the structures and signalling functions of these cell surface receptors provides a unique opportunity for the design of therapeutic reagents which target these proteins, with the goal of interrupting an autocrine activation cycle, downregulating the receptor, or otherwise inhibiting its signalling activity.

The necessity of receptor tyrosine kinases (RTKs) to dimerize (41), thereby allowing interreceptor transphosphorylation and activation, offers a means by which to inhibit these receptors. EGF-induced receptor dimers have been detected both in cell-free systems (53) and in living cells (6). The purified EGF-R extracellular domain, alone, undergoes ligand-induced oligomerization, which indicates that this function is an intrinsic property of the ligand-binding domain (27). In addition, the A431 cell-derived, purified extracellular domain was shown to inhibit EGF-R phosphorylation activity in vitro (1), a result which suggests that receptor dimerization not only is a consequence of ligand interaction but also is essential for biological signal generation. This requirement has not yet been demonstrated for the mutated EGF-R derivative v-*erb*B.

Recent studies have shown that an EGF-R mutant lacking most of the cytoplasmic domain is able to form heterodimers with wild-type (wt) receptors when expressed in the same cell. These heterodimers are not subject to EGF-induced tyrosine autophosphorylation. Furthermore, coexpression of mutant and wt receptors diminished the number of high-affinity EGF binding sites and reduced the rate of ligand-induced receptor degradation (20). In other studies, a kinase-negative EGF-R point mutant was coexpressed in cells with an active EGF-R mutant which lacked carboxy-terminal sequences. While the kinase-negative mutant was transphosphorylated, its expression in NIH 3T3 cells increased the ligand requirement for EGF-stimulated DNA synthesis (18). These experiments demonstrate extensive cross-talk and transactivation between EGF-R monomers, properties that render this signalling pathway potentially sensitive to inactivation by expression of receptor mutant polypeptides.

* Corresponding author.

To further investigate the biological consequences of dominant-negative EGF-R mutants in intact cells, we generated a series of recombinant retroviruses that encode EGF receptors bearing point or deletion mutations and examined their growth-inhibitory and anti-oncogenic potential upon coexpression with wt EGF-R or the v-*erb*B oncogene product in NIH 3T3 cells.

MATERIALS AND METHODS

Generation of recombinant retroviruses. The retroviral expression vectors pN2, pNTK2, pNTK-v-erbBES4, and pNTK-HERc have been described previously (21, 44, 50). pNTK-HERK721A was generated by cloning a *Bgl*II fragment from CMV-HERK721A into pNTK-HERc. pNTK-HERCD-533 was created by generating *Cla*I restriction sites on both sides of an *Xba*I-*Xho*I 2-kb fragment from pLSXNA8 (29), using standard cloning procedures, and ligating the 2-kb *Cla*I fragment with *Cla*I-digested pNTK2. The NTK-HERCD-566 construct was created by cloning a *Cla*I fragment from CVNHERXCD (19a) into the *Cla*I site of pNTK2. Ecotrophic recombinant retrovirus stocks were prepared from the helper virus-free producer line GP+E-86 (31). Stable GP+E-86 producer lines were generated by using a modified infection protocol (33). Low-titer amphotrophic virus, which was generated by transient transfection of retrovirus expression plasmids into the helper virus-free packaging cell line PA 317 (34), was used to infect GP+E-86 secondary packaging cells, followed by selection of GP+E-86 producer line clones in G418 (1 mg/ml). The virus titer was determined by infecting NIH 3T3 cells with serial dilutions of retrovirus-containing cell-free GP+E-86 supernatants and determining the number of G418-resistant colonies. A retrovirus (ψ2TGFα) containing TGFα gene sequences was kindly provided by David Lee (3). The titers were about 5×10^5/ml for wt and mutant receptor viruses and 5×10^4/ml for the ψ2TGFα virus.

Retrovirus-mediated gene transfer. Subconfluent NIH 3T3 cells (10^5 cells per 6-cm plate) were incubated with supernatants of GP+E-86 cells releasing high-titer NTK-HERc or NTK v-erbBES4 virus (5×10^5 G418^r CFU/ml; multiplicity of infection [MOI] of 5) for 4 to 12 h in the presence of Polybrene (4 μg/ml; Aldrich) and afterwards incubated in supernatant of GP+E-86 cells releasing high titers of either N2, NTK-HERK721A, NTK-HERCD-533, or NTK-HERCD-566 virus. The level of receptor expression was increased by multiple rounds of infection (4). In the experiments described, infection was carried out once with 1 ml of a diluted supernatant (MOI of 1.25) or one or four times with the same volume of undiluted supernatants (MOI of 5 and 20) of GP+E-86 cells releasing high titers of either N2, NTK+HERK721A, NTK-HERCD-533, or NTK-HERCD-566 virus.

Receptor phosphorylation in intact cells. Cells infected as described above were grown in 10-cm plates to 90% confluence, washed, and grown for 16 h in methionine-free Dulbecco modified Eagle medium (DMEM; GIBCO) supplemented with 1% fetal calf serum (FCS) containing 50 μCi of [^{35}S]methionine (Amersham) per ml. Cells were stimulated for 10 min with EGF (20 ng/ml; kindly provided by Amgen Corp.) and lysed in 0.5 ml lysis buffer (50 mM *N*-2-hydroxyethylpiperazine-*N'*-2-ethanesulfonic acid [HEPES; pH 7.2], 150 mM NaCl, 1.5 MM MgCl, 1 mM EGTA, 10% glycerol, 1% Triton X-100, 1 mM phenylmethylsulfonyl fluoride, 10 mg of aprotinin per ml, 100 μM sodium orthovanadate) at 4°C. The lysates were centrifuged for 10 min at 4°C in an Eppendorf centrifuge (~12,000 × *g*). The supernatants were then incubated with an excess of monoclonal antibody (MAb) 108.1 or polyclonal rabbit peptide antibody RK2 (24) and protein A-Sepharose for 4 h at 4°C. Immunoprecipitates were washed twice with HNTG (20 mM HEPES [pH 7.3], 150 mM NaCl, 0.1% Triton X-100, 10% glycerol). The pellet was then resuspended in sample buffer, boiled for 5 min, and analyzed by sodium dodecyl sulfate (SDS)-polyacrylamide gel electrophoresis (PAGE). Proteins were transferred electrophoretically to nitrocellulose and subsequently incubated with a mouse monoclonal antiphosphotyrosine antibody (5E2; 11). For detection, the nitrocellulose filter was incubated with a peroxidase-coupled goat anti-mouse antibody, followed by an enhanced chemiluminescence (ECL) substrate (Amersham) reaction. After detection of the ECL substrate reaction on Kodak X-Omat film, nitrocellulose filters were washed with phosphate-buffered saline (PBS) containing 0.2% Tween 20. Subsequently, [^{35}S]methionine-labeled proteins were detected by autoradiography. The intensity of the bands was determined by densitometry.

[^{3}H]thymidine incorporation. Subconfluent NIH 3T3 cells (10^5 cells per 6-cm plate) were coinfected as described with NTK-HERc, followed by four cycles of infection with either N2, NTK-HERK721A, NTK-HERCD-533, or NTK-HER CD-566. Cells were split in 12-well Costar dishes. After reaching confluence, the cell monolayers were starved for 24 h in 0.5 ml of DMEM–0.5% FCS, and 18 h after EGF addition, cells were labeled with 0.5 μCi of [*methyl*-^{3}H]thymidine (Amersham) for 4 h. Cells were washed twice with PBS and then precipitated with 10% trichloroacetic acid for 1 h on ice. The precipitate was washed with 10% trichloroacetic acid and solubilized in 200 μl of 0.2 N NaOH–0.2% SDS. Lysates were neutralized, and the incorporated radioactivity was quantitated by scintillation counting.

Transformation assays. To examine the ability of NIH 3T3 cells to form colonies in soft agar, subconfluent NIH 3T3 cells (10^5 cells per 6-cm plate) were infected with NTK-HERc or NTK-v-erbBES4 virus (MOI of 5), followed by four cycles of infection with either N2, NTK-HERK721A, NTK-HERCD-533, or NTK-HERCD-566 (MOI of 5 each). In cases in which an autocrine stimulus was to be created, cells were superinfected with ψ2TGFα virus (MOI of 0.2). Cells were plated in a 6-cm dish in the presence or absence of EGF (10 ng/ml) in a top layer of 3 ml of DMEM containing 10% FCS and 0.2% agar (GIBCO). The bottom layer contained DMEM, 10% FCS, and 0.4% agar. Visible colonies were scored after 4 weeks.

For focus formation assays, subconfluent NIH 3T3 cells (10^5 cells per 6-cm plate) were coinfected with NTK-HERc (MOI of 0.1) or NTK-v-erbBES4 (MOI of 0.05), followed by four cycles of infection (MOI of 5 each) with either N2, NTK-HERK721A, NTK-HERCD-533, or NTK-HERCD-566. Infected cells were grown on 6-cm dishes with DMEM containing 4% FCS in the presence or absence of EGF (10 ng/ml). Medium was changed every 3 days. Plates were stained with crystal violet, and foci were scored on day 18. Under superinfection conditions with ψ2TGFα virus (MOI of 0.01), an MOI of 5 was used for the NTK-HERc virus.

RESULTS

To investigate the effects of various EGF-R mutants on the biological signalling activities of either wt EGF-R or the v-*erb*BES4 oncogene product, we infected NIH 3T3 cells with replication-defective retroviruses containing wt viral and signalling-defective mutant receptor genes under the

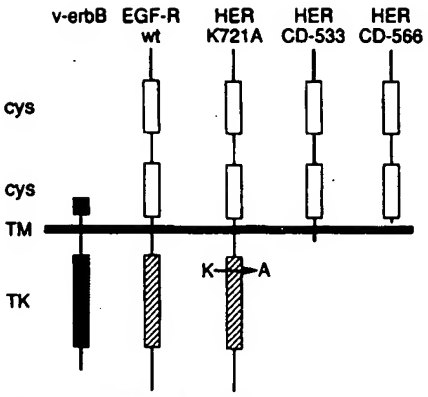

FIG. 1. Schematic representation of human wt and mutant EGF-R. Locations of cysteine-rich (cys), tyrosine kinase (TK), and transmembrane (TM) receptor domains are indicated. HERK721A carries a point mutation at position 721 (Lys → Ala), while HERCD-533 and HERCD-566 have C-terminal deletions of 533 and 566 amino acids, respectively (17, 19a, 29).

control of the mouse thymidine kinase promoter. Simultaneous infection with signalling-competent and -defective mutant EGF-R viruses at different relative MOIs provided quantitatively defined coexpression of different proteins in the same cell and circumvented the need for lengthy selection procedures and the risk of clonal influences on the cellular responses measured. In this manner, we determined the effects of various levels of mutant receptor expression on wt EGF-R and v-*erb*BES4 phosphorylation and tyrosine kinase-mediated mitogenic and oncogenic signal generation. This experimental approach made it possible to characterize even severely negative effects of specific EGF-R mutants (Fig. 1).

Inhibition of EGF-R and v-*erb*B phosphorylation in living cells. Ligand binding to the EGF-R activates its tyrosine kinase activity, which triggers rapid phosphorylation of five tyrosine residues in the C-terminal tail region (10, 30, 51). This phosphorylation of receptor tyrosines is an early and crucial event in the signal transduction process, and there is increasing evidence that it is the consequence of receptor dimerization and transphosphorylation (18, 25). In addition, structural alterations, including extensive truncations, deletions, and point mutations, can lead to constitutive activation of the EGF-R kinase, as exemplified by the activities of the v-*erb*B oncogene product (26). Whether the generation of a transforming signal by this oncoprotein also involves intermolecular activation in a dimeric complex remains to be established.

Cells infected with either wt EGF-R virus alone at an MOI of about 5 or doubly infected with the same amount of wt receptor virus and increasing doses (MOIs of 1.25, 5, and 20) of mutant receptor viruses were labeled with [^{35}S]methionine, incubated in the presence or absence of EGF for 10 min, lysed, and immunoprecipitated with a mouse anti-human EGF-R antibody (MAb 108). Samples were subjected to SDS-PAGE and transferred to nitrocellulose filters, and tyrosine phosphorylation was detected by using the mouse antiphosphotyrosine-specific antibody 5E2 (11) (Fig. 2A). The amount of receptor present in the immunoprecipitates was detected by autoradiography of the same nitrocellulose filter (Fig. 2B).

As shown in Fig. 2A (lanes b and c), EGF addition to

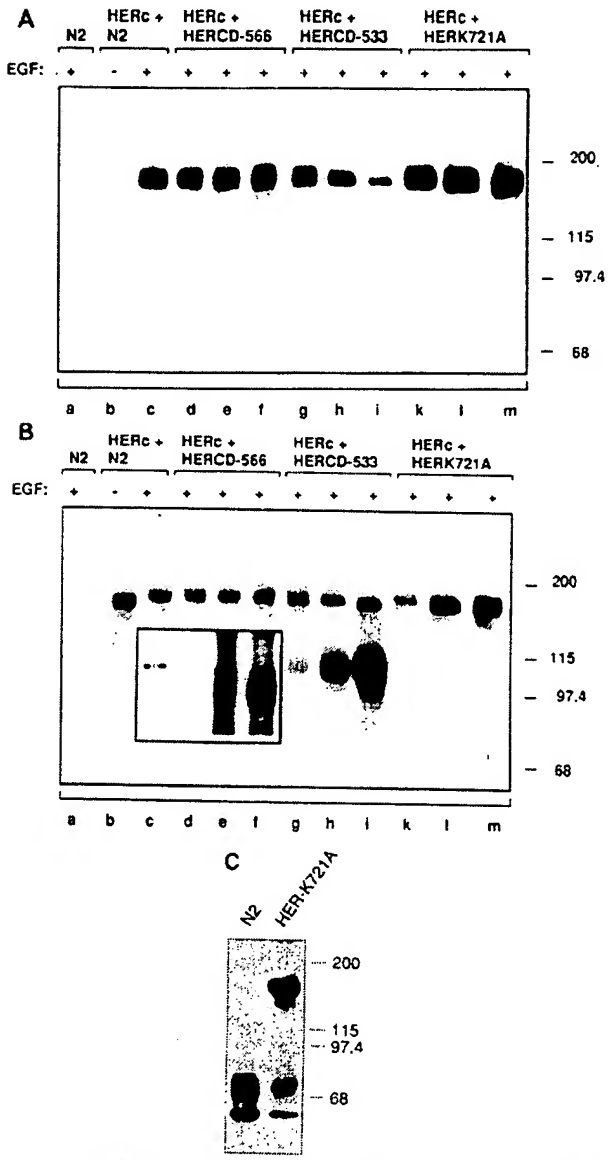

FIG. 2. Effect of mutant EGF-R expression on wt receptor phosphorylation. NIH 3T3 cells were infected with NTK-HERc virus (MOI of 5) and subsequently superinfected at MOIs of 1.25, 5, and 20 with N2, NTK-HERK721A, NTK-HERCD-533, or NTK-HERCD-566 virus. (A) Tyrosine phosphorylation of EGF-R in intact NIH 3T3 cells coexpressing EGF-R mutants. Cells infected with either wt receptor virus alone or doubly infected with wt and mutant receptor viruses were labeled overnight with [^{35}S]methionine and, after stimulation with EGF (20 ng/ml) for 10 min and solubilization, precipitated with anti-EGF-R MAb 108, separated by SDS-PAGE, and analyzed by immunoblotting with antiphosphotyrosine antibody 5E2, followed by the ECL detection system. (B) Receptor expression on NIH 3T3 cells. The nitrocellulose filters from panel A were reused to detect expression of wt and mutant receptors in infected cells. After the filter was washed with PBS containing 0.2% Tween 20, [^{35}S]methionine-labeled proteins were detected by autoradiography. (C) Effect of kinase-negative coexpression on v-*erb*B phosphorylation on tyrosine. NIH 3T3 cells were infected with NTK-v-erbBES4 virus (MOI of 5) and subsequently superinfected at an MOI of 20 with the NTK-HERK 721A virus. Cells were then solubilized, precipitated with EGF-R antibody RK2, separated by SDS-PAGE, and analyzed by immunoblotting with antiphosphotyrosine antibody 5E2 and the ECL detection system. Positions of size markers are shown in kilodaltons on the right.

intact NIH 3T3 cells infected with wt EGF-R virus strongly induced tyrosine phosphorylation of the 170-kDa EGF-R band. Phosphorylation decreased the electrophoretic mobility of the EGF-R in SDS-PAGE compared with unphosphorylated EGF-R (Fig. 2B, lanes b and c). This level of EGF-stimulated wt receptor phosphorylation was not diminished upon coexpression of the soluble EGF-R extracellular domain, encoded by the NTK-HERCD-566 virus genome, even when the extracellular domain was expressed at a significant excess relative to the wt receptor (Fig. 2A, lanes d to f; Fig. 2B, lanes d to f).

In contrast, in an analogous experiment using a virus expressing the membrane-anchored EGF-R deletion mutant HERCD-533 (Fig. 1), a strong dose-dependent inhibition of EGF-induced, wt EGF-R phosphorylation was observed (Fig. 2A, lanes g to i), even though the level of 170-kDa EGF-R protein remained constant (Fig. 2B, lanes g to i). The intensity of the tyrosine phosphorylation signal bands decreased from 100 to 71 to 30%. Under these conditions, the wt EGF-R displayed the same electrophoretic characteristics as an unphosphorylated receptor (Fig. 2B, lane i), which was consistent with its state of tyrosine phosphorylation, detected by MAb 5E2 (Fig. 2A, lane i).

When cells were coinfected with constant doses of wt receptor (MOI of 5) and increasing amounts of virus encoding the kinase-negative mutant HERK721A, increased tyrosine phosphorylation of the 170-kDa band was detected in lysates of EGF-stimulated cells (Fig. 2A, lanes k to m). The intensity of the receptor tyrosine phosphorylation signal in Fig. 2A (lanes k to m) increased from 251 to 337 to 450%, as measured by densitometric analysis of autoradiographs (not shown). As the wt receptor and the kinase-negative mutants are of the same size, the increased 170-kDa signal in Fig. 2B (lanes k to m) likely reflects the sum of phosphorylation of both receptors and was apparently the result of transphosphorylation between active HERc and multiple kinase-defective HERK721A receptors.

Similarly, we examined the consequences of NTK-v-erbBES4 and signalling-defective mutant virus coinfection on the phosphorylation states of the coexpressed proteins. Neither HERCD-566 nor HERCD-533 had any apparent effect on v-*erb*BES4 phosphorylation in coinfected cells (not shown). Simultaneous expression of v-*erb*BES4 and the kinase-defective HERK721A point mutant in coinfected cells resulted in a marked and reproducible decrease of v-*erb*BES4 66- and 74-kDa band phosphorylation in comparison with the control experiment in which the N2 virus was used (Fig. 2C).

Concomitant with the reduction in v-*erb*BES4 phosphotyrosine content, strong tyrosine phosphorylation of the 170-kDa HERK721A mutant receptor was observed, which suggested interaction and transphosphorylation between the oncogene product and HERK721A. However, it is important to note that the intensity of the phosphorylation signal did not reflect the relative expression levels of p66/74 versus p170 polypeptide (about 1:4), as determined by immunoblotting with RK2 polyclonal antiserum (not shown).

Inhibition of EGF-induced mitogenic response. EGF stimulates a mitogenic response in NIH 3T3 fibroblasts expressing the EGF receptor (37, 39). To determine the consequences of receptor mutations, we investigated the effects of mutant receptors on wt EGF-R mitogenic signalling by measuring induction of DNA synthesis in quiescent, confluent cell monolayers.

DNA synthesis in cells infected with the NTK-HERc virus (MOI of 5) and the N2 virus control (MOI of 5), as determined by [^{3}H]thymidine incorporation, was maximally stimulated by EGF at 2 ng/ml, with half-maximal stimulation (50% effective dose) at 0.66 ng/ml (Fig. 3). Similar to earlier observations (16, 39), higher EGF concentrations resulted in lower levels of [^{3}H]thymidine incorporation, as indicated by the decline in the dose-response curve (Fig. 3). Coexpression of EGF-R (single infection, MOI of 5) with HERCD-533 and HERK721A (four sequential infection cycles, MOI of 5 each) led to a marked shift of the dose-response curve to higher EGF concentrations (Fig. 3A and B), indicating that the cells had become less responsive to the growth factor compared with HERc/N2 cells. The deletion mutant HERCD-533 and the kinase-deficient point mutant HERK721A (Fig. 1) had similar effects on wt EGF-R mito-

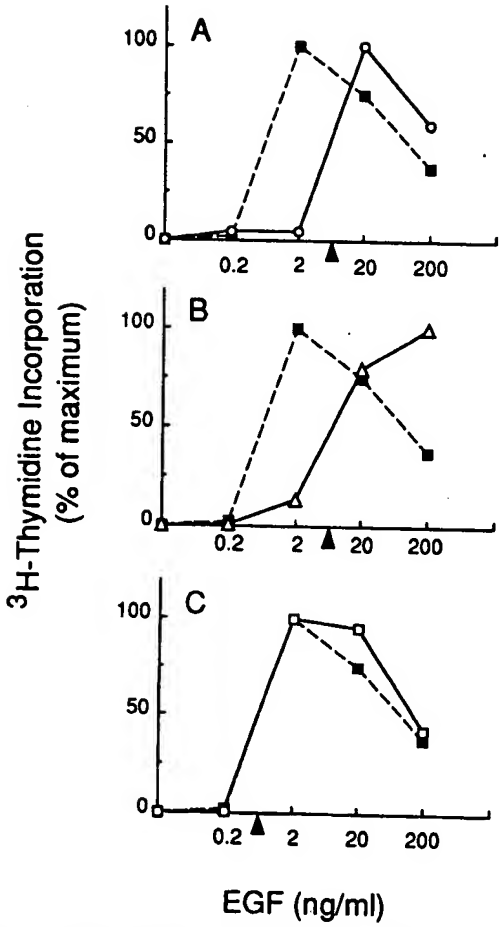

FIG. 3. EGF-stimulated [^{3}H]thymidine incorporation. Cells were infected with either wt receptor virus alone (dashed lines) or with wt and mutant receptor viruses under conditions described in Materials and Methods. HERc/HERK721A (A), HERc/HERCD-533 (B), and HERc/HERCD-566 (C) were grown to confluence in 12-well Costar dishes and starved for 2 days in DMEM containing 0.5% FCS, after which 10% FCS or different concentrations of EGF were added. At 18 h after EGF addition, [^{3}H]thymidine (0.5 μCi per well) was added for 4 h, and its incorporation into DNA was determined. The mitogenic response was scaled to demonstrate dose-response relationships. The values were corrected for basal thymidine incorporation, and the maximal observed response to EGF was defined as 100%. The arrowhead indicates half-maximal thymidine incorporation. Numbers represent averages of two independent experiments.

TABLE 1. Effects of dominant negative mutants on EGF-R/v-*erb*B-mediated colony formation[a]

Infection	No. of colonies/10^6 CFU		
	+ EGF (10 ng/ml)	+ ψ2 TGFα	No ligand
N2	0	0	
NTK-HERK721A	0	0	
NTK-HERCD-533	0	0	
NTK-HERCD-566	0	0	
NTK-HERc/N2	246	148	
NTK-HERc/NTK-HERK721A	8	2	
NTK-HERc/NTK-HERCD-533	6	4	
NTK-HERc/NTK-HERCD-566	128	100	
NTK-v-erbB-ES4/N2			180
NTK-v-erbB-ES4/NTK-HERK721A			68
NTK-v-erbB-ES4/NTK-HERCD-533			128

[a] Colonies were counted after 4 weeks. Numbers represent averages of three (v-*erb*B) or four (HERc) independent experiments with duplicate determinations and maximal 10 to 15% variation observed between experiments.

TABLE 2. Inhibition of NIH 3T3 cell focus formation by dominant negative EGF-R mutant viruses[a]

Infection	No. of foci/10^6 CFU		
	+ EGF (10 ng/ml)	+ ψ2 TGFα	No ligand
N2	0	0	
NTK-HERK721A	0	0	
NTK-HERCD-533	0	0	
NTK-HERCD-566	0	0	
NTK-HERc/N2	920	480	
NTK-HERc/NTK-HERK721A	40	18	
NTK-HERc/NTK-HERCD-533	90	14	
NTK-HERc/NTK-HERCD-566	910	500	
NTK-v-erbB-ES4/N2			3,000
NTK-v-erbB-ES4/NTK-HERK721A			2,850
NTK-v-erbB-ES4/NTK-HERCD-533			2,770
NTK-v-erbB-ES4/NTK-HERCD-566			2,800

[a] Foci were counted after 14 to 16 days. Numbers represent averages of three (v-*erb*B) or four (HERc) independent experiments with duplicate determinations and maximal 10 to 15% variation observed between experiments.

genic signalling, causing a 10-fold increase of the 50% effective dose to 6.6 ng of EGF per ml. In contrast, superinfection with NTK-HERCD-566 virus had no significant effect on wt EGF-R-mediated stimulation of DNA synthesis by EGF (Fig. 3C).

Anti-oncogenic activity of EGF-R mutants. Overexpression of EGF-R causes EGF-dependent cell transformation of NIH 3T3 cells (8, 39, 49). To examine whether the oncogenic activity of overexpressed EGF-R could be inhibited with either of the three mutant receptors, we performed double-infection experiments with NTK-HERc virus and either of the mutant receptor viruses and determined their ability to induce the formation of colonies in soft agar or foci in cell monolayers. Stimulation of overexpressed EGF-R was achieved by either EGF addition to the medium or by infection with a TGFα expression virus (ψ2TGFα) to create an autocrine activation system (Table 1; average numbers from four experiments are given).

After infection with NTK-HERc virus (MOI of 5) and N2 control (MOI of 20), NIH 3T3 cells formed about 250 soft-agar colonies in the presence of 10 ng of EGF per ml. Upon coinfection with ψ2TGFα virus (MOI of 0.2), formation of an average of 148 colonies was observed under otherwise identical conditions (Table 1). However, when NTK-HERc virus-infected cells were superinfected with either NTK-HERK721A or NTK-HERCD-533 virus (four cycles, MOI of 20 each), the colony-forming capacity was almost completely suppressed. Coexpression of EGF-R with the secreted extracellular domain HERCD-566 reduced the colony-forming capacity by about 50% when stimulated with added EGF and by about 33% under autocrine stimulation conditions after infection with ψ2TGFα virus.

Similarly, we determined the focus-forming potential of NTK-HERc virus in NIH 3T3 monolayers, either in the presence of EGF at 10 ng/ml (resulting in an average of 920 foci per 10^6 viruses) or after coinfection with ψ2TGFα virus (resulting in 480 foci per 10^6 NTK-HERc viruses). Superinfection with NTK-HERK721A or NTK-HERCD-533 virus suppressed the number of foci by more than 90% when stimulated with added EGF or ψ2TGFα virus, respectively (Table 2).

In contrast to the result obtained in the soft-agar colony formation assay, cells coexpressing wt EGF-R and HERCD-566 after infection with the respective viruses formed about the same number of foci as did EGF-R-expressing cells coinfected with N2 control virus, both when stimulated with EGF and when stimulated with ψ2TGFα virus.

Analogous experiments with NTK-v-erbBES4 virus as the transforming agent demonstrated a significant inhibitory effect (~60%) of the HERK721A mutant in the soft-agar colony growth assay, which correlated with the observed reduction of v-*erb*BES4 phosphorylation (Table 1). A reproducible but significantly weaker inhibition of colony formation in soft agar was obtained even with the HERCD-533 deletion mutant (Table 1). Interestingly, however, no inhibition by any EGF-R mutant was observed on v-*erb*BES4-induced focus formation in NIH 3T3 monolayers, even though the ratios of signalling-defective to transforming receptor viruses used in these experiments were 400:1 rather than 4:1 as in the colony formation experiments (Table 2).

DISCUSSION

RTKs represent complex biological signal-generating molecules that span the plasma membrane and permit the cell to communicate with its environment. RTK signalling activities are regulated by conformational changes within their extracellular or cytoplasmic domains, by interactions between these domains across the plasma membrane barrier, and by intermolecular contacts with intracellular substrates and regulatory factors. Many details of the intricate process by which ligand binding on the cell surface leads to diverse cellular responses are still poorly understood. However, a wealth of experimental data supports a mechanism for the generation of a molecular signal by RTKs within the cell, which includes receptor dimerization and transphosphorylation followed by phosphorylation of polypeptide substrates and interaction with cellular regulatory factors (48).

Disruption of this process of receptor activation and signal generation by mutations which either impair the ligand-binding function of the receptor, affect its transport to the cell surface, prevent dimerization, inactivate its tyrosine kinase, or interfere with substrate interaction lead to a partial or complete loss of biological function (48). This hypothesis is supported by experimental evidence with

kinase-deficient and truncated receptors in vitro, in intact cells, and in vivo (1, 5, 18, 20, 32, 35, 36, 38, 45).

In stable cell lines, a kinase-negative EGF-R carrying a point mutation in the ATP binding site was shown previously to be transphosphorylated by a C-tail deletion mutant and to reduce the response of NIH 3T3 cells to EGF (18). The use of recombinant retrovirus infection allowed us to modulate the relative expression levels of signalling-competent and -defective receptors and thereby facilitated quantitative analyses, which had been previously hampered by the clonal nature of doubly transfected cell lines. In such an experiment, by increasing the levels of HERK721A expression relative to the level of wt EGF-R in the same cells, we detected a proportionally elevated phosphotyrosine signal (Fig. 2A). This result demonstrated that the formation of dimers and the subsequent transphosphorylation reaction represented a dynamic enzyme-substrate interaction, which even in the intact cell appeared to be stoichiometric. Thus, at least for the monomeric subclass 1 receptors, a transphosphorylation/activation cascade originating from a few ligand-activated molecules appears to be possible; phosphorylated dimers may dissociate into activated monomers, which are subsequently internalized and degraded. Alternatively, however, the inability of the HERK721A receptor to phosphorylate the wt EGF-R within the dimer leads to a failure in creating a productive complex. Accordingly, overexpression of the kinase-negative EGF-R relative to intact, wt receptor in the same cell had a strong inhibitory effect on EGF-induced DNA synthesis in NIH 3T3 cells and suppressed two transformation parameters, soft-agar colony formation and focus formation, in cell monolayers with comparable potency. The observation that the inhibitory effects of HERK721A may be overcome by high ligand concentrations likely reflects the equilibrium between free and ligand-bound, wt and mutant receptors in their monomeric and dimeric forms and lends support to a transphosphorylation cascade model.

Similar results were obtained with the receptor deletion mutant HERCD-533, which is missing almost the entire cytoplasmic portion of the receptor. Previous analyses in stable cell lines showed that cross-linked heterodimers between HERCD-533 and wt EGF-R were not tyrosine phosphorylated (20). In our experiments, this mutant inhibited wt receptor phosphorylation in a dose-dependent manner (Fig. 2A) and potently suppressed its mitogenic and oncogenic signals in intact NIH 3T3 cells (Fig. 3; Tables 1 and 2). Again, the growth-inhibitory and anti-oncogenic effects of the HERCD-533 mutant could be prevented by overstimulation of cells with high ligand concentrations. Thus, the deletion mutant behaves similarly to the kinase-defective point mutant under comparable expression conditions in intact cells. Since the HERCD-533 deletion mutant displays an approximately 30-fold-lower affinity for EGF than does the wild-type receptor (29), it is highly unlikely that the observed inhibitory effects are the result of competition for the ligand.

Interestingly, coexpression of wt EGF-R with a fourfold excess of the soluble extracellular domain did not inhibit wt receptor phosphorylation in intact cells and had no detectable effects on EGF-induced proliferation or focus formation. These findings were inconsistent with earlier reports that demonstrated heterodimer formation of soluble EGF-R extracellular domain with wt receptor and suppression of its kinase activity in vitro (1, 27). Soft-agar colony formation experiments with the soluble, extracellular domain, however, demonstrated a partial (33 to 50%) inhibition of EGF- or TGFα-stimulated transforming activity. The soft-agar growth conditions may prevent rapid diffusion of secreted extracellular domain molecules, which accumulate near the cell surface and eventually reach inhibitory concentrations. These levels could not be attained with monolayer cultures under normal experimental conditions for focus formation. Analogously, A431 epidermoid carcinoma cells, which because of gene amplification and rearrangement overexpress the EGF-R and produce a soluble form of EGF-R, are still tumorigenic (47).

Transformation by the avian v-*erb*BES4 oncogene product, as measured by soft-agar colony formation, was suppressed (60%) by the kinase-negative HERK721A mutant and less efficiently (30%) by the HERCD-533 mutant. For the kinase-defective receptor, this effect correlated with a decrease of v-*erb*BES4 protein phosphorylation in coexpressing NIH 3T3 cells. Under these conditions, HERK721A was found to be tyrosine phosphorylated, although at a lower stoichiometry than when coexpressed with comparable molar amounts of activated wt EGF-R. These observations suggest that the cytoplasmic domains of v-*erb*BES4 and EGF-R are able to interact and that these interactions are sufficient for transphosphorylation. This finding is also consistent with our earlier results demonstrating transphosphorylation of the HERK721A mutant by a chimeric receptor consisting of insulin receptor extracellular and EGF-R cytoplasmic domains (25). Although we cannot exclude an involvement of the extracellular or transmembrane sequences present in v-*erb*BES4, the weak inhibitory effect of the HERCD-533 mutant on v-*erb*BES4-induced colony formation indicates that these sequences play a relatively minor role. Nevertheless, comparison of equivalent overexpression of HERK721A with activated EGF-R or v-*erb*BES4 and its effect on transformation strongly supports a predominant role of extracellular domain determinants in receptor dimerization and therefore dominant-negative inhibition of signalling functions.

Transphosphorylation of HERK721A by v-*erb*BES4 and the reduced phosphorylation signal of $p66/74^{v\text{-}erbBES4}$ suggest that even this truncated oncogene product is activated by transphosphorylation rather than intramolecular autophosphorylation. In addition, our observations suggest that the formation of dimers and transphosphorylation are dynamic processes in which the binding constant for dimerization is defined by structural determinants located in extracellular, cytoplasmic, and possibly transmembrane domains of the receptor. A minimization of such determinants may have occurred during the evolution of oncogenic receptor mutants, generating membrane proteins that can transiently dimerize and become transphosphorylated, without subsequent removal from the cell surface. This would lead to constant reactivation of the oncogenic signal despite the presence of cellular tyrosine phosphatases.

None of the EGF-R mutants had a significant effect on v-*erb*BES4-induced focus formation. This finding may indicate that there is no quantitative correlation between phosphorylation levels and this biological response. Alternatively, a secreted molecule could be involved which accumulates in soft agar and causes inhibition of transformation but fails to reach a critical concentration in monolayer cultures.

In summary, EGF-R mutants with either a defective kinase or large cytoplasmic domain deletions exhibited antiproliferative and anti-oncogenic potencies in intact cells in culture. These effects are likely analogous to those evoked by certain mouse *W* locus mutations, as well as genetic

lesions identified in association with syndromes of insulin resistance in humans (46). The capacity of mutant RTKs to inhibit wt receptor signals may have great potential for the investigation of the biological roles of the many members of this family; such function knockout experiments offer many of the possibilities otherwise achieved by gene knockout, using the homologous recombination approach. Moreover, these mutant receptors serve as potential therapeutic options for the cure of malignant cancer by virus-mediated therapy in the future.

ACKNOWLEDGMENTS

We thank David Lee for making the ψ2TGFα virus available and Khash Khazaie for support of this project. We are grateful to Suzanne Pfeffer for editorial advice and Jeanne Arch for expert preparation of the manuscript.

REFERENCES

1. **Basu, A., M. Raghunath, S. Bishayee, and M. Das.** 1989. Inhibition of tyrosine kinase activity of the epidermal growth factor (EGF) receptor by a truncated receptor form that binds to EGF: role for interreceptor interaction in kinase regulation. Mol. Cell. Biol. 9:671–677.
2. **Berger, M. S., C. Greenfield, W. J. Gullick, J. Haley, J. Downward, D. E. Neal, A. L. Harris, and M. D. Waterfield.** 1987. Evaluation of epidermal growth factor receptors in bladder tumours. Br. J. Cancer 56:533–537.
3. **Blasband, A. J., D. M. Gilligan, L. F. Winchell, S. T. Wong, N. C. Luetteke, K. T. Rogers, and D. C. Lee.** 1990. Expression of the TGF-α integral membrane precursor induces transformation of nrk cells. Oncogene 5:1213–1221.
4. **Bordignon, C., S.-F. Yu, C. A. Smith, P. Hantzopoulos, G. E. Ungers, C. A. Keever, R. J. O'Reilly, and E. Gilboa.** 1989. Retroviral vector-mediated high-efficiency expression of adenosine deaminase (ADA) in hematopoietic long-term cultures of ADA-deficient marrow cells. Proc. Natl. Acad. Sci. USA 86: 6748–6752.
5. **Chou, C. K., T. J. Dull, D. S. Russell, R. Gherzi, D. Lebwohl, A. Ullrich, and O. M. Rosen.** 1987. Human insulin receptors mutated at the ATP-binding site lack protein tyrosine kinase activity and fail to mediate postreceptor effects of insulin. J. Biol. Chem. 262:1842–1847.
6. **Cochet, C., O. Kashles, E. M. Chambaz, I. Borrello, C. R. King, and J. Schlessinger.** 1988. Demonstration of epidermal growth factor-induced receptor dimerization in living cells using a chemical covalent cross-linking agent. J. Biol. Chem. 263:3290–3295.
7. **Derynck, R., D. V. Goeddel, A. Ullrich, J. U. Gutterman, R. D. Williams, T. S. Bringman, and W. H. Berger.** 1987. Synthesis of mRNAs for transforming growth factors-α and -β and the epidermal growth factor receptor by human tumors. Cancer Res. 47:707–712.
8. **Di Fiore, P. P., J. H. Pierce, T. P. Fleming, R. Hazan, A. Ullrich, C. R. King, J. Schlessinger, and S. A. Aaronson.** 1987. Overexpression of the human EGF receptor confers an EGF-dependent transformed phenotype to NIH 3T3 cells. Cell 51:1063–1070.
9. **Di Marco, E., J. H. Pierce, T. P. Fleming, M. H. Kraus, C. J. Molloy, S. A. Aaronson, and P. P. Di Fiore.** 1989. Autocrine interaction between TGFα and the EGF-receptor: quantitative requirements for induction of the malignant phenotype. Oncogene 4:831–838.
10. **Downward, J., P. Parker, and M. D. Waterfield.** 1984. Autophosphorylation sites on the epidermal growth factor receptor. Nature (London) 311:483–485.
11. **Fendly, B. M., M. Winget, R. M. Hudziak, M. T. Lipari, M. A. Napier, and A. Ullrich.** 1990. Characterization of murine monoclonal antibodies reactive to either the human epidermal growth factor receptor or HER2/*neu* oncogene. Cancer Res. 50:1550–1558.
12. **Frykberg, L., S. Palmieri, H. Beug, T. Graf, M. J. Hayman, and B. Vennström.** 1983. Transforming capacities of avian erythroblastosis virus mutants deleted in the erbA or erbB oncogenes. Cell 32:227–238.
13. **Fung, T., W. G. Lewis, H.-J. Kung, and L. B. Crittenden.** 1983. Activation of the cellular oncogene c-erbB by LTR insertion: molecular basis for induction of erythroblastosis by avian leukosis virus. Cell 33:357–368.
14. **Graf, T., B. Royer-Pokora, G. E. Schubert, and H. Beug.** 1976. Evidence for the multiple oncogenic potential of cloned leukemia virus: in vitro and in vivo studies with avian erythroblastosis virus. Virology 71:423–433.
15. **Gullick, W. J., J. J. Marsden, N. Whittle, B. Ward, L. Bobrow, and M. D. Waterfield.** 1986. Expression of epidermal growth factor receptors on human cervical, ovarian and vulval carcinomas. Cancer Res. 46:285–292.
16. **Honegger, A. M., T. J. Dull, F. Bellot, E. Van Obberghen, D. Szapary, A. Schmidt, A. Ullrich, and J. Schlessinger.** 1988. Biological activities of EGF-receptor mutants with individually altered autophosphorylation sites. EMBO J. 7:3045–3052.
17. **Honegger, A. M., T. J. Dull, S. Felder, E. Van Obberghen, F. Bellot, D. Szapary, A. Schmidt, A. Ullrich, and J. Schlessinger.** 1987. Point mutation at the ATP binding site of EGF receptor abolishes protein-tyrosine kinase activity and alters cellular routing. Cell 51:199–209.
18. **Honegger, A. M., A. Schmidt, A. Ullrich, and J. Schlessinger.** 1990. Evidence for epidermal growth factor-induced intermolecular autophosphorylation of the EGF receptor in living cells. Mol. Cell. Biol. 10:4035–4044.
19. **Hudziak, R. M., J. Schlessinger, and A. Ullrich.** 1987. Increased expression of the putative growth factor receptor $p185^{HER2}$ causes transformation and tumorigenesis of NIH 3T3 cells. Proc. Natl. Acad. Sci. USA 84:7159–7163.

19a. **Hudziak, R. M., and A. Ullrich.** Submitted for publication.

20. **Kashles, O., Y. Yarden, R. Fischer, A. Ullrich, and J. Schlessinger.** 1991. A dominant negative mutation suppresses the function of normal epidermal growth factor receptors by heterodimerization. Mol. Cell. Biol. 11:1454–1463.
21. **Keller, G., C. Paige, E. Gilboa, and E. F. Wagner.** 1985. Expression of a foreign gene in myeloid and lymphoid cells derived from multipotent haematopoietic precursors. Nature (London) 318:149–154.
22. **Kern, J. A., D. A. Schwartz, J. E. Nordberg, D. B. Weiner, M. I. Greene, L. Torney, and R. A. Robinson.** 1990. $p185^{neu}$ expression in human lung adenocarcinomas predicts shortened survival. Cancer Res. 50:5184–5191.
23. **Khazaie, K., T. J. Dull, T. Graf, J. Schlessinger, A. Ullrich, H. Beug, and B. Vennström.** 1988. Truncation of the human EGF receptor leads to differential transforming potentials in primary avian fibroblasts and erythroblasts. EMBO J. 7:3061–3071.
24. **Kris, R., I. Lax, W. Gullick, M. D. Waterfield, A. Ullrich, M. Fridkin, and J. Schlessinger.** 1985. Antibodies against a synthetic peptide as a probe for the kinase activity of the avian EGF-R and v-erbB protein. Cell 40:619–625.
25. **Lammers, R., E. Van Obberghen, R. Ballotti, J. Schlessinger, and A. Ullrich.** 1990. Transphosphorylation as a possible mechanism for insulin and epidermal growth factor receptor activation. J. Biol. Chem. 265:16886–16890.
26. **Lax, I., R. Kris, I. Sasson, A. Ullrich, M. J. Hayman, H. Beug, and J. Schlessinger.** 1985. Activation of c-erb-B in avian leukosis virus-induced erythroblastosis leads to the expression of a truncated EGF receptor kinase. EMBO J. 4:3179–3182.
27. **Lax, I., A. Mitra, C. Ravera, D. Hurwitz, M. Rubinstein, A. Ullrich, R. Stroud, and J. Schlessinger.** 1991. EGF induces oligomerization of soluble, extracellular, ligand binding domain of EGF-receptor and a low resolution projection structure of the ligand binding domain. J. Biol. Chem. 266:13828–13833.
28. **Libermann, T. A., H. R. Nusbaum, N. Razon, R. Kris, I. Lax, H. Soreq, N. Whittle, M. D. Waterfield, A. Ullrich, and J. Schlessinger.** 1985. Amplification, enhanced expression and possible rearrangement of EGF receptor gene in primary human brain tumours of glial origin. Nature (London) 313:144–147.
29. **Livneh, E., R. Prywes, O. Kashles, N. Reiss, I. Sasson, Y. Mory, A. Ullrich, and J. Schlessinger.** 1986. Reconstitution of human epidermal growth factor receptors and its deletion mutants in

cultured hamster cells. J. Biol. Chem. 260:12490–12497.
30. **Margolis, B. L., I. Lax, R. Kris, M. Dombalagian, A. M. Honegger, R. Howk, D. Givol, A. Ullrich, and J. Schlessinger.** 1989. All autophosphorylation sites of epidermal growth factor (EGF) receptor and HER2/*neu* are located in their carboxy-terminal tails. J. Biol. Chem. 264:10667–10671.
31. **Markowitz, D., S. Goff, and A. Bank.** 1988. A safe packaging line for gene transfer: separating viral genes on two different plasmids. J. Virol. 62:1120–1124.
32. **McClain, D. A., H. Maegawa, J. Lee, T. J. Dull, A. Ullrich, and J. M. Olefsky.** 1987. A mutant insulin receptor with defective tyrosine kinase displays no biologic activity and does not undergo endocytosis. J. Biol. Chem. 262:14663–14671.
33. **Miller, A. D., and C. Buttimore.** 1986. Redesign of retrovirus packaging cell lines to avoid recombination leading to helper virus production. Mol. Cell. Biol. 6:2895–2902.
34. **Miller, A. D., M.-F. Law, and I. M. Verma.** 1985. Generation of helper-free amphotropic retrovirus that transduce a dominant-acting, methotrexate-resistant dihydrofolate reductase gene. Mol. Cell Biol. 5:431–437.
35. **Nocka, K., S. Majumder, B. Chabot, P. Ray, M. Cervone, A. Bernstein, and P. Besmer.** 1989. Expression of c-*kit* gene products in known cellular targets of *W* mutations in normal and *W* mutant mice—evidence for an impaired c-*kit* kinase in mutant mice. Genes Dev. 3:816–826.
36. **Nocka, K., J. C. Tan, E. Chin, T. Chu, P. Ray, P. Traktman, and P. Besmer.** 1990. Molecular bases of dominant negative and loss of function mutations at the murine c-*kit*/white spotting locus: W^{37}, W^{v}, W^{41} and *W*. EMBO J. 9:1805–1813.
37. **Prywes, R., E. Livneh, A. Ullrich, and J. Schlessinger.** 1986. Mutations in the cytoplasmic domain of EGF receptor affect EGF binding and receptor internalization. EMBO J. 5:2179–2190.
38. **Reith, A. D., R. Rottapell, E. Giddens, C. Brady, L. Forrester, and A. Bernstein.** 1990. ω mutant mice with mild or severe developmental defects contain distinct point mutations in the kinase domain of the c-kit receptor. Genes Dev. 4:390–400.
39. **Riedel, H., S. Massoglia, J. Schlessinger, and A. Ullrich.** 1988. Ligand activation of overexpressed epidermal growth factor receptors transforms NIH 3T3 mouse fibroblasts. Proc. Natl. Acad. Sci. USA 85:1477–1481.
40. **Sainsbury, J. R. C., J. R. Farndon, G. V. Sherbert, and A. L. Harris.** 1985. Epidermal growth factor receptors and oestrogen receptors in human breast cancer. Lancet i:364–366.
41. **Schlessinger, J.** 1988. Signal transduction by allosteric receptor oligomerization. Trends Biochem. Sci. 13:443–447.
42. **Slamon, D. J., G. M. Clark, S. G. Wong, W. J. Levin, A. Ullrich, and W. L. McGuire.** 1987. Human breast cancer: correlation of relapse and survival with amplification of the HER-2/neu oncogene. Science 235:177–182.
43. **Slamon, D. J., W. Godolphin, L. A. Jones, J. A. Holt, S. G. Wong, D. E. Keith, W. J. Levin, S. G. Stuart, J. Udove, A. Ullrich, and M. F. Press.** 1989. Studies of the HER-2/neu proto-oncogene in human breast and ovarian cancer. Science 244:707–712.
44. **Stewart, C. L., S. Schuetze, S. Vanek, and E. F. Wagner.** 1987. Expression of retroviral vectors in transgenic mice obtained by embryo infection. EMBO J. 6:383–388.
45. **Tan, J. C., K. Nocka, P. Ray, P. Traktman, and P. Besmer.** 1990. The dominant W^{42} *spotting* phenotype results from a missense mutation in the c-*kit* receptor kinase. Science 247:209–212.
46. **Taylor, S. I., A. Cama, H. Kadowaki, T. Kadowaki, and D. Accili.** 1990. Mutations of the human insulin receptor gene. Trends Endocrinol. Metabol. 2:134–139.
47. **Ullrich, A., L. Coussens, J. S. Hayflick, T. J. Dull, A. Gray, A. W. Tam, J. Lee, Y. Yarden, T. A. Libermann, J. Schlessinger, J. Downward, E. L. V. Mayes, N. Whittle, M. D. Waterfield, and P. H. Seeburg.** 1984. Human epidermal growth factor receptor cDNA sequence and aberrant expression of the amplified gene in A431 epidermoid carcinoma cells. Nature (London) 309:418–425.
48. **Ullrich, A., and J. Schlessinger.** 1990. Signal transduction by receptors with tyrosine kinase activity. Cell 61:203–212.
49. **Velu, T. J., L. Beguinot, W. C. Vass, M. C. Willingham, G. T. Merlino, I. Pastan, and D. R. Lowy.** 1987. Epidermal growth factor-dependent transformation by a human EGF receptor proto-oncogene. Science 237:1408–1410.
50. **von Rüden, T., and E. F. Wagner.** 1988. Expression of functional human EGF receptor on murine bone marrow cells. EMBO J. 7:2749–2756.
51. **Walton, G. M., W. S. Chen, M. G. Rosenfeld, and G. N. Gill.** 1990. Analysis of deletions of the carboxyl terminus of the epidermal growth factor receptor reveals self-phosphorylation at tyrosine 992 and enhanced in vivo tyrosine phosphorylation of cell substrates. J. Biol. Chem. 265:1750–1754.
52. **Yamamoto, T., N. Kamata, H. Kawano, S. Shimizu, T. Kuroki, K. Toyoshima, K. Rikimaru, N. Nomura, R. Ishizaki, I. Pastan, S. Gamou, and N. Shimizu.** 1986. High incidence of amplification of the epidermal growth factor receptor gene in human squamous carcinoma cell lines. Cancer Res. 46:414–416.
53. **Yarden, Y., and J. Schlessinger.** 1987. Self-phosphorylation of epidermal growth factor receptor: evidence for a model of intermolecular allosteric activation. Biochemistry 26:1443–1451.

BIOLOGY OF REPRODUCTION 68, 797–803 (2003)
Published online before print 23 October 2002.
DOI 10.1095/biolreprod.102.005520

Epidermal Growth Factor-Receptor Tyrosine Kinase Activity Regulates Expansion of Porcine Oocyte-Cumulus Cell Complexes In Vitro[1]

Radek Prochazka,[2,3] Petr Kalab,[4] and Eva Nagyova[3]

Institute of Animal Physiology and Genetics,[3] Academy of Sciences of the Czech Republic, 277 21 Libechov, Czech Republic
Department of Molecular and Cellular Biology,[4] University of California at Berkeley, Berkeley, California 94720

ABSTRACT

We have recently shown that epidermal growth factor (EGF) strongly stimulates expansion of porcine oocyte-cumulus complexes (OCCs) isolated from large follicles (>6 mm) and does not promote expansion of OCCs from small (3–4-mm) follicles. In order to elucidate the role of EGF in OCCs expansion, in the present study, we first examined the presence of EGF receptors (EGFRs) in cumulus cells isolated from follicles of different sizes. Surprisingly, immunoblotting showed that cumulus cells obtained from all follicular size categories contained similar amounts of EGFR protein. On the other hand, we found a dramatic difference in the pattern of protein tyrosine phosphorylation in a comparison of cumulus cells isolated from small and large follicles treated by EGF. Furthermore, tyrosine-phosphorylated EGFR was specifically immunoprecipitated with anti-phosphotyrosine antibodies from EGF-treated cumulus cells isolated from the large follicles. This result strongly indicates that only OCCs from the large follicles contain mature EGFRs that are capable of becoming activated by EGF. Remarkably, preincubation of cumulus cells from small follicles (3–4 mm) with FSH strongly increased EGF-stimulated tyrosine phosphorylation to levels comparable with OCCs from large follicles. The FSH-dependent activation of EGFRs was beneficial for expansion of OCCs isolated from the small follicles since OCCs treated sequentially by FSH (3 h) and EGF (1 h) underwent expansion significantly better then OCCs cultured in FSH or EGF alone. We conclude that a FSH-dependent pathway has an important role in the maturation of the EGFR in cumulus cells and that activation of EGFR-dependent signaling is sufficient to induce expansion.

cumulus cells, follicle-stimulating hormone, growth factors, oocyte development, signal transduction

INTRODUCTION

In mammalian ovarian follicles committed for ovulation, two major events occur following the preovulatory surge of gonadotropins. The residing oocytes resume and complete meiotic maturation and the cumulus cells, representing several layers of granulosa cells surrounding the oocyte, undergo a process of expansion. The morphology of cumulus cells changes dramatically, inclusive of an extensive rearrangement of cytoskeleton, namely assembly of actin microfilaments [1–3]. This process is followed by increased synthesis of hyaluronic acid-enriched extracellular matrix [4–6] and modification of the gap junctions between cumulus cells and the oocyte [7]. Presumably, the expansion facilitates release of the oocyte-cumulus complexes (OCCs) from the follicles during ovulation, their capture by oviductal fimbria, and a passage through the oviduct [8] and maintains viability of the ovulated oocytes within the oviduct [9]. In addition, expansion of the cumulus creates the proper microenvironment for sperm activation and motility [10, 11]. Therefore, the expansion is crucial for oocyte fertilization under both in vivo and in vitro conditions. Better understanding of mechanisms regulating cumulus expansion will thus lead to improvement of conditions for successful maturation and fertilization of mammalian oocytes under in vitro conditions.

In vitro, cumulus expansion can be induced by FSH [5, 6], and in mouse, pig, cattle, and rabbit, also by epidermal growth factor (EGF) [12–16]. The intrinsic tyrosine kinase of EGF-receptor (EGFR) is activated by binding of EGF, resulting in EGFR autophosphorylation and subsequent tyrosine phosphorylation of numerous substrates within the cell [17]. The tyrosine phosphorylation of the EGFR enables interaction with exchange proteins and a downstream activation of several signaling pathways, including mitogen-activated protein (MAP) kinase [18], phosphoinositol 3-kinase [19], STAT [20, 21], and phospholipase Cγ [22] pathways. So far, it is not known what signaling pathway is involved in regulation of EGF-stimulated cumulus expansion.

Recently, we reported that expansion of cumulus cells in the pig is developmentally regulated; while EGF stimulates expansion of OCCs originating from large antral and preovulatory follicles, OCCs from small follicles (<4 mm) do not expand following EGF treatment [3]. We have also shown that the failure of porcine OCCs from the small follicles to undergo expansion is accompanied by their inability to undergo rearrangement of F-actin and increase production of hyaluronic acid following EGF stimulation [3]. Nevertheless, these OCCs were able to respond to FSH and undergo full expansion accompanied by rearrangement of F-actin and increased secretion of hyaluronic acid. Therefore, we supposed that the failure of porcine OCCs to respond to EGF was caused by the absence or immaturity of EGFR. Alternatively, the absence of response to EGF could result from insufficient development of an EGFR downstream pathway.

Here we report that, while only expansion-capable OCCs

[1]This work was supported by grants 524/01/0903 from Grant Agency of the Czech Republic, A5045102 from Grant Agency of the Academy of Sciences of the Czech Republic, and LN 00A065 from Czech Ministry of Education.
[2]Correspondence: Radek Prochazka, Academy of Sciences of the Czech Republic, Institute of Animal Physiology and Genetics, Rumburska 89, 277 21 Libechov, Czech Republic. FAX: 420 315 69 71 86; e-mail: prochazka@iapg.cas.cz

Received: 12 April 2002.
First decision: 6 May 2002.
Accepted: 10 September 2002.

ISSN: 0006-3363. http://www.biolreprod.org

from large follicles respond to EGF by a prominent tyrosine phosphorylation of EGFR, the amount of EGFR protein is comparable in OCCs from all follicle sizes. We also provide evidence that pretreatment of OCCs from small follicles by FSH strongly increases their response to EGF both in terms of EGFR tyrosine phosphorylation and OCCs expansion, indicating that the function of EGFR in OCC expansion is FSH dependent.

MATERIAL AND METHODS

Chemicals, Supplies, and Antibodies

Culture medium M-199 with Hanks balanced salt solution was purchased from Sevac (Prague, Czech Republic), fetal calf serum (FCS) from Veterinary University in Brno (Czech Republic), culture dishes from Nunclon (Roskilde, Denmark), human recombinant FSH from N.V. Organon (Oss, Netherlands), human recombinant EGF from Genzyme Diagnostics (Russelheim, Germany), polyvinylidene difluoride (PVDF)-membrane Immobilon-P from Millipore (Bedford, MA). We used monoclonal antiphosphotyrosine antibodies PY 20 from Transduction Laboratories (Lexington, KY) and PT 66 from Sigma-Aldrich (Prague, Czech Republic). Rabbit anti-EGFR antibody was from Santa Cruz Biotechnology (Santa Cruz, CA). Peroxidase-conjugated anti-mouse or anti-rabbit IgG and D-[6-^{3}H] glucosamine hydrochloride were from Amersham (Uppsala, Sweden). The enhanced chemiluminescence (ECL) kit was purchased from Amersham and protein G agarose beads (P 4691) from Sigma-Aldrich. All other listed chemicals were purchased from Sigma-Aldrich.

Isolation and Culture of Oocyte-Cumulus Complexes, Cumulus, and Mural Granulosa Cells

Ovaries of slaughtered gilts were collected at a local abattoir and transported to the laboratory in a thermos. OCCs were released from follicles by aspiration and washed in M-199 supplemented with 6.25 mM Hepes, 20 mM sodium bicarbonate, 0.91 mM sodium pyruvate, 1.62 mM calcium lactate, and antibiotics. OCCs were isolated from 3–4-mm and 6–7-mm follicles, which we will refer to as small and large follicles, respectively.

Only OCCs surrounded by compact multilayered cumulus were selected for experiments; special attention was paid to selecting OCCs with the same size of cumulus within each experimental group. Twenty OCCs were cultured in 1 ml M-199 with 5% fetal calf serum in four-well dishes at 38.5°C, 5% CO_2 in air. To stimulate expansion of cumulus cells, the culture medium was supplemented with FSH or EGF at a concentration of 10 ng/ml, as reported previously [3].

To quantify EGFR on different types of cells during follicular growth, we prepared samples with defined numbers of cumulus and mural granulosa cells. For this purpose, we isolated OCCs and pieces of mural granulosa cells (about 300 μm in diameter) from 1–2-, 3–4-, and 6–7-mm follicles by the procedures described above. Cumulus cells, stripped mechanically from 50–100 OCCs, or 100 pieces of mural granulosa cells were vortexed in 0.5 ml of calcium and magnesium-free PBS with 3 mg/ml polyvinylpyrrolidone in a tube for 1 min to prepare the cell suspension. The number of cells in the suspension was determined by hemacytometer and the volume adjusted to contain 5×10^4 cells. The tube was centrifuged at 3000 rpm for 3 min, the excess PBS removed, and samples processed for immunoblotting with EGFR antibodies.

Assessment of Cumulus Expansion

Cumulus expansion was assessed 24 h after the onset of culture using a subjective scoring method [23]. Briefly, no response was scored as 0, minimum observable response was scored as 1, expansion of outer OCCs layers was scored as 2, expansion of all OCCs layers except the corona radiata was scored as 3, and expansion of all OCCs layers was scored as 4.

Production of Hyaluronic Acid by OCCs

Total hyaluronic acid (released in culture medium and retained by OCCs) was measured in this experiment. Groups of 10 OCCs were cultured in 100 μl of the culture medium supplemented with 2.5 μCi of D-[6-^{3}H]glucosamine hydrochloride. The cultures were terminated by adding 10 μl of a solution containing 50 mg/ml pronase and 10% Triton X-100 in 0.2 M Tris buffer, pH 7.8. The samples were incubated for 2 h at 38°C and then transferred to Whatman 3MM filter paper disks. The disks were air dried and then washed three times in 0.5% cetylpyridinium chloride with 10 mM nonradioactive glucosamine hydrochloride for 45 min each. The disks were dried once again, and radioactivity was measured using a liquid scintillation counter.

Immunoblotting

At selected intervals, groups of OCCs or defined numbers of cumulus and mural granulosa cells were lysed in 15 μl of sample buffer for SDS PAGE [24], heated at 100°C for 3 min, and stored at −80°C until use. Proteins of the samples were separated on 7% polyacrylamide gel modified as described [25] and transferred to PVDF membrane. Blots were blocked 1 h with 5% FCS and incubated 2 h with antiphosphotyrosine or anti-EGFR antibody. After incubation with secondary antibodies (1:5000) for 1 h, blots were extensively washed and signal developed by ECL. Following detection of phosphotyrosine, antibodies were stripped in some experiments by incubation of blots in 25 mM TRIS with 2% β-mercaptoethanol and 0.2% SDS at 70°C for 20 min. The blots were then reprobed with anti-EGFR antibody as described above. The intensity of the bands was analyzed by densitometry using the Advanced Image Data Analyzer software (Raytest Isotopenmessgeraete GmbH, Strawbenhardt, Germany). After detection, the blots were stained by Coomassie blue to assess amount of proteins in each lane.

Immunoprecipitation

Cumulus cells (3×10^5/sample) were lysed in 0.3 ml ice-cold buffer A (50 mM Hepes, pH 7.5, 1% NP-40, 150 mM NaCl, 0.5% sodium deoxycholate, 1 mM sodium vanadate, 1mM 4-(2-aminoethyl) benzensulfonyl fluoride, 1 mM p-nitrofenylphosphate, 0.2 μM aprotinin, 2 μM leupeptin, and 30 μM tosyl-L-phenylalanine) [26] for 25 min. The cell lysate was centrifuged and precleared by incubation with 5 μl protein G agarose beads for 60 min at 4°C. After preclearing, the lysates were centrifuged at 10^4 rpm and supernatants transferred to new tubes. Antiphosphotyrosine PY 20 was added to cell lysates (2 μl/sample) and incubated for 2 h. The lysates were then supplemented with 5 μl protein G and incubated on a rotator at 4°C overnight. Beads were washed five times with 0.2 ml buffer A, immune complexes were extracted by boiling with 2× concentrated SDS sample buffer, and samples were processed for immunoblotting as described above.

Statistics

Analysis of variance (ANOVA) was used to compare results of densitometry on immunoblots and production of hyaluronic acid. The chi-square test for independence and Fisher exact test were used to analyze data on the expansion of OCCs. The differences were considered significant when $P < 0.05$.

RESULTS

OCCs Isolated from Small and Large Follicles Contain Similar Amounts of EGFR

Immunoblotting with EGFR antibodies revealed that OCCs isolated from follicles of all size categories contain similar amounts of 170 kDa EGFR (Fig. 1). In contrast, the amount of EGFR protein in mural granulosa cells decreased by 30% with increasing follicle size. No signal of EGFR was detectable in oocytes. Thus, we concluded that the failure of OCCs from small follicles to expand after EGF treatment reported previously [3] was not caused by the absence or lower numbers of EGFRs in the cumulus cells.

EGF Induces Tyrosine Phosphorylation of EGFR and Other Cumulus Cell Proteins

EGF treatment of OCCs from large follicles induced robust and reproducible tyrosine phosphorylation of a number of proteins (Fig. 2A, top). Particularly prominent appeared to be the phosphotyrosine content of 42-, 116-, and 170-kDa proteins. As expected, based on the size of pig EGFR [27], the 170-kDa tyrosine phosphorylated protein exactly comigrated with the signal of the EGFR (Fig. 2A, bottom).

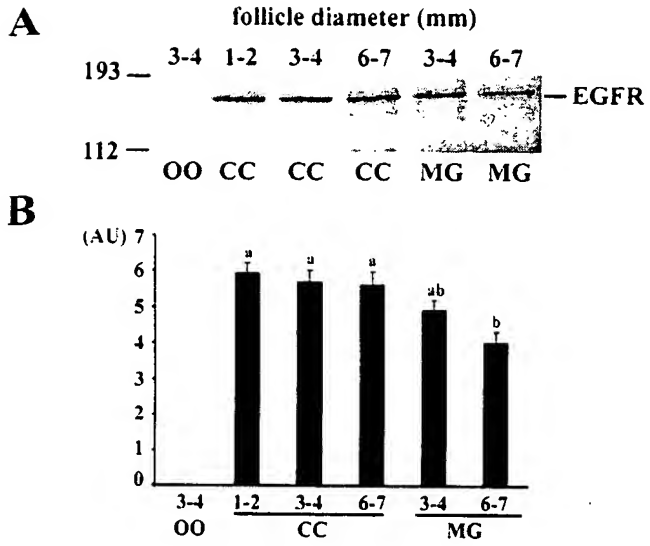

FIG. 1. The comparison of EGFR content in oocytes and cumulus and mural granulosa cells by immunoblotting with anti-EGFR antibodies. A) A typical result showing detection of EGFR in samples containing extracts of 50 oocytes (lane 1; OO) and of 5×10^4 cells (lanes 2–6; CC, cumulus cells; MG, mural granulosa cells), respectively. The size of respective follicles (mm) is shown above individual lanes; the position of molecular weight markers is shown on the left. B) Quantification of EGFR on immunoblots by densitometry. Results of three experiments as shown in A are summarized and expressed in arbitrary units as a mean ± SEM. Note the absence of detectable EGFR in oocytes and a decrease of EGFR content in mural granulosa cells with follicle growth compared with its stable expression in cumulus cells. Bars with no common letters indicate significant differences ($P < 0.05$).

Immunoprecipitation with antiphosphotyrosine antibody followed by development of blots with EGFR antibody confirmed that the 170-kDa phosphoprotein is indeed identical to EGFR (Fig. 2B). The ability of EGF to stimulate expansion of cumulus cells is therefore likely to be specifically transduced by the action of 170-kDa EGFR that becomes transiently phosphorylated on tyrosine upon activation. This result also suggests that the tyrosine phosphorylation of many other proteins that we have detected is specifically linked to the tyrosine kinase activity of EGFR itself or of kinase(s) regulated by EGFR.

EGF-Induced Protein Tyrosine Phosphorylation in Cumulus Cells Is Follicle-Size Dependent

Next, we assessed the pattern of tyrosine phosphorylation of the EGFR in cumulus cells isolated from small and large follicles. In cumulus cells from the small follicles, the phosphorylation of the EGFR occurred within 1–3 min, reaching approximately a 2-fold increase over the basal level (Fig. 3, A and B). On the contrary, in cumulus cells from the large follicles, the p170/EGFR tyrosine phosphorylation increased 10–12-fold over the basal level at 10 min after stimulation. In OCCs from both small and large follicles, the EGF-stimulated p170/EGFR tyrosine phosphorylation returned to the basal level within 1 h, with a sharp drop by 30 min after the start of activation (data not shown). Importantly, the low level of EGFR tyrosine phosphorylation correlated with the inability of cumulus cells from small follicles to undergo expansion after EGF stimulation reported previously [3].

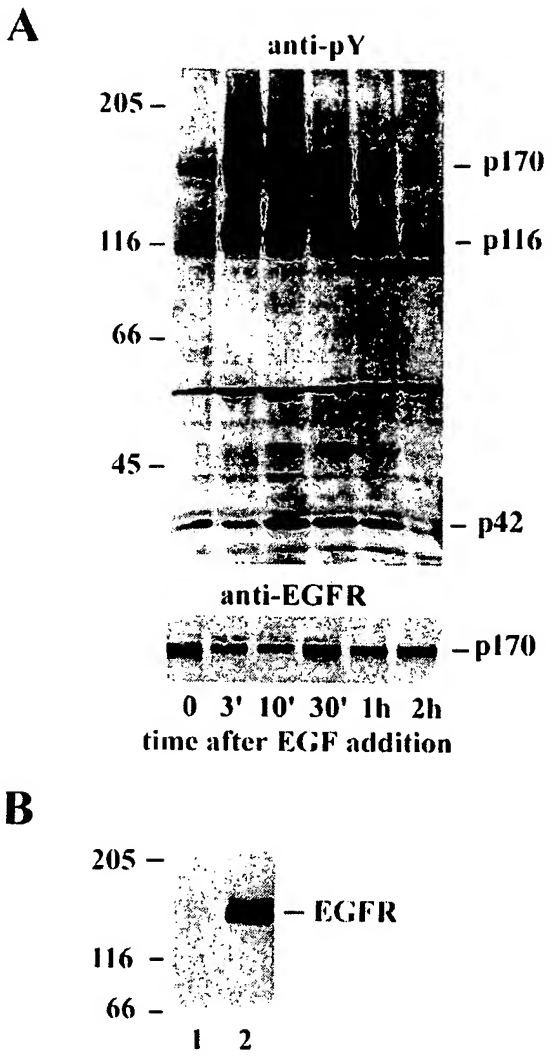

FIG. 2. Treatment of OCCs from large follicles with EGF induces transient tyrosine phosphorylation of EGFR. A) Top: Detection of phosphotyrosine in samples of 50 OCCs at various times after the start of EGF. Proteins (p170, p116, p42) displaying particularly prominent tyrosine phosphorylation are marked on the right of the immunoblot, molecular weight standards on the left. Bottom: Blot with stripped antiphosphotyrosine antibodies was reprobed with anti-EGFR antibody. The position of the EGFR matched with the position of 170-kDa protein. Note transient shift in electrophoretic mobility of the phosphorylated EGFR at 3–10 min after EGF addition, coinciding with strongest phosphotyrosine signal of p170 in top panel. B) Immunoprecipitation confirms that EGFR from EGF-treated cumulus cells are phosphorylated on tyrosine. Cumulus cells (3×10^5) from large follicles were stimulated with EGF for 10 min, their extracts immunoprecipitated with antiphosphotyrosine antibody and immunoblots developed with anti-EGFR antibody. Lane 1: control sample processed without antiphosphotyrosine antibody; lane 2: cells precipitated with antiphosphotyrosine antibody. Positions of molecular weight markers are on the left. Experiments were done in three replicates and representative results are shown.

FSH Enhances EGF-Induced Phosphorylation of EGFR

FSH is known to increase binding of EGF to granulosa cells and to induce and maintain EGFR in the follicle [28–31]. We therefore examined what the effect of FSH is on the pattern of tyrosine phosphorylation of EGFR in cumulus cells of small follicles. OCCs from small follicles were cultured in medium with or without FSH for 3 h and were stimulated by EGF afterward. In control groups pre-

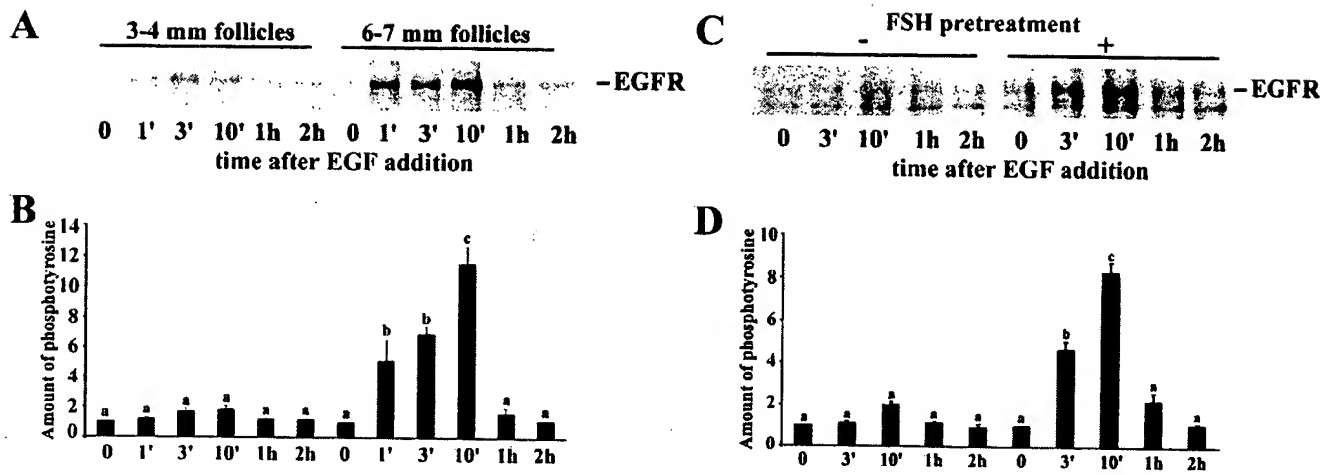

FIG. 3. The EGF-induced p170/EGFR tyrosine phosphorylation is regulated developmentally and promoted by FSH treatment in vitro. A) OCCs isolated from small and large follicles were treated with EGF and p170/EGFR tyrosine phosphorylation detected on immunoblots with phosphotyrosine antibodies at various times after the start of EGF treatment. B) Quantification of three experiments as shown in A by densitometry. Note that EGF induced 5–6-fold lower tyrosine phosphorylation of p170/EGFR in OCCs isolated from 3–4 mm as compared with OCCs from 6–7 mm follicles. C) Comparison of EGF induced p170/EGFR tyrosine phosphorylation in OCCs from 3–4-mm follicles that either were (right lanes) or were not (left) treated with FSH. D) Quantitative summary of three replicates of experiments shown in C. The samples in A and C contained 15 OCCs/lane and represent three parallel experiments with similar results. Densitometric quantification shown in B and D is expressed as a fold-increase over the basal level detected in OCCs at Time 0, ± SEM. Different letters above bars indicate significant differences ($P < 0.05$, at least).

incubated without FSH, the phosphorylation of EGFR increased about 2-fold over the base level. However, in the group of OCCs preincubated with FSH, the EGF-induced tyrosine phosphorylation of EGFR was about 9-fold over the base level, and the overall pattern of tyrosine phosphorylation resembled EGF-treated OCCs from large follicles (Fig. 3, C and D). FSH itself did not affect tyrosine phosphorylation of EGFR (Fig. 3C). In summary, these results suggest that FSH treatment in vitro is sufficient to induce development of a mature EGF response in cumulus cells of small follicles. This effect of FSH was not caused by increasing numbers of EGFRs on cumulus cells during the time of preincubation (Fig. 4).

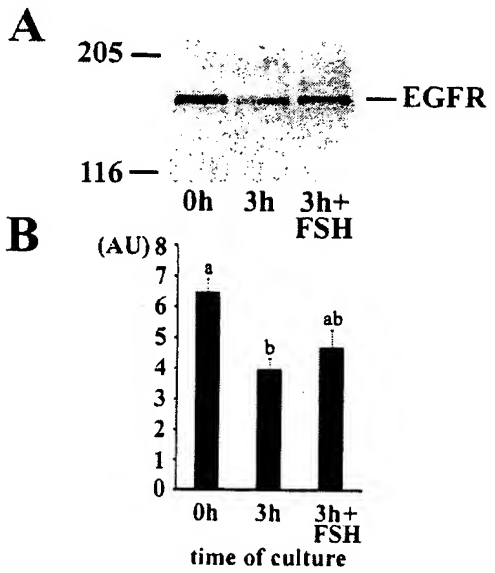

FIG. 4. FSH treatment does not significantly increase EGFR expression in OCCs from small follicles. A) OCCs isolated from 3–4-mm follicles were treated as indicated and immunoblotted with EGFR antibody. Each lane represents 50 OCCs and shown is a result representative of three replicates. Positions of molecular weight markers (kDa) are on the left. B) The results of experiments in A were quantified by densitometry and EGFR concentration is expressed in arbitrary units ± SEM. Bars with no common letters indicate significant differences ($P < 0.05$).

FSH-Enhanced Phosphorylation of EGFR Promotes Expansion of OCCs

In the next experiment, we asked whether sequential treatment by FSH and EGF promotes production of hyaluronic acid and expansion of OCCs from small follicles. As expected, based on our previous results [3], OCCs from small follicles did not expand following stimulation by EGF alone, irrespective of the length of stimulation (1 or 24 h; Fig. 5A). In contrast, more than 85% of OCCs cultured in FSH-supplemented medium for 24 h underwent expansion. Thirty percent of OCCs cultured in FSH for 4 h and subsequently in control medium for 20 h underwent expansion, while sequential treatment with FSH (3 h) followed by EGF (1 h) and control medium (20 h) induced expansion in 53% of OCCs ($P < 0.05$). In concert with these data, production of hyaluronic acid was significantly higher in OCCs stimulated by the sequential treatment than in OCCs stimulated by FSH or EGF (Fig. 5B). The FSH-dependent development of a mature level of EGF-induced EGFR phosphorylation (Fig. 3C) is therefore strongly correlated with increased ability of OCCs to produce hyaluronic acid and to undergo expansion.

EGFR Tyrosine Kinase Activity Is Essential for EGF-Induced Expansion of OCCs

The results of the above experiments suggest that activity of the intrinsic EGFR-tyrosine kinase is involved in regulation of EGF-induced expansion. To confirm this, we assessed the effect of EGFR-tyrosine kinase-specific inhibitor tyrphostin 46 [32] on expansion of porcine OCCs from large follicles. As shown in Figure 6, tyrphostin inhibited expansion in a dose-dependent manner, with full inhibition at a concentration of 10 μM.

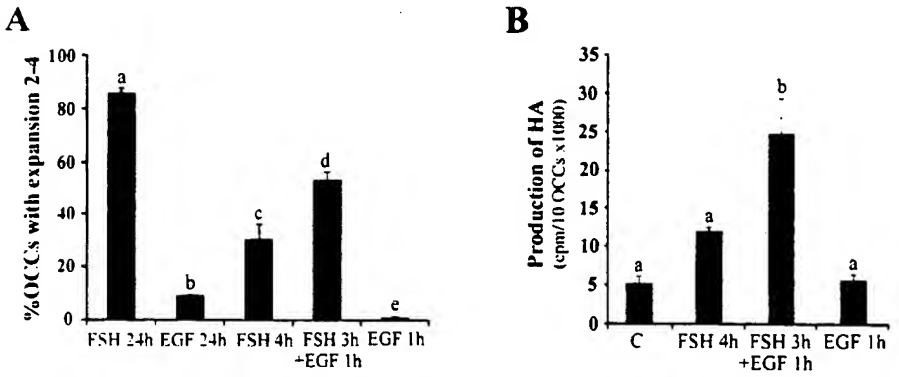

FIG. 5. FSH and EGF act synergistically to promote production of hyaluronic acid and expansion of OCCs from small follicles. OCCs obtained from 3–4-mm follicles were treated by FSH and EGF for indicated periods of time, washed, and cultured in control medium. A) The percentages of OCCs displaying expansion 2–4 times (see *Materials and Methods*) were scored at 24 h of culture in all groups. Experiment was repeated three times using 528 OCCs in total. B) OCCs were cultured for the last 20 h of culture in control medium with D-[6-^{3}H] glucosamine hydrochloride. Production of hyaluronic acid is expressed in cpm for 10 OCCs ± SEM (three replicates). HA, Hyaluronic acid; C, control medium without FSH and EGF. Bars with different superscripts are significantly different ($P < 0.05$).

DISCUSSION

Our data proved that EGFRs are present on cumulus cells of both small and large follicles in similar quantities. This is in accord with the data obtained by Singh et al. [33], who detected, by RT-PCR and immunostaining, EGFR on porcine cumulus, granulosa, and theca cells of all follicle stages. These results suggest that the failure of EGF to stimulate expansion of OCCs isolated from the small follicles is not caused by an absence of the EGFR.

EGF binding to its receptor causes activation of the intrinsic receptor tyrosine kinase, which results in autophosphorylation of the EGFR [17]. Tyrosine kinase activity of EGFR is essential for activation of the downstream signaling pathways [18, 20, 34, 35], regulation of gene expression [36, 37], cell proliferation [35], and apoptosis [38]. Also, effects of EGF on regulation of bovine oocyte maturation [39] and EGF-induced production of hyaluronic acid by mouse OCCs [40] are mediated through a tyrosine kinase pathway. Similarly, we found in the present study that tyrphostin 46 is able to eliminate EGF-induced expansion of porcine OCCs, providing evidence that tyrosine kinase activity is required in this process.

We found three cumulus cell proteins heavily phosphorylated on tyrosine residues after stimulation with EGF. First was a protein of 170 kDa, which showed the highest increase in phosphorylation and which we identified in the next experiments as the EGFR; second was a protein of 116 kDa that showed a similar pattern of phosphorylation as the EGFR. We assume that this protein may be the product of the Cbl proto-oncogene that was also identified as a 116-kDa tyrosine phosphorylated protein in a variety of EGF-stimulated cells [41, 42]. Finally, the 42-kDa protein might be identical to the MAP kinase because it comigrated on one-dimensional immunoblots with activated ERK-2 protein (data not shown).

The comparison of tyrosine phosphorylation of EGFR localized on small and large follicles indicates that the extent of EGFR phosphorylation may play a pivotal role in regulation of EGF-stimulated expansion of OCCs. Only expanding cumulus cells from large follicles contained EGFR capable of extensive tyrosine phosphorylation following stimulation by EGF. In contrast, EGFR in nonexpanding cumulus cells from small follicles exhibited only low levels of EGF-induced tyrosine phosphorylation. There are several possible explanations of this feature.

OCCs from small follicles may contain EGFR with a decreased binding of EGF. To our knowledge, no data on EGF binding capacity of cumulus cells during folliculogenesis have been reported so far. In mural granulosa cells, the EGFR binding capacity was primarily affected by their luteinization and decreased with follicle enlargement due to a decrease in receptor number with no change in receptor affinity [28]. However, it is unlikely that a similar scenario would apply in the case of cumulus cells that are under the influence of oocyte-secreted paracrine factors preventing them from luteinization [23]. Indeed, our immunoblotting data revealed that EGFR concentration decreases in mural granulosa cells and remains stable in cumulus cells during follicular growth.

Although all EGFRs in EGFR-expressing cells are molecularly identical, they can be divided into two classes that have either low or high affinity to EGF [43]. The mechanisms responsible for transmodulation of EGFR have been

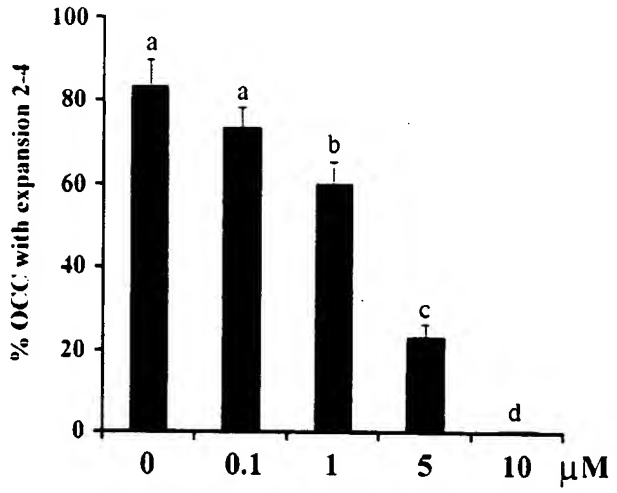

FIG. 6. EGFR tyrosine kinase inhibitor tyrphostin 46 inhibits EGF-stimulated expansion. OCCs isolated from 6–7-mm follicles were treated with EGF and indicated concentrations of tyrphostin 46. The control group of OCCs (0 μM) was cultured in medium with 0.1% DMSO that was used to dissolve the tyrphostin. Percentages of OCCs displaying expansion 2–4 times (see *Material and Methods*) were scored 24 h after the onset of culture. Bars with different superscripts are significantly different ($P < 0.05$). The experiment was repeated three times using 226 OCCs in total.

extensively studied but remain still unclear. The increase in the fraction of high-affinity EGFR, associated with a high level of EGF-induced autophosphorylation, was attributed to binding of the EGFR to filamentous actin [44]. However, removal of the actin-binding site from the receptor did not affect the affinity of EGFR to EGF [43]. Next, EGFR can form homodimers or heterodimers with other members of the EGFR family, including ErbB2 [45]. These dimeric forms of EGFR were shown to bind EGF with high affinity [46, 47]. On the other hand, substances that disrupt high-affinity EGF-EGFR interaction in HeLa cells had no effect on the EGFR homo- or heterodimerization [48]. Instead, the presence of specific EGFR-affinity modulating proteins has been suggested [43, 48]. This idea is supported by the discovery of a peptide that induces conformational change of the EGFR and thus provides access to additional tyrosine autophosphorylation sites [49]. In addition, tyrosine kinase activity of the EGFR was enhanced 10-fold after binding with the oncogenic form of c-Cbl in EGF-stimulated lymphoma cells, suggesting that Cbl protein acts as a regulator of receptor tyrosine kinases [50]. We propose that one of these mechanisms may be responsible for the differing extents of phosphorylation of EGFR in cumulus cells from small and large follicles. It should be noted at this point that, in our experiments, the extensive phosphorylation of EGFR was regularly accompanied by increased tyrosine phosphorylation of the 116-kDa protein, which, as discussed above, may be identical to the Cbl.

Gonadotropins and EGF have a synergistic effect on the range of functions of follicular cells. FSH was shown to increase the number of EGFRs and binding of EGF on cultured granulosa cells in a dose-dependent manner [28–31, 51]. In our experiment, we demonstrated that FSH promotes maturation of the EGF-response pathway in OCCs from small follicles, as evidenced by a strong increase in EGF-induced EGFR tyrosine phosphorylation, production of hyaluronic acid, and OCCs expansion. Surprisingly, a 3-h preincubation of OCCs in FSH-supplemented medium was sufficient to induce a significant increase in EGFR phosphorylation without an increase in EGFR concentration. These data indicate that FSH may be implicated in mechanism(s) regulating EGFR tyrosine phosphorylation in porcine cumulus cells. We suggest that FSH-dependent maturation of EGFR may also function in vivo and regulate expansion of cumulus cells in preovulatory follicles.

REFERENCES

1. Sutovsky P, Flechon JE, Pavlok A. Microfilaments, microtubules and intermediate filaments fulfill different roles in gonadotropin induced expansion of bovine cumulus oophorus. Reprod Nutr Dev 1994; 34: 415–425.
2. Sutovsky P, Flechon JE, Pavlok A. F-actin is involved in control of bovine cumulus expansion. Mol Reprod Dev 1995; 41:521–529.
3. Prochazka R, Srsen V, Nagyova E, Miyano T, Flechon JE. Developmental regulation of effect of epidermal growth factor on porcine oocyte-cumulus cell complexes: nuclear maturation, expansion, and F-actin remodeling. Mol Reprod Dev 2000; 56:63–73.
4. Dekel N, Hillensjo Y, Kraicer PF. Maturation effects of gonadotropins on the cumulus-oocyte complex of the rat. Biol Reprod 1979; 20:191–197.
5. Eppig JJ. FSH stimulates hyaluronic acid synthesis by oocyte-cumulus cell complexes from mouse preovulatory follicles. Nature 1979; 281: 483–484.
6. Salustri A, Yanagishita M, Underhill CB, Laurent TC, Hascall VC. Localization and synthesis of hyaluronic acid in the cumulus cells and mural granulosa cells of the preovulatory follicle. Dev Biol 1992; 151: 541–551.
7. Sutovsky P, Flechon JE, Flechon B, Motlik J, Peynot N, Heyman Y. Dynamic changes of gap junctions and cytoskeleton during in vitro culture of cattle oocyte cumulus complexes. Biol Reprod 1993; 49: 1277–1287.
8. Salustri A, Hascall VC, Camaioni A, Yanagihista M. Oocyte-granulosa cell interactions. In: Adashi EY, Leung PCK (eds.), The Ovary. New York: Raven Press; 1993: 209–225.
9. Hess KA, Chen L, Larsen WJ. Inter-α-inhibitor binding to hyaluronan in the cumulus extracellular matrix is required for optimal ovulation and development of mouse oocytes. Biol Reprod 1999; 61:436–443.
10. Chen L, Russel PT, Larsen WJ. Functional significance of cumulus expansion in the mouse: roles for the preovulatory synthesis of hyaluronic acid within the cumulus mass. Mol Reprod Dev 1993; 34: 87–93.
11. Tesarik J, Pilka L, Drahorad J, Cechova D, Veselsky L. The role of cumulus cell-secreted proteins in the development of human sperm fertilizing ability: implication in IVF. Hum Reprod 1988; 3:129–132.
12. Downs SM. Specificity of epidermal growth factor action on maturation of the murine oocyte and cumulus oophorus in vitro. Biol Reprod 1989; 41:371–379.
13. Boland NI, Gosden RG. Effects of epidermal growth factor on the growth and differentiation of cultured mouse ovarian follicles. J Reprod Fertil 1994; 101:369–374.
14. Singh B, Barbe GJ, Armstrong DT. Factors influencing resumption of meiotic maturation and cumulus expansion of porcine oocyte-cumulus cell complexes in vitro. Mol Reprod Dev 1993; 36:113–119.
15. Lorenzo PL, Illera MJ, Illera JC, Illera M. Enhancement of cumulus expansion and nuclear maturation during bovine oocyte maturation in vitro by the addition of epidermal growth factor and insulin-like growth factor I. J Reprod Fertil 1994; 101:697–701.
16. Lorenzo PL, Rebollar PG, Illera MJ, Illera C, Illera M, Alvarino JMR. Stimulatory effect of insulin-like growth factor I and epidermal growth factor on the maturation of rabbit oocytes in vitro. J Reprod Fertil 1996; 107:109–117.
17. Carpenter G, Cohen S. Epidermal growth factor. J Biol Chem 1990; 265:7709–7712.
18. Keel BA, Hildebrant JM, May JV, Davis JS. Effects of epidermal growth factor on tyrosine phosphorylation of mitogen activated protein kinases in monolayer cultures of porcine granulosa cells. Endocrinology 1995; 136:1197–1204.
19. Bjorge JD, Chan TO, Antczak M, Kung HJ, Fujita DJ. Activated type I phosphatidylinositol kinase is associated with the epidermal growth factor (EGF) receptor following EGF stimulation. Proc Natl Acad Sci U S A 1990; 87:3816–3820.
20. David M, Wong L, Flawell R, Thompson SA, Wells A, Larner AC, Johnson GR. STAT activation by epidermal growth factor (EGF) and amphiregulin. Requirement for the EGF receptor kinase but not for tyrosine phosphorylation sites or JAK1. J Biol Chem 1996; 271:9185–9188.
21. Nakamura N, Chin H, Miyasaka N, Miura O. An epidermal growth factor receptor/Jak2 tyrosine kinase domain chimera induces tyrosine phosphorylation of Stat5 and transduces a growth signal in hematopoietic cells. J Biol Chem 1996; 271:19483–19488.
22. Houslay MD. "Crosstalk": a pivotal role for protein kinase C in modulating relationships between signal transduction pathways. Eur J Biochem 1991; 195:9–27.
23. Vanderhyden BC, Cohen JN, Morley P. Mouse oocytes regulate granulosa cell steroidogenesis. Endocrinology 1993; 133:423–426.
24. Laemmli UK. Cleavage of structural proteins during the assembly of the head of bacteriophage T4. Nature 1970; 227:680–685.
25. Kalab P, Kubiak JZ, Verlhac MH, Colledge WH, Maro B. Activation of p90rsk during meiotic maturation and first mitosis in mouse oocytes and eggs: MAP kinase-independent and -dependent activation. Development 1996; 122:1957–1964.
26. Dvorak P, Hampl A, Jirmanova L, Pacholikova J, Kusakabe M. Embryoglycan ectodomains regulate biological activity of FGF-2 to embryonic stem cells. J Cell Sci 1998; 111:2945–2952.
27. Zhang Y, Paria BC, Dey SK, Davis DL. Characterization of the epidermal growth factor receptor in preimplantation pig conceptus. Dev Biol 1992; 151:617–621.
28. Buck PA, Schomberg DW. [^{125}I]iodo-epidermal growth factor binding and mitotic responsiveness of porcine granulosa cells are modulated by differentiation and follicle stimulating hormone. Endocrinology 1988; 122:28–33.
29. Feng P, Knecht M, Catt K. Hormonal control of epidermal growth factor receptors by gonadotropins during granulosa cell differentiation. Endocrinology 1987; 120:1121–1126.
30. Fujinaga H, Yamoto M, Nakano R, Shima K. Epidermal growth factor

binding sites in porcine granulosa cells and their regulation by follicle-stimulating hormone. Biol Reprod 1992; 46:705–709.
31. Fujinaga H, Yamoto M, Shione T, Nakano R. FSH and LH up-regulate epidermal growth factor receptors in rat granulosa cells. J Endocrinol 1994; 140:171–177.
32. Gazit A, Osherov N, Posner I, Yaish P, Poradosu E, Gilson C, Levitzki A. Tyrphostins. 2. Heterocyclic and alpha-substituted benzylidenemalononitrile tyrophostins as potent inhibitors of EGF receptor and ErbB2/neu tyrosine kinases. J Med Chem 1991; 34:1896–1907.
33. Singh B, Rutledge JM, Armstrong DT. Epidermal growth factor and its receptor gene expression and peptide localization in porcine ovarian follicles. Mol Reprod Dev 1995; 40:391–399.
34. Margolis B, Bellot F, Honneger AM, Ullrich A, Schlesinger J, Zilb A. Tyrosine kinase activity is essential for association of phospholipase C-gamma with the epidermal growth factor receptor. Mol Cell Biol 1990; 10:435–441.
35. Chen WS, Lazar CS, Poenie M, Tsien RY, Gill GN, Rosenfeld MG. Requirement for intrinsic protein tyrosine kinase in the immediate and late actions of the EGF receptor. Nature 1987; 328:820–823.
36. Honneger AM, Szapary D, Schmidt A, Lyall R, Van Obberghen E, Ullrich A, Schlessinger J. A mutant epidermal growth factor receptor with defective tyrosine kinase is unable to stimulate proto-oncogene expression and DNA synthesis. Mol Cell Biol 1987; 7:4568–4571.
37. Reddy KB, Keshamouni VG, Chen YQ. The level of tyrosine kinase activity regulates the expression of p21/WAF1 in cancer cels. Int J Oncol 1999; 15:301–306.
38. Musallam L, Ethier C, Haddad PS, Bilodeau M. Role of EGF receptor tyrosine kinase activity in antiapoptotic effect of EGF on mouse hepatocytes. Am J Physiol Gastrointest Liver Physiol 2001; 280:G1360–G1369.
39. Lorenzo PL, Liu IK, Illera JC, Picazo RA, Carniero GF, Illera MJ, Conley AJ, Enders AC, Illera M. Influence of epidermal growth factor on mammalian oocyte maturation via tyrosine-kinase pathway. J Physiol Biochem 2001; 57:15–22.
40. Tirone E, D'Alessandris C, Hascall VC, Siracusa G, Salustri A. Hyaluronan synthesis by mouse cumulus cells is regulated by interactions between follicle-stimulating hormone (or epidermal growth factor) and soluble oocyte factor (or transforming growth factor β_1). J Biol Chem 1997; 272:4787–4794.
41. Fukazawa T, Miake S, Band V, Band H. Tyrosine phosphorylation of Cbl upon epidermal growth factor (EGF) stimulation and its association with EGF receptor and downstream signaling proteins. J Biol Chem 1996; 271:14554–14559.
42. Jope RS, Song L, Grimes CA, Zhang L. Oxidative stress oppositely modulates protein tyrosine phosphorylation stimulated by muscarinic G protein coupled with epidermal growth factor receptors. J Neurosci Res 1999; 55:329–340.
43. Van der Heyden MA, Nievers M, Verkleij AJ, Boonstra J, van Bergen en Henegouwen PM. Identification of an intracellular domain of the EGF receptor required for high-affinity binding of EGF. FEBS Lett 1997; 410:268–268.
44. Diakonova M, Payrastre B, van Velzen AG, Hage WJ, van Bergen en Henegouwen PM, Boonstra J, Cremes FF, Humbel BM. Epidermal growth factor induces rapid and transient association of phospholipase C-gamma 1 with EGF receptor and filamentous actin a membrane ruffles of A431 cells. J Cell Sci 1995; 108:2499–2509.
45. Heldin CH. Dimerization of cell surface receptors in signal transduction. Cell 1995; 80:213–223.
46. Sherrill JM, Kyte J. Activation of epidermal growth factor receptor by epidermal growth factor. Biochemistry 1996; 35:5705–5718.
47. Wilkinson JC, Staros JV. Effect of ErbB2 coexpression on the kinetic interactions of epidermal growth factor with its receptor in intact cells. Biochemistry 2002; 41:8–14.
48. Johanessen LE, Haugen KE, Ostvold AC, Stang E, Madshus IH. Heterodimerization of the epidermal-growth-factor (EGF) receptor and ErbB2 and the affinity of EGF binding are regulated by different mechanisms. Biochem J 2001; 356:87–96.
49. Poppleton HM, Wiepz GJ, Bertics PJ, Patel TB. Modulation of the protein tyrosine kinase activity and autophosphorylation of the epidermal growth factor receptor by its juxtamembrane region. Arch Biochem Biophys 1999; 363:227–236.
50. Thien CB, Langdon WY. Tyrosine kinase activity of the EGF receptor is enhanced by expression of oncogenic 70Z-Cbl. Oncogene 1997; 15: 2909–2919.
51. Hattori MA, Yoshino E, Shinohara Y, Horiuchi R, Kojima I. A novel action of epidermal growth factor in rat granulosa cells: its potentiation of gonadotrophin action. J Mol Endocrinol 1995; 15:283–291.

Sign in

Google

Web Images Video News Maps more »

Y1214 kdr/flk-1 Search Advanced Search Preferences

Web

Results 11 - 20 of about 61 for Y1214 kdr/flk-1. (0.28 seconds)

VEGF Receptor 2 (phospho Y1214) antibody (ab31480) datasheet
VEGF Receptor 2 (phospho **Y1214**) antibody (ab31480) datasheet. ... A single autophosphorylation site on **KDR/Flk-1** is essential for VEGF-A-dependent ...
www.abcam.com/index.html?datasheet=31480&icn=6 - 44k - Cached - Similar pages

VEGF Receptor 2 antibody (ab31326) datasheet
Detects endogenous levels of VEGFR2 protein around **Y1214** ... A single autophosphorylation site on **KDR/Flk-1** is essential for VEGF-A-dependent activation of ...
www.abcam.com/index.html?datasheet=31326&icn=6 - 45k - Cached - Similar pages

Anti-phospho-VEGFR-2 antibody - MPR Summary: pY1175, pY951, pY996 ...
Anti-phospho-**KDR/Flk-1**/VEGFR2 (Tyr1054), clone D1W (05-894) ... **Y1214**, Y1212, PKFHpYDNTA, 450. VEGFR2 [pY1214] (44-1052) · Biosource, P (Rabbit) ...
mpr.nci.nih.gov/MPR/MPRAntibodiesForProteinPage.aspx?GI=11321597 - 23k - Cached - Similar pages

Blackwell Synergy: Histopathology, Vol 43, Issue 1, pp. 33-39: The ...
... number 469 against peptide containing the tyrosine residue **Y1214**, ... Frelin C. Rapid transactivation of the VEGF receptor **KDR/Flk-1** by the bradykinin ...
www.blackwell-synergy.com/doi/abs/10.1046/j.1365-2559.2003.01644.x - Similar pages

GTX25475-VEGF Receptor 2 (phospho Y1214) antibody-GeneTex Inc.
VEGF Receptor 2 (phospho **Y1214**) antibody 44-1052 GTX25475 25475 GTX25475 VEGF ... also known as **KDR / FLK 1**) is a 200 kDa member of a receptor tyrosine ...
www.genetex.com/commerce/catalog/product.jsp;jsessionid=2F14471B1F5AFD91171F389F90EFB800?product_id=15398... - 47k - Cached - Similar pages

THE USE OF AN EPITOPE OF VASCULAR ENDOTHELIAL GROWTH FACTOR ...
Thus, according to the first aspect of the present invention there is provided the use of the **KDR/Flk-1** epitope **Y1214** as a marker in the measurement of a ...
www.freepatentsonline.com/EP1487876.html - 52k - Cached - Similar pages

(WO/2003/078465) THE USE OF AN EPITOPE OF VASCULAR ENDOTHELIAL ...
... THE USE OF AN EPITOPE OF VASCULAR ENDOTHELIAL GROWTH FACTOR RECEPTOR **KDR/FLK-1** ... The invention also relates to the use of KDR/F1k-1 epitope **Y1214** as a ...
www.wipo.int/pctdb/en/wo.jsp?WO=2003/078465 - 38k - Cached - Similar pages

KDR - kinase insert domain receptor (a type III receptor tyrosine ...
The human **KDR/flk-1** gene contains a functional initiator element that is bound and ... We conclude that phosphorylation of **Y1214** on VEGFR2 is required to ...
www.ihop-net.org/UniPub/iHOP/gs/89664.html - 326k - Cached - Similar pages

[PDF] Vascular Endothelial Growth Factor Receptor Family Genes: When Did ...
File Format: PDF/Adobe Acrobat
and **Y1214** on human VEGFR2 could be autophosphory-. lated (Cunningham et al., 1997; ... A Single autophosphorylation site on **KDR/Flk-1** is essential ...
www.atypon-link.com/WDG/doi/pdf/10.1515/BC.2002.177 - Similar pages

ScienceDirect - Human Pathology : Expression and cellular ...
... phosphorylated at residue **Y1214**, and characterized by Western blotting and ... [8] T. Takahashi and M. Shibuya, The 230 kD mature form of **KDR/Flk-1** ...
linkinghub.elsevier.com/retrieve/pii/S0046817705002674 - Similar pages

www.bioone.org/perlserv/?request=get-document&doi=10.1379%2F1466-1268(2003)8%3C37%3AIVRFVA%3E2.0.CO%3B2 - Similar pages

Result Page: **Previous** 1 2 3 4 5 **Next**

Y1214 kdr/flk-1 Search

Search within results | Language Tools | Search Tips

Sign in

Google

Web Images Video News Maps more »

Y1214 kdr/flk-1 Search Advanced Search Preferences

Web

Results 21 - 30 of about 60 for **Y1214 kdr/flk-1**. (0.15 seconds)

[PDF] Phosphorylated KDR is expressed in the neoplastic and stromal ...
File Format: PDF/Adobe Acrobat
including the **Y1214** and Y1059 tyrosine residues,. respectively, with specificity of the ... autophosphorylation site on **KDR/Flk-1** is essential for VEGF- ...
doi.wiley.com/10.1002/path.1520 - Similar pages

AZD2171: A Highly Potent, Orally Bioavailable, Vascular ...
... generated to phosphorylated **Y1214**), KDR (Santa Cruz Biotechnology), ... Involvement of VEGFR-2 (**kdr/flk-1**) but not VEGFR-1 (flt-1) in VEGF-A and VEGF-C ...
cancerres.aacrjournals.org/.../full/65/10/4389?ijkey=LMN5l94cOe5BU&keytype=ref&siteid=aacrjnls - Similar pages

[PDF] 04-4409 4389..4400
File Format: PDF/Adobe Acrobat
against pKDR (rabbit polyclonal generated to phosphorylated **Y1214**), KDR ... Involvement of VEGFR-2 (**kdr/flk-1**) but not VEGFR-1 ...
cancerres.aacrjournals.org/cgi/reprint/65/10/4389.pdf - Similar pages

Blackwell Synergy - Traffic, Volume 7 Issue 9 Page 1270 ...
... and Y1175 and **Y1214** in the carboxyl terminal tail (5,6,8). ... Chida K, Shibuya M. A single autophosphorylation site on **KDR/Flk-1** is essential for ...
www.blackwell-synergy.com/doi/abs/10.1111/j.1600-0854.2006.00462.x - Similar pages

Vascular Endothelial Growth Factor Signaling Pathways: Therapeutic ...
A second major autophosphorylation site in human VEGFR-2 is **Y1214**, ... Chida K, Shibuya M. A single autophosphorylation site on **KDR/Flk-1** is essential for ...
clincancerres.aacrjournals.org/cgi/content/full/12/17/5018 - Similar pages

Rabbit Anti-VEGF Receptor 2, phospho (Tyr1214) Polyclonal Antibody ...
Rabbit polyclonal to VEGF Receptor 2 (phospho **Y1214**) Vascular Endothelial Growth Factor Receptor 2 (VEGFR 2, also known as **KDR / FLK 1**) is a 200 kDa member ...
www.biocompare.com/itemdetails.asp?itemid=380551 - 37k - Cached - Similar pages

[PDF] 06-1520 5018..5022
File Format: PDF/Adobe Acrobat - View as HTML
ylation site in human VEGFR-2 is **Y1214**, which is involved in ... single autophosphorylation site on **KDR/Flk-1** is. essential for VEGF-A-dependent activation ...
www.uth.tmc.edu/gsbs/courses/Cancer%20Biology/2006%20Materials/Ferrara_review_CCR_2006.pdf - Similar pages

[PDF] The vascular endothelial growth factor (VEGF)/ VEGF receptor ...
File Format: PDF/Adobe Acrobat - View as HTML
Y1214 appears to be required to trigger the sequential activation of Cdc42 and p38 MAPK. ... (2001) A single autophosphorylation site on **KDR/Flk-1** ...
www.clinsci.org/cs/109/0227/1090227.pdf - Similar pages

[PDF] Signal transduction in angiogenesis
File Format: PDF/Adobe Acrobat
domain, and Y1175 and **Y1214** in the carboxyl terminal tail [38, 39]. ... **KDR/Flk-1** is essential for VEGF-A-dependent activation of PLC-gamma and DNA ...
www.springerlink.com/index/w7vt738347n42g7g.pdf - Similar pages

BIOONE Online Journals - Integrin αvβ3 requirement for VEGFR2 ...

... sites on VEGFR2 have been ascribed as Y1175 and **Y1214** (Takahashi et al 2001). ... A single autophosphorylation site on **KDR/Flk-1** is essential for ...

Result Page: **Previous** 1 2 3 4 5 **Next**

Y1214 kdr/flk-1 Search

Search within results | Language Tools | Search Tips

Google Home - Advertising Programs - Business Solutions - About Google